

**SINGLE CRYSTAL X-RAY CHARACTERIZATION AND
STRUCTURE CORRELATION OF PENTACYCLIC
FRIEDELANE RING SYSTEM**

Mr. Auphatham Phothikanith

A Thesis Submitted in Partial Fulfillment of the Requirements

For the Degree of Doctor of Philosophy in Chemistry

Suranaree University of Technology

Academic Year 2003

ISBN 974-533-294-1

การศึกษาโครงสร้างสารในกลุ่มฟรีเดเลนที่มีระบบวงแหวนห้าวงโดยวิธี
รังสีเอกซ์ผลึกเดี่ยวและสหสัมพันธ์ของโครงสร้าง

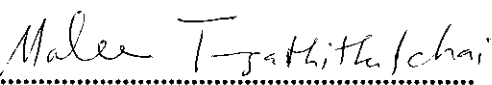
นายอุปถัมภ์ โปธิกนิษฐ์

วิทยานิพนธ์นี้เป็นส่วนหนึ่งของการศึกษาตามหลักสูตรปริญญาวิทยาศาสตรดุษฎีบัณฑิต
สาขาวิชาเคมี
มหาวิทยาลัยเทคโนโลยีสุรนารี
ปีการศึกษา 2546
ISBN 974-533-294-1

**SINGLE CRYSTAL X-RAY CHARACTERIZATION AND
STRUCTURE CORRELATION OF PENTACYCLIC
FRIEDELANE RING SYSTEM**

Suranaree University of Technology has approved this thesis submitted in
partial fulfillment of the requirements for the Degree of Doctor of Philosophy

Thesis Examining Committee


.....

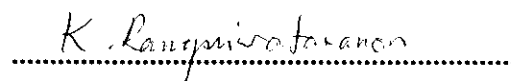
(Asst. Prof. Dr. Malee Tangsathitkulchai)
Chairperson


.....

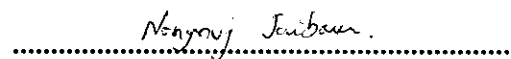
(Assoc. Prof. Dr. Kenneth J. Haller)
Member (Thesis Advisor)


.....

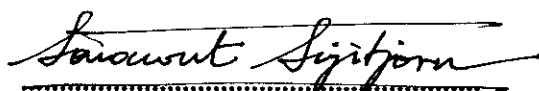
(Asst. Prof. Dr. James R. Ketudat-Cairns)
Member


.....

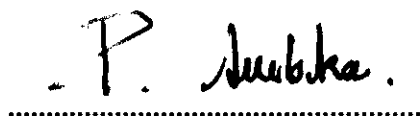
(Asst. Prof. Dr. Kunwadee Rangsiwatananon)
Member


.....

(Asst. Prof. Dr. Nongnuj Jaiboon)
Member


.....

(Assoc. Prof. Dr. Sarawut Sujitjorn)
Vice Rector for Academic Affairs


.....

(Assoc. Prof. Dr. Prasart Suebka)
Dean of the Institute of Science

อุปถัมภ์ โปชนิกนิษฐ์: การศึกษาโครงสร้างสารในกลุ่มฟริเดแลนที่มีระบบวง
แหวนห้าวงโดยวิธีรังสีเอกซ์ผลึกเดี่ยวและสหสัมพันธ์ของโครงสร้าง (SINGLE
CRYSTAL X-RAY CHARACTERIZATION AND STRUCTURE
CORRELATION OF PENTACYCLIC FRIEDELANE RING SYSTEM)

อาจารย์ที่ปรึกษา : รศ. ดร. เต็มเนท เจ. แสลดอร์, 139 หน้า. ISBN 974-533-294-1

วิทยานิพนธ์นี้ เป็นการศึกษาโครงสร้างสารประกอบซึ่งมีวงแหวนหกเหลี่ยมห้าวงต่อกันในกลุ่มฟริเดแลน โดยวิธีสหสัมพันธ์ของโครงสร้างและ วิธีรังสีเอกซ์ผลึกเดี่ยว โดยวิธีสหสัมพันธ์ของโครงสร้างจากความสัมพันธ์ระหว่างความยาวพันธะของคาร์บอนกับออกซิเจน ($C\cdots O$) กับผลรวมของมุมพันธะที่อะตอมคาร์บอนตำแหน่งที่ 3 ได้แสดงให้เห็นถึงความผิดปกติในโครงสร้างของตำแหน่งออกซิเจนอะตอม ความผิดปกตินี้สามารถอธิบายได้โดยการศึกษาโครงสร้างของสารที่ผิดปกติ โดยเทคนิครังสีเอกซ์ผลึกเดี่ยว สารดังกล่าวคาร์บอนอะตอมตำแหน่งที่ 3 เกิดพันธะกับทั้งหมู่ไฮดรอกซีและหมู่คาร์บอนิล โดยหมู่ไฮดรอกซีมีค่าออกคิวแพนซี 0.680(3) ความยาวพันธะของคาร์บอน-ออกซิเจนสำหรับหมู่ไฮดรอกซีเท่ากับ 1.426 อังสตรอม และหมู่คาร์บอนิลเท่ากับ 1.251 อังสตรอม เมื่อหาค่าเฉลี่ยน้ำหนักออกคิวแพนซีของทั้งสองหมู่ จะได้ค่าความยาวพันธะของคาร์บอน-ออกซิเจน และมุมพันธะเป็น 1.361 อังสตรอมและ 341.18 องศา ตามลำดับ ตรงกับค่าที่แสดงความผิดปกติที่ได้จากกราฟการกระจาย คือ 1.33 อังสตรอม และ 343.1 องศา ของวิธีสหสัมพันธ์ของโครงสร้าง การพิสูจน์โครงสร้างที่ผิดปกตินี้ได้อาร์แฟคเตอร์ที่ 0.0563 ที่ความหนาแน่นของอิเล็กตรอน 0.22(3) ต่อลูกบาศก์อังสตรอม

ผลึกสารประกอบ 25-26-oxidofiedelan-1,3-dione ซึ่งสกัดได้จากต้นตะไคร้ (*Salacia Chinensis* Linn.) อยู่ในระบบผลึกโมโนคลินิก สเปซกรุ๊ป P_2 , สูตรโมเลกุล $C_{30}H_{46}O_3$, MW 454.67, $a = 7.6688(1) \text{ \AA}$, $b = 16.1829(2) \text{ \AA}$, $c = 10.7132(2) \text{ \AA}$, $\beta = 109.861(1)^\circ$, $V = 1250.46(3) \text{ \AA}^3$, $Z = 2$, และ $R_I = 0.042$ สำหรับ 2903 ของข้อมูลรังสีสะท้อน ที่อุณหภูมิ 150 เคลวิน โมเลกุลของสารในระบบของแข็งยึดเหนี่ยวกันโดยพันธะไฮโดรเจน ผ่านหมู่คาร์บอนิล ($C=O\cdots H$) และแรงระหว่างขั้วระหว่างหมู่คาร์บอนิลกับอีเทอร์ ($>C(\delta^+)\cdots O(\delta^-)$)

สาขาวิชาเคมี

ปีการศึกษา 2546

ลายมือชื่อนักศึกษา

ลายมือชื่ออาจารย์ที่ปรึกษา

ลายมือชื่ออาจารย์ที่ปรึกษาร่วม

ลายมือชื่ออาจารย์ที่ปรึกษาร่วม

AUPHATHAM PHOTHIKANITH: SINGLE CRYSTAL X-RAY CHARACTERIZATION
AND STRUCTURE CORRELATION OF PENTACYCLIC FRIEDELANE RING SYSTEM
THESIS ADVISOR: ASSOCIATE PROFESSOR KENNETH J. HALLER,
Ph.D., 139 PP. ISBN 974-533-294-1

Structural studies of the five fused six-membered ring friedelane skeleton with structure correlation and single crystal x-ray analysis methods are presented. The correlation between the sum of angles about C3 and C3–O bond distances identified an anomalous of structure in the database. Structure correlation to examine the hybridization of carbon C3 in friedelane and oleanane triterpene structures revealed one anomalous compound in the structure database. Redetermination of the structure of the anomalous compound clearly demonstrates that the oxygen at C3 is disordered. The major component of the structure is epifriedelin-3-ol with a refined occupancy of 0.680(3). The minor component is friedelin-3-one, the only difference being the ketone at C3. The bond lengths of the disordered components are $d[\text{C–O}] = 1.426(5)$ and $d[\text{C=O}] = 1.251(6)$ Å, giving occupancy weighted averages of 1.370 Å and 341.4° for $d[\text{C–O}]$, nearly the same as the 1.33 Å and 343.1° values previously reported for the anomalous structure. Refinement converged with a conventional R_I of 0.0563 and the highest peak on the electron density difference map of $0.22(3) \text{ e } \text{Å}^{-3}$.

The crystal and molecular structure of 25,26-oxidofriedel-1,3-dione, isolated from *Salacia Chinensis* Linn is reported. The compound crystallizes in the monoclinic space group $P2_1$, $MW = 454.67$, $a = 7.6688(1)$ Å, $b = 16.1829(2)$ Å, $c = 10.7132(2)$ Å, $\beta = 109.861(1)^\circ$, $V = 1250.46(3)$ Å³, $T = 150$ K, and $Z = 2$, and refines to $R_I = 0.0412$ for 2903 reflections. The crystal

packing of the structure contains C–H···O hydrogen bonds and a previously undescribed supramolecular building block involving dipolar intermolecular contacts between the positive polarity carbon atom of a carbonyl group and the negative polarity oxygen atom of the ether linkage, C(δ^+)···O(δ^-). The new linkage has been characterized from the structure and data in the Cambridge Crystal Structure Database.

School of Chemistry

Student's Signature

Academic Year 2003

Advisor's Signature

Co-advisor's Signature

Co-advisor's Signature

Acknowledgments

I would like to express my sincerest gratitude to my advisor, Assoc. Prof. Dr. Kenneth J. Haller for his kindness to me during my study time at SUT. Without his supervision and patient help this thesis would not be successful.

I would also like to thank the Thai Government Scholarship, Secondary Education Quality Improvement Project, Ministry of Education for the scholarship for my study.

I would like to express my gratitude to all the teachers of the School of Chemistry for giving me good opportunity to study in the School of Chemistry. I wish to express my special thanks to the Head of the School of Chemistry, Asst. Prof. Dr. Malee Tangsathitkulchai also to Asst. Prof. Dr. Kunwadee Rangriwatananon, and Asst. Prof. Dr. James R. Ketudat-Cairns for their warm hearted support, encouragement, and help.

Thanks to Suranaree University of Technology for travel grants to support my attendance at the 25th and 26th Science and Technology of Thailand meetings in Phisanulok and Bangkok, Thailand and for partial support of the research (grant SUT1-102-41-36-07). Thanks to the Asian Crystallographic Association for a Bursary Award to support my attendance at AsCA'01, the 4th meeting of the Asian Crystallographic Association in Bangalore, India; unfortunately, due to illness I was unable to attend the meeting.

I would also like to thank the forester at Herbarium Hall, Department of Forestry for plant identification, the School of Chemistry, Rajabhat Institute of Nakhon Ratchasima for use of the separations laboratory to support this work. Thanks to Mr. Ed Fraser for assistance with the disordered friedelin data set, and Professors Ton Spec and

Martin Lutz at the University of Utrecht for collecting the data for 25,26-oxidofriedel-1,3-dione.

I would like to thank all my friends in our research group for their help and encouragement throughout my study time at SUT.

Finally, I would like to express my deepest appreciation and sincere gratitude to my family for their love, devotion, understanding, consolation, and encouragement for my success in my studies.

Auphatham Phothikanith

Contents

	Page
Abstract in Thai	I
Abstract in English	II
Acknowledgements	IV
Contents	V
List of Tables	IX
List of Figures	XI
List of Abbreviations	XIII
Chapters	
I Introduction	1
II Theory	14
2.1 X-ray Crystallography.....	14
2.2 Structure Correlation.....	32
III Experiment	39
3.1 Structure Correlation.....	39
3.2 Isolation.....	42
3.3 Single Crystal X-ray Crystallography.....	43
IV X-ray Structural Characterization of Disordered Epifriedelin-3-ol and Friedelin-3-one	45
4.1 Introduction.....	45

Contents (Continued)

	Page
4.2 Experimental.....	47
4.3 Results and Discussion.....	51
4.4 Conclusion.....	67
V 25,26-Oxidofriedalan-1,3-dione.....	68
5.1 Introduction.....	68
5.2 Experimental.....	73
5.3 Results and Discussion.....	75
5.4 The Geometry of the Carbonyl Ether Intermolecular Interaction.....	85
5.5 Conclusion.....	88
VI Conclusions.....	89
6.1 Conclusions.....	89
6.2 Suggestions for Further Study.....	91
References.....	92
Appendices.....	101
Appendix A Search of the Cambridge Structure Database	102
Appendix B1 Scatterplot Type 1.....	109
Appendix B2 Scatterplot Type 2.....	125
Appendix B3 Scatterplot Type 3.....	128
Appendix C Least-Squares Mean Planes.....	131
Appendix D Isolation Study.....	137
Curriculum Vitae.....	139

List of Tables

Table	page
1.1 The Character of R–H···O=C Hydrogen Bonds.....	12
2.1 Crystal Systems.....	15
3.1 The Compounds for Structure Correlation.....	41
4.1 Crystal Data and Structure Refinement Details.....	49
4.2 The Compounds for Structure Correlation	51
4.3 Crystal Data for the Different Friedelin Structures.....	52
4.4 Fractional Monoclinic Coordinates and Isotropic Atomic Displacement Parameters for the Nonhydrogen Atoms.....	55
4.5 Fractional Monoclinic Coordinates and Isotropic Atomic Displacement Parameters for the Hydrogen Atoms.....	56
4.6 Anisotropic Atomic Displacement Parameters	58
4.7 Selected Torsional Angles.....	59
4.8 Selected Interatomic Distances.....	61
4.9 Selected Bond Angles.....	62
4.10 Least-Squares Mean Planes and Atomic Deviations from the Planes.....	63
4.11 Torsion Angles Across Ring Junctions	65
5.1 Experimental Details for 25,26-oxidofriedel-1,3-dione.....	74

List of Tables (Continued)

Table		page
5.2	Fractional Monoclinic Coordinates and Equivalent Isotropic Displacement Parameters	76
5.3	Selected Bond Distances for 25,26-oxidofriedel-1,3-dione.....	78
5.4	Selected Bond Angles for 25,26-oxidofriedel-1,3-dione.....	78
5.5	Least-Squares Mean Planes for 25,26-oxidofriedel-1,3-dione.....	81
5.6	The Characteristics of C–H···O Weak Hydrogen Bonds at O3.....	82

List of Figures

Figure	page
1.1 The five fused six-membered ring search fragment.....	3
1.2 Structure diagrams of triterpenes containing the search fragment.....	4
1.3 Structures of friedelin and derivatives.....	5
1.4 Carbonyl and ethereal acceptor motifs of C–H···O interactions.....	10
1.5 Geometry of C–H···O hydrogen bonds.....	11
1.6 The geometries of carbonyl-carbonyl interaction.....	13
2.1 Bravais lattices.....	16
2.2 Different sets of planes in a two dimensional lattice.....	18
2.3 The incident and reflected beams relative to the planes.....	20
2.4 A diffraction pattern.....	22
2.5 The relationship between crystal and reciprocal lattices.....	23
2.6 The relationship between atomic scattering factors and $\sin \theta/\lambda$	26
2.7 In plane bonding orbitals of regular hexagon.....	35
2.8 Out-of-plane deformations.....	35
4.1 Scatterplot of the sum of bond angles about C(3) versus C(3)–O bond distances.....	54
4.2 Ring A fragment with oxygen bound to sp^2 and sp^3 carbon at C3.....	54
4.3 Distribution of oxygen atoms related to sp^2 and sp^3 hybridization.....	55
4.4 The structure of disordered epifriedelin-3-ol and friedelin-3-one.....	60

List of Figures (Continued)

Figure	page
5.1 Carbonyl and ethereal acceptor motifs of C–H···O interactions.....	69
5.2 Geometry of the C–H···O hydrogen bond.....	70
5.3 The ideal geometries of carbonyl-carbonyl interactions.....	71
5.4 The structure of 25,26-oxidofriedel-1,3-dione	80
5.5 Perspective view showing the weak intermolecular C–H···O hydrogen bond at O3.....	82
5.6 Perspective view of the >C(δ^+)···O(δ^-) dipole-dipole interaction	83
5.7 The weak C–H···O hydrogen bonds and noncovalent >C(δ^+)···O(δ^-) carbonyl-ether dipole-dipole interaction in the 25,26-oxidofriedel-1,3-dione crystal structure.....	84
5.8 The geometric parameters of the carbonyl-ether dipole-dipole interaction.....	85
5.9 Histograms of the >C(δ^+)···O(δ^-) carbonyl-ether dipole-dipole interaction.....	87

List of Abbreviations

A, B	Values of $ F_{(hkl)} \cos \delta$ and $f_j \sin \delta$
A	A centered lattice
a, b, c	Unit cell vectors of the direct lattice
a, b, c	Unit cell axial lengths in direct space
a^*, b^*, c^*	Unit cell vectors of the reciprocal lattice
a^*, b^*, c^*	Unit cell axial lengths in reciprocal lattice
B	B centered lattice
B_{iso}	Isotropic vibration parameter
C	C centered lattice
d	Space between the lattice planes in crystal
F	F centered lattice
$ F_o , F_c $	Amplitude of observed and calculated structure factor
$F_{(hkl)}$	The structure factor
f	Atomic scattering factor
h, k, l	Miller indices to identify a family of planes or a reflection
I	I centered lattice
I	Intensity of light
P	Primitive lattice
psi	Pounds per square inch, unit of pressure
R	Primitive lattice for a rhombohedral crystal system

List of Abbreviations (Continued)

R_I	Conventional discrepancy index = $\frac{\sum (F_o - F_c)}{\sum F_o }$
(μ^2)	Mean square amplitude of atomic vibration
2θ	Angle between incident and diffracted x-ray beams
δ	Phase angle
α, β, γ	Angles between unit cell axes in direct space
$\alpha^*, \beta^*, \gamma^*$	Angles between unit cell axes in reciprocal space
λ	Wavelength of x-rays used in a given diffraction experiment
$\rho(xyz)$	Electron density

Chapter I

Introduction

Chemists have always been interested in the structure of molecules. The meaning of the word structure has changed as more and more sophisticated methods of looking at molecules have been developed. Among the first probes of molecules for the determination of their atomic compositions were molecular weight measurements and elemental analysis. With the help of spectrometers and diffractometers, chemists established the existence of chemical bonds holding atoms in a molecule and then indicating the positions of the atoms in three-dimensional space, *i.e.* stereochemistry. From the information about the spatial location of the atoms of a molecule it is natural to try to proceed to get the complete geometrical characterization of the molecule by calculating bond distances, bond angles, and torsion angles. Some molecules may have two or more conformations with similar, or even equal stability, and energy barriers between them small enough so that, even at room temperature, the molecule fluctuates among the possible conformations, which can lead to different reaction products. Structural information is essential in chemistry not only for determining the geometrical arrangement of atoms within a molecule or a crystal, but also because each structure may tell something about the electron distribution, the type and properties of bonds connecting the atoms in their potential energy minimum, and to some extent, about their reactivity.

Structure-reactivity relationships are often sensitive to very small differences in bond distance, even at the level of hundredths or thousandths of an Ångstrom. X-ray diffraction is one of very few techniques that is able to determine this information for virtually all atoms in the molecule and is now the most popular and reliable method of solid state structure analysis for all but the very smallest molecules. The analysis is carried out on crystalline solids, preferably, on single crystals. Nowadays, the structure determination of small and medium sized organic molecules, including biologically important polymers, is readily achieved. The number of structures determined by x-ray crystallography is such that computer-assisted systematic searches in the Cambridge Structure Database, presently containing more than 270,000 organic structures (CCDC, 2002), permits a new approach to structure analysis. Chemical information may be extracted from these data through extensive comparisons between large numbers of related molecules.

Generally the compounds have been divided into families. One can describe a family of molecules with a common fragment in terms of a modified incidence matrix. The incidence matrix contains the atoms and bonds, which are the same for all members of the family, and a number of variable substituents. The constant part of the matrix defines the fragment in terms of connectivity and perhaps chemical information (Burgi and Dunitz, 1994a). The structure parameters define a multidimensional coordinate axes of configuration space and each molecule or fragment is represented by a single point in this space, with coordinates corresponding to the values of its bond distances, bond angles, and torsion angles. The different fragment structures are represented by different points, and distances between these are taken as a measure of structural similarity where small distance corresponds to

high similarity (Domenicano and Hargittai, 1992). The comparisons between many structure parameters from many different molecules (all containing the same fragment) has been called structure correlation. Many examples including studies on hydrogen bonding in first row transition metal carbonyl complexes (Braga, Grepioni, Biradha, Pedireddi, and Desiraju, 1995; Paquette, Stepanian, Branan, Edmondson, Bauer, and Rogers, 1996) have been reported. In favorable cases structure correlation extends very far into configuration space and may even map a reaction coordinate or pathway from reactants to products (Burgi and Dunitz, 1994a).

Primarily natural products related to the polycyclic triterpene friedelane will be investigated in this study. Compounds of this family exhibiting antileukemic activity, (Lee and Nozaki, 1984) cytotoxicity, (Zheng, 1994) and antiviral activity (Chen, Shi, Kashiwada, Zhang, Hu, Jin, Nozaki, Kilkuskie, Tramontano, Cheng, McPhail, McPhail, and Lee, 1992) have been investigated. The fragment used to define the structure type is five fused six-member rings containing only carbon atoms connected by single bonds as shown in the skeletal diagram in Figure 1.1.

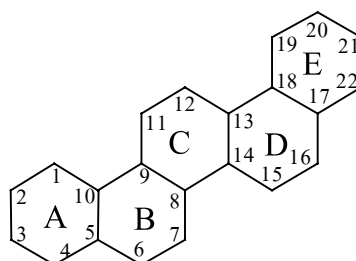


Figure 1.1. The five fused six-membered ring search fragment.

The conventional numbering scheme for this twenty-two atom polycyclic system is indicated on the diagram. The rings are assigned letters A through E for

convenience in comparison and discussion. Type compounds of four triterpenes with this five fused six-member ring system skeleton, but with different patterns of eight substituent groups are shown in Figure 1.2.

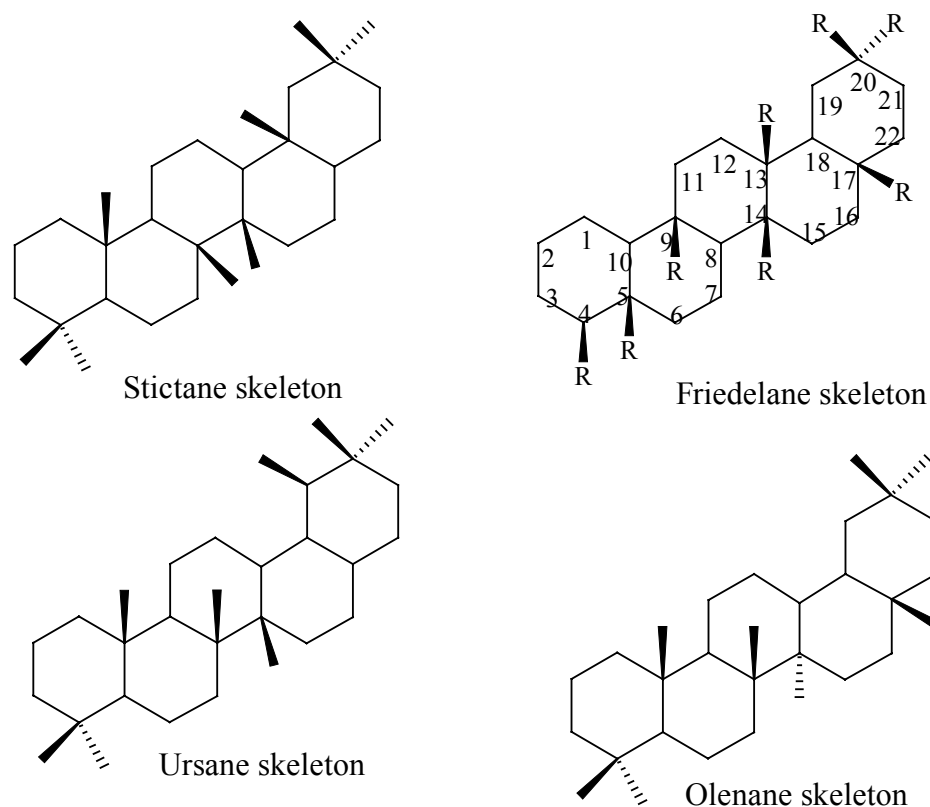
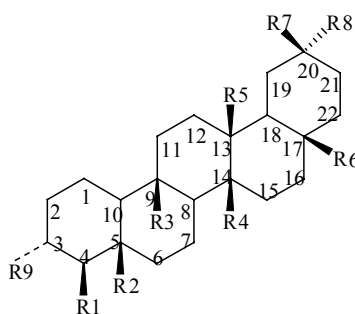


Figure 1.2. Structure diagrams of triterpenes containing the search fragment.

For consideration of the conformation of a saturated six-membered ring like cyclohexane, Pickett and Strauss (1970) suggested that the out-of-plane coordinates of motion relative to a planar regular hexagon describe a chair form, a boat form, and a twist form of cyclohexane. Dunitz and Waser (1972) established geometric constraints for six- and eight-membered rings. For six-membered rings they

considered rigid and flexible ring conformations that relate to the symmetry of the ring conformations. They indicated that with a given bond distance or rigid bond angle the six-membered ring exhibits chair forms and belongs to the nondegenerate vibration B_{2g} of the out-of-plane normal vibration of a regular hexagon. However, if the bond distances or bond angles of the six-membered ring are flexible the ring exhibits boat forms or twist forms and belongs to the degenerate E_{2u} out-of-plane vibration. Consideration of the conformation of six-membered rings out-of-plane coordinates and torsion angles are natural for x-ray analysis, and most helpful in characterizing fused ring systems.



	R1	R2	R3	R4	R5	R6	R7	R8	R9
1	Me	H	Me	Me	Me	Me	Me	Me	OC ₁₀
2	Me	Me	CH ₂ OR ₄	CH ₂ OR ₃	Me	Me	Me	Me	O
3	Me	Me	Me	Me	Me	Me	Me	Me	OAc
4	Me	Me	Me	Me	Me	Me	Me	Me	OH, H
5	Me	Me	Me	Me	Me	Me	Me	Me	O
6	Me	Me	Me	CH ₂ OH	Me	Me	Me	Me	O
7	Me	Me	Me	Me	Me	COOMe	Me	Me	O
8	Me	CH ₂ OR ₉	Me	Me	Me	Me	Me	COOH	OH, OR ₂
9	Me, CH ₂ R ₂	CH ₂ R ₁	Me	Me	Me	Me	Me	Me	O
10	Me	Me	Me	Me	Me	CH ₂ OH	CH ₂ OH	Me	O
11	Me	Me	Me	Me	Me	OOH	Me	Me	O
12	Me	Me	Me	Me	COOH	Me	Me	Me	OH, H
13	Me	Me	Me	Me	Me	CH ₂ OH	Me	Me	O
14	Me	Me	Me	Me	Me	Me	COOMe	Me	O
15	Me	CH ₂ OR ₉	Me	Me	Me	Me	Me	COOH	OH, OR ₂

Figure 1.3. Structures of friedelin and derivatives.

Several structures of friedelane type triterpenes have been previously determined by single crystal x-ray structural analysis and/or NMR spectroscopy. Masaki, Niwa, and Kikuchi (1975) suggested two possible conformations of the five fused six-membered ring skeletons of friedelane triterpene by interpretation of NMR spectroscopic results from pachysandiol derivatives. First, the chair-chair-chair-boat-boat for the five rings A through E, respectively, giving a system they called the stretched conformation and denoted as the S form. Second, the all chair for the five rings, giving a system they called the folded conformation and denoted as the F form.

White, Fayos, and Clardy (1973), and later Mo (1977), studied the structure of campanulin(1)^{n¹³} in which ring A has an additional cyclic component, an epoxy bridge between C3 and C10. Additional cyclic linkages such as this will obviously affect the stereochemistry of the ring skeleton.

Rogers, Williams, Joshi, Kamat, and Viswanathan (1974) studied the structure of 2,2-dibromo-25,26-oxido-friedel-1,3-dione(2) and found that the conformation of the five ring system was the S form. This structure, as well as most of the other older single crystal results, includes substituents containing a heavy atom such as bromine. The bromine atoms were deliberately added, and were generally necessary to obtain a structure solution in the days prior to the advent of powerful direct methods techniques that enable routine solution of light atom structures. However, one must proceed with caution when doing ring stereochemical analysis since the two heavy atom substituents are two bromine atoms on C2, positions normally occupied by hydrogen atoms. Masaki, Niwa, and Kikuchi (1975) confirmed the S form for

^{n¹³} The number in parentheses corresponds to the numbered entry in Figure 1.3 giving the ring substituents. This notation is used throughout Chapter I.

friedelane type triterpenes with the x-ray structure determination of 3-O-acetyl-16-O-p-bromo-benzoylpachysandiol(3). In this case the heavy atom substituent is the bromine containing $-\text{OCO}-\text{C}_6\text{H}_4\text{Br}$ connected to C16, occupying the β position. The substituent is in the axial position to relieve steric effects of the normal friedelin substituent groups at C13 and C17. In addition to the intramolecular steric effects, the molecular packing often occasions $\text{C}-\text{H}\cdots\text{O}$ hydrogen bond contacts, as for example those at O2 and O4 to the heavy atom substituent phenyl ring in this structure with nonbond distances of 3.40 and 3.08 Å, respectively, and a $\text{C}-\text{H}\cdots\text{O}$ bond angle of 131° .

Laing, Burke-Laing, Bartho, and Weeks (1977) studied the structure of epifriedelinol(4) and concluded the S form is the favored lower energy solid state conformation of the friedelane skeletons. Additional support for the S form comes from the study of diketo-friedelane skeletons in the structures of prionastemmadione(5) (Monache, Marini-Bettolo, Pomponi, de Mello, King, and Thomson, 1979), 26-methoxy-friedelan-1,3-dione(6) (Rogers, Phillips, Joshi, and Viswanathan, 1980), 29-hydroxyfriedelan-3-one acetate(7) (Betancor, Freire, Gonzalez, Salazar, Pascard and Prange, 1980), (2R,3R,4R,5S,8S,9R,10S,13S,14R,17R,20R)-2,24-dihydroxy-3-oxofriedelan-29-oic acid hemiketal monohydrate(8) containing strong hydrogen bonds at $\text{O}2\text{H}\cdots\text{O}4$ with distance 2.66 Å and with the hydrate water molecule (Gonzalez, Fraga, Gonzalez, Gonzalez, Ravelo, Ferro, Dominquez, Martinez, Perales, and Fayos, 1983) and $5\beta,24$ -cyclofriedelan-3-one (Connolly, Freer, Anjaneyulu, Ravi, and Sambasivarao, 1986).

Prakash, Roy, Grag, and Bhakuni (1987) studied structures of nine friedelan-7-one derivatives by ^{13}C NMR and found both the D and E rings to be in boat conformations.

Nozaki, Suzuki, Lee, and McPhail (1982) studied the structures of maytenfolic acid and maytenfoliol. Maytenfoliol(10) is in the S form while maytenfolic acid, which belongs to the oleanane class is in the F form, similar to the structure of maytensifolin-A(11) that belongs to the friedelane skeleton system (Lee, Nozaki, and McPhail, 1984). Tanaka, Matsunaga, and Ishida (1988) revised the structure of 3β -hydroxy-D:A-friedo-oleanan-27-oic acid(12) finding coexistence of the S and F forms, apparently to relieve strains of the α -side and β -side interactions arising from a C27 carbonyl group. Subramanian, Selladurai, Sivakumar, Ponnuswamy, and Sukumar (1989) studied the structure of 28-hydroxyfriedelan-3-one(13) and found rings A, B and C are chair forms while rings D and E are twist boat and distorted chair forms respectively. The molecular packing is due to van der Waals forces.

Mo, Winther, and Scrimgeour (1989) studied the conformation of friedelane skeletons with accurate single crystal x-ray analysis and force-field calculation methods on friedelin-3-one(5). They found that for x-ray analysis the S forms are more favored while force-field calculations suggest F forms to be lower in energy than S forms by about 3.85 kJ mol^{-1} . This implies that the conformation of friedelane skeletons depends on two factors; one, intermolecular forces, and two, the change in substitution. The molecular packing has the relatively weak intermolecular force associated with $\text{O}\cdots\text{C3}$ at $3.17(1) \text{ \AA}$ and van der Waals interactions. In any event the results are not contradictory as it has long been known that crystal lattice stabilization

energies can be several kJ mol^{-1} . Cota, Mascarenhas, Silva, and de Souza (1990) found the structure of methyl 3-oxofriedelan-20 α -oate(14) to be in the F form, but Chen, Shi, Kashiwada, Zhang, Hu, Jin, Nozaki, Kilkuskie, Tramontano, Cheng, McPhail, McPhail, and Lee (1992) studied salaspermic acid(15), an inhibitor of HIV reverse transcriptase and HIV replication in H9 lymphocyte cells, and confirmed the S forms to be more favored for friedelane skeletons in the solid state.

Generally molecular packing of organic compounds are held together by attractive electrostatic forces based on charge localization in the molecule, the strongest of which are the hydrogen bonds, and/or van der Waals interactions, also called dispersion bonds. van der Waals interactions occur when equal atoms are in contact and induced dipoles interact to give small short-term attractive forces.

Most organic molecules have hydrogen bond donor sites and hydrogen bond acceptor sites of varying strengths on the different parts of the molecule. These donor and acceptor sites bind to each other as $\text{D-H}\cdots\text{A-X}$ (D = donor, A = acceptor, X = atom bonded to acceptor) when a crystal is formed, thereby stabilizing the solid phase. The criteria for classifying hydrogen bonds are distance and directionality (Steed and Atwood, 2000). Strong hydrogen bonds, those with energies of about 20-40 kJ mol^{-1} , (*e.g.* $\text{O-H}\cdots\text{O}$, $\text{N-H}\cdots\text{O}$, and $\text{O-H}\cdots\text{N}$) have $\text{H}\cdots\text{A}$ distances of about 1.60-1.80 Å and $\text{D-H}\cdots\text{A}$ angles close to 180°. Weak hydrogen bonds (*e.g.* $\text{C-H}\cdots\text{O}$, $\text{C-H}\cdots\text{N}$, and $\text{C-H}\cdots\text{Cl}$) were established unambiguously by Taylor and Kennard (1982) by using structure correlation based on the wealth of structures in the Cambridge Structure Database. There is of course a near continuum of hydrogen bond strengths going through intermediate strength to the weak hydrogen bonds. Near the

lower energy limit are the nontraditional hydrogen bonds, such as $\text{O-H}\cdots\pi$ and $\text{C-H}\cdots\pi$ with energies as low as $1\text{-}2\text{ kJ mol}^{-1}$. Several other weak interactions, such as the $\text{Cl}\cdots\text{Cl}$ interaction (Sarma and Desiraju, 1986) have also been established, especially through the work of Desiraju and his coworkers.

The weak hydrogen bonds, especially the $\text{C-H}\cdots\text{O}$ bonds are necessary in understanding the molecular packing of crystalline natural products. A nice review of early crystal engineering work with $\text{C-H}\cdots\text{O}$ hydrogen bonds and a methodology for considering their interaction in the crystal in terms of two alternative motifs was given by Sarma and Desiraju (1986). They suggested the interaction may be considered and characterized by either $\text{C}\cdots\text{O}$, (D), or $\text{H}\cdots\text{O}$, (d), distance as shown in Figure 1.4.

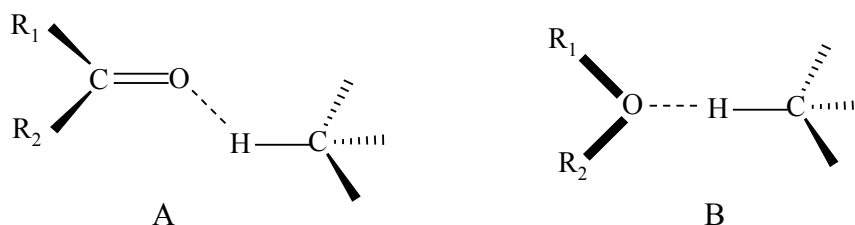


Figure 1.4. Carbonyl (A) and ethereal (B) acceptor motifs of $\text{C-H}\cdots\text{O}$ interactions.

For carbonyl and ethereal acceptors the $\text{C-H}\cdots\text{O}$ contact tends to lie in the plane defined by the oxygen atom and its lone pairs and to be between the hydrogen atom and an oxygen lone pair. This has the effect of making the $\text{H}\cdots\text{O}=\text{C}$ angle in a carbonyl interaction close to 120° (sp^2 oxygen) with the hydrogen atom in the plane of the $\text{O}=\text{C}(\text{R}_1)\text{R}_2$, and making the $\text{H}\cdots\text{O}-\text{C}(\text{R}_1)\text{R}_2$ angle in an ether interaction nearer

the tetrahedral value (sp^3 oxygen) with the hydrogen atom tending to lie in the plane bisecting the R_1OR_2 angle.

Desiraju (1991) elucidated the significance of the carbonyl $C-H\cdots O$ hydrogen bond in organic crystals when he considered $C-H\cdots O$ lengths and angles in conjunction with spectroscopic data. The $C-H\cdots O$ interaction geometry was characterized with $C-H\cdots O$ lengths and angles as θ and ϕ as shown in Figure 1.5. The value of D was dependent on the acidity of the hydrogen atom with $3.0 \text{ \AA} < D < 4.0 \text{ \AA}$ as common values for weak hydrogen bonds. The $C-H\cdots O$ angles (θ) cluster in the range $150\text{-}160^\circ$ with longer length correlating with more linear values and the $C=O\cdots H$ generally around 120° .

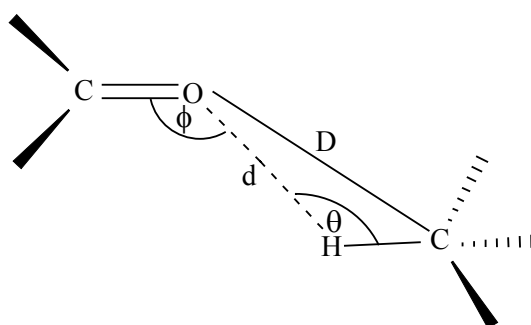


Figure 1.5. Geometry of $C-H\cdots O$ hydrogen bonds.

Steiner and Desiraju (1998) described the fundamental difference between the $C-H\cdots O$ hydrogen bond and the van der Waals interaction in terms of the different length and angle directionality characteristics of the interactions. The contact of $R-H\cdots O=C$ depends on the acidity of the R groups as given in Table 1.1.

Table 1.1. The Character of R–H···O=C Hydrogen Bonds.

Contact type	mean H···O (Å)	mean R···O (Å)	mean >C–O···H (°)
C(sp ³)–O–H···O=C	2.36(4)	3.31(2)	152(2)
C≡C–H···O=C	2.67(1)	3.56(2)	143(1)
C=CH ₂ –H···O=C	2.761(6)	3.590(7)	137.1(7)

Burgi, Dunitz, and Shefter (1974) established the short O=C···O contacts in crystals with structure correlation. They found that for O=C···O distances shorter than 3 Å the carbon is displaced from the plane of the carbonyl group towards the nearby oxygen atom and the O=C···O angle lies in the range 100-110°. Allen, Baalham, Lommerse, and Raithby (1998) indicated geometries and attractive energies of carbonyl-carbonyl interactions (not hydrogen bonds) by using a combination of systematic crystallographic database analysis and high level *ab initio* molecular orbital calculations. Three motifs of these interactions, the perpendicular motif, the parallel motif, and the anti-parallel motif, shown in Figure 1.6 were considered. They examined all motifs for which the C···O contact distance was less than 3.6 Å. The attractive energy less than 20 kJ mol⁻¹ indicated these are medium strength C···O interactions.

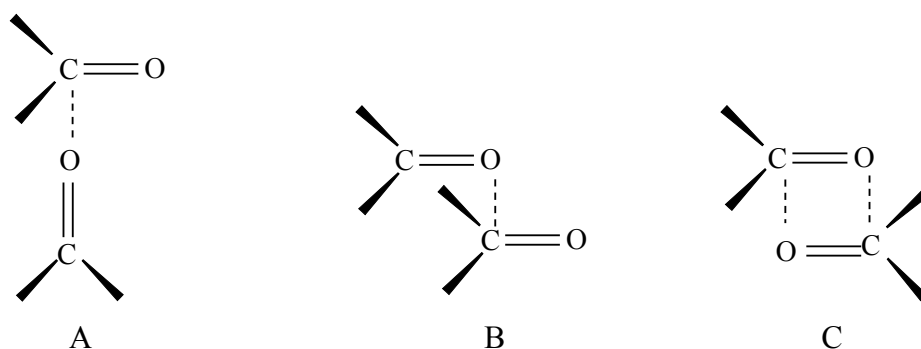


Figure 1.6. The geometries of carbonyl-carbonyl interaction.

The anti-parallel motif involves two short $C\cdots O$ interactions and is the most common of three, while the perpendicular motif and the parallel motif both involve a single short $C\cdots O$ interaction. Assuming a perfect rectangular anti-parallel dimer having both $d(C\cdots O) = 3.02 \text{ \AA}$ gave an attractive energy of $-22.3 \text{ kJ mol}^{-1}$ and attractive energies less than -20 kJ mol^{-1} over the $d(C\cdots O)$ range $2.92\text{-}3.32 \text{ \AA}$. Intermolecular perturbation theory calculation gave an attractive interaction energy of -7.6 kJ mol^{-1} for the single $d(C\cdots O)$, again at 3.02 \AA , in the perpendicular motif. They established the importance of dipolar interactions between carbonyl groups in stabilizing the packing modes of small organic molecules and confirmed that the contribution of these interactions to supramolecular recognition processes is comparable to that of medium-strength hydrogen bonds.

Chapter II

Theory

2.1 X-Ray Crystallography

X-ray crystallography is the most powerful method for the structure analysis of solids. The advent of modern high speed computers, automated diffractometers, area detectors, and powerful structure solution programs has contributed to x-ray diffraction becoming widely accepted as a necessary standard technique. An x-ray diffraction experiment may be carried out in as little as a few hours or may take several days depending on the experimental conditions and the information desired.

Crystals

The characteristic of the crystalline state is that it is composed of atoms, ions, or molecules which have a regular arrangement in three dimensions to give a highly ordered structure that is usually bounded by flat faces which intersect at straight edges. Crystals may be regarded as being built up by the continuing three dimensional translational repetition of some basic structure pattern called the *unit cell*, which may contain one or more atoms, a molecule, or a complex assembly of molecules. If each unit cell is replaced by a point, the result is a regular three-dimensional arrangement of points that leads to a *crystal lattice*. This array of identical points, equivalent to each other by translation is a type of symmetry, which occurs in all crystalline solids, whether or not they also show other forms of symmetry such as rotation or reflection.

In three dimensions the unit cell has three sides or edges called a , b , and c and three angles α , β , and γ arranged such that α lies between the b and c axes, β lies between the a and c axes and γ lies between the a and b axes. If the crystal contains rotation or reflection symmetry relating molecules or parts of molecules to each other, there are restrictions, in addition to those from the lattice and unit cell, imposed on the geometry. For example a square unit cell with two equal sides and a 90 degree angle is required for a two dimensional lattice pattern that includes four-fold rotation symmetry in the unit cell. Reflection symmetry gives a 90 degree angle but still allows the two sides to be of different lengths. In the absence of any rotation and reflection symmetry the three axes may have different lengths and the three angles may be different from each other and from 90 degrees. On the basis of these rotation and reflection restrictions, crystal symmetry is broadly divided into seven types, called the seven *crystal systems*. The names, minimum symmetry, and unit cell geometries are shown in Table 2.1 and the fourteen Bravais lattices in Figure 2.1.

Table 2.1. Crystal Systems.

Crystal system	Minimum symmetry of a crystal	restrictions on unit cell
Triclinic	none	none
Monoclinic	two-fold axis parallel to b	$\alpha = \gamma = 90^\circ$
Orthorhombic	three mutually perpendicular two-fold axes	$\alpha = \beta = \gamma = 90^\circ$
Tetragonal	four-fold axis parallel to c	$a = b$; $\alpha = \beta = \gamma = 90^\circ$
90°Trigonal/Rhombohedral	three-fold axis parallel to $(a+b+c)$	$a = b = c$; $\alpha = \beta = \gamma \neq 90^\circ$
Hexagonal	six-fold axis parallel to c	$a = b$; $\alpha = \beta = 90^\circ$; $\gamma = 120^\circ$
Cubic	three-fold axes along the cube diagonals	$a = b = c$; $\alpha = \beta = \gamma = 90^\circ$

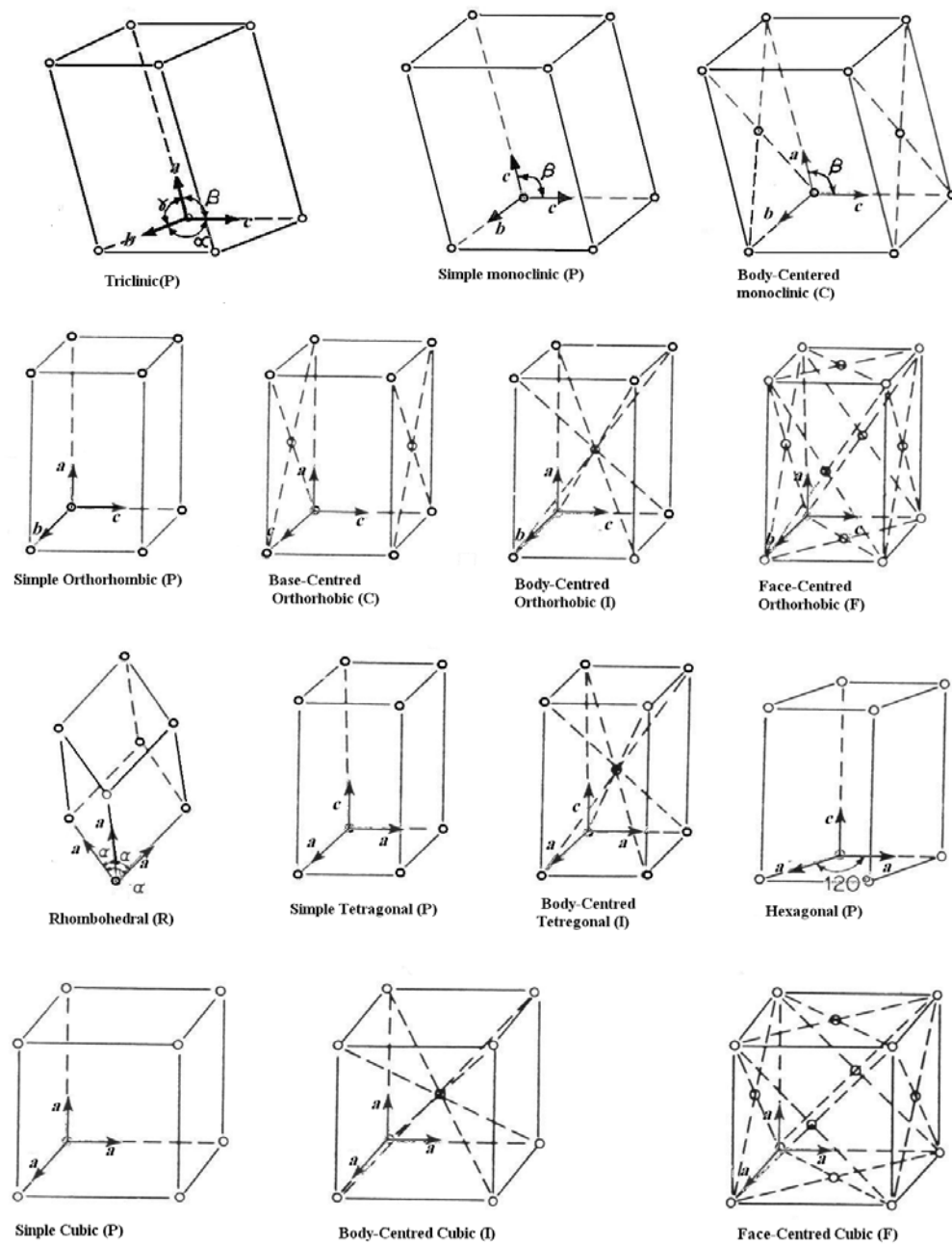


Figure 2.1. Bravais lattices (redrawn after Douglas, McDaniel, and Alexander, 1993).

The crystal can have other types of symmetry elements in which rotation or reflection is combined with translation to give *screw axes* and *glide planes*. A screw

axis involves rotation about an axis through an angle. $2\pi/n$, followed by a translation parallel to the axis. If the translation equals m/n of the identity period along the axis, where m is an integer less than n , then repetition of this operation n times is equivalent to a translation along m periods. In the Hermann-Mauguin notation, a screw axis is symbolized by n_m , e.g. 2_1 corresponds to rotation through $2\pi/2=180^\circ$, followed by a translation of one-half of one lattice translation. A glide plane involves reflection across a plane followed by translation parallel to the plane by a distance equal to one-half of one lattice translation. In the Hermann-Mauguin notation, a glide plane is symbolized by a , b , or c if the translation element is parallel to a crystal axis or n if it is parallel to a face diagonal or d if the lattice translation involved corresponds to a body centering of the unit cell. The presence of these additional symmetry elements leads to the standard compilation of 17 plane groups and 230 space groups as contained in Volume A of the *International Tables for X-ray Crystallography* (Hahn, 1992). It is necessary to consider sets of parallel lattice planes constructed so that for any given set every lattice point lies on some member of the set of planes. Constructions showing some examples of such planes in a two dimensional lattice are shown in Figure 2.2.

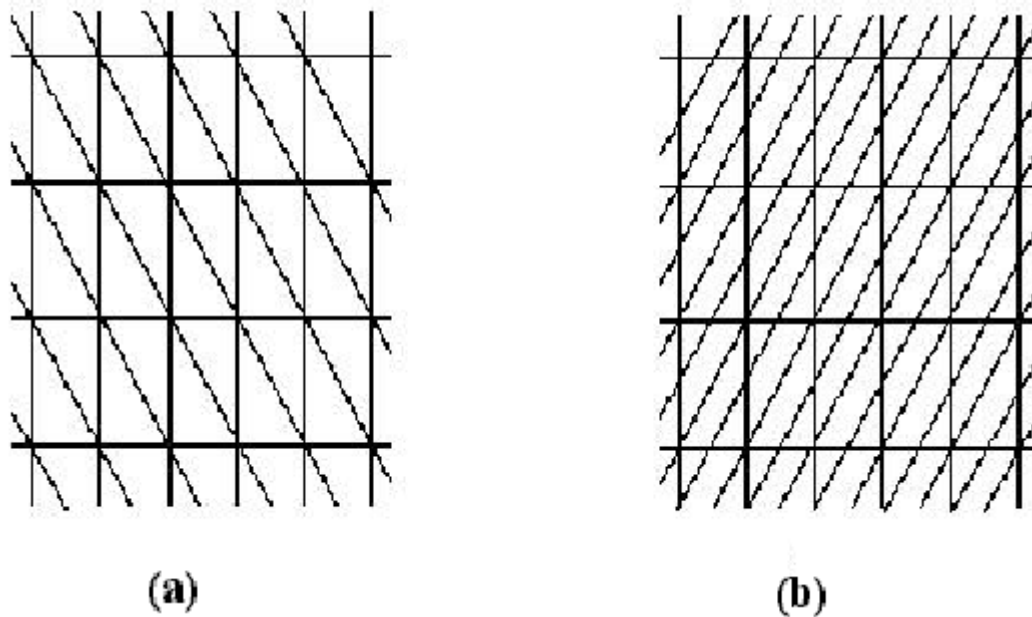


Figure 2.2. Different sets of planes in a two dimensional lattice.

These sets of planes are identified by three numbers in the three dimensional case, one corresponding to each axis. It follows from the repetitive nature of the lattice that when such planes cut at the edge of the unit cell the edge is always divided into an integral number of equal parts. These are common fractions of the unit translation; $1/1$, $1/2$, ..., $1/n$. The fraction intercepts on the three unit cell axes are used as the basis for a triple of numbers known as indices, the indices that uniquely characterize each possible set of planes. These indices are obtained by considering some lattice point as the origin and proceeding from it along the axes until the first number of a set of planes is reached. When the intercepts of the plane on the axes are expressed as fractions of the unit cell edge, their reciprocals are just the desired indices, such that a plane that has intercepts $\frac{1}{2}$, $\frac{1}{2}$, 1 on the x, y, and z axes then has

indices (2,2,1). By convenience in x-ray diffraction the set of lattice planes is assigned the symbol (h,k,l) and the numbers h , k , and l are called Miller indices.

Diffraction of X-rays by Molecules and Crystals

Many spectroscopic techniques measure the variation of intensity of radiation passing through the sample as its frequency (or wavelength) is varied, thus involving processes of differing energy in the sample. In x-ray crystallography we usually keep the wavelength fixed and measure the variation of intensity with direction, *i.e.* the scattering of monochromatic radiation is measured. The intensity variation is caused by interference effects, also known as diffraction. In other words, when electromagnetic radiation passes through matter the electrons are made to oscillate with the rapidly oscillating electric field and are set into oscillation about their nuclei with a frequency identical to the incident radiation. Thus each electron in the medium acts as a source of radiation that travels outward with a spherical wave front. A convenient and conceptually easy way to describe diffraction of x-rays from crystals is to consider that diffracted beams are reflected from planes in the crystal lattice analogous to the reflection of light waves from a mirror. Bragg's law gives the mathematical expression used to describe how x-rays interact with crystals to produce a diffraction pattern;

$$n\lambda = 2d \sin \theta$$

where n is an integer, λ is the wavelength of the radiation, d is the perpendicular spacing between adjacent planes in the crystal lattice, and θ is the angle of incidence and reflection of the x-ray beam as show in Figure 2.3.

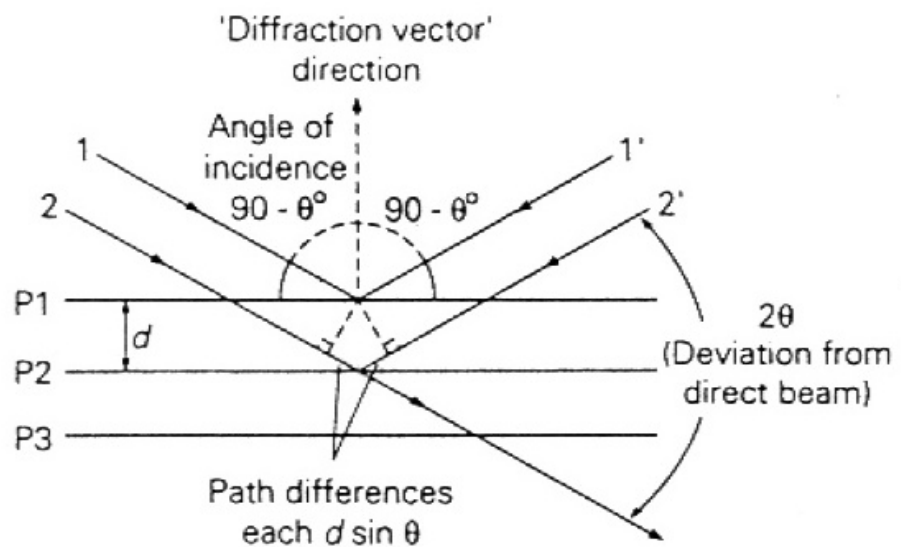


Figure 2.3. The incident and reflected beams relative to the planes.

The electromagnetic beams 1 and 2 strike planes P1 and P2 at points A and B, respectively, making the angle θ . For a diffracted intensity to occur, it is necessary for the reflected beams (1' and 2') from points A and B to exhibit constructive interference (be in phase), which occurs when the path lengths traveled are an integral multiple of the wavelength, $n\lambda$, that must be equal $2d(\sin\theta)$. In other words for diffraction by a three-dimensional lattice there are three equations, corresponding to the lattice plane equations, that all have to be satisfied simultaneously. The first equation contains the lattice spacing along the a direction with angles relative to the a

axis of the unit cell, and an integer h . The other two equations, correspondingly, involve the unit cell axes b and c and integers k and l , respectively. The Bragg equation can be rewritten into this form as

$$n\lambda = 2d_{hkl} \sin \theta$$

In practice the value of n can always be set to 1 by considering planes with smaller spacing ($n = 2$ for planes hkl is equivalent to $n = 1$ for planes $2h, 2k, 2l$ which have exactly half the spacing) giving Bragg's law in the form

$$\lambda = 2d_{hkl} \sin \theta$$

Thus, Bragg's law allows each diffracted beam to be uniquely labeled with its three indices, and for its net scattering angle (2θ from the direct beam direction) to be calculated from the unit cell geometry, of which each d_{hkl} spacing is a function.

$$\sin \theta = (\lambda/2)(1/d_{hkl})$$

The distance of each spot from the center of an x-ray diffraction pattern is proportional to $\sin \theta$ and hence to $1/d_{hkl}$ for some set of lattice planes. This demonstrates mathematically the reciprocal nature of the geometrical relationship between the crystal lattice and its diffraction pattern, already seen pictorially.

An example of a single layer of an x-ray diffraction pattern is given in Figure 2.4. There are three properties of interest in the x-ray diffraction pattern which correspond to three properties of the crystal structure. First, the pattern has a particular geometry. The intensity spots lie in certain positions which are clearly not random. The pattern geometry is related to the lattice and unit cell of the crystal structure and tell us the repeat distances of the unit cells and the directions of the unit

cell axes. Second, the pattern has symmetry, not only in the regular arrangement of the spots but also in the equal intensities of spots which lie in symmetry related positions relative to the center of the pattern. The pattern symmetry is closely related to the symmetry of the crystal system and space group. Third, apart from this symmetry, there is no apparent relationship among the intensities of the individual spots, which vary widely; some are very intense, while others are too weak to be seen. These intensities hold all the available information about the positions of the atoms in the unit cell of the crystal structure, because it is the relative atomic positions, which, through the combination of their individual interactions with the x-rays, generate different amplitudes for different directions of scattering.

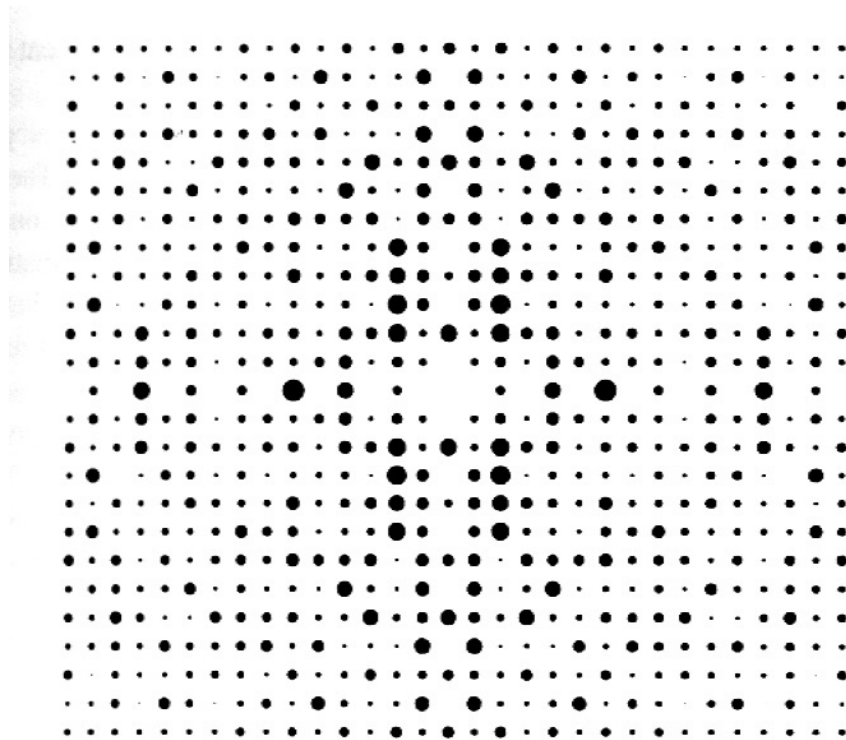


Figure 2.4. A diffraction pattern (redrawn after Clegg, 1998).

As a result, structures having large d -spacing exhibit compressed diffraction patterns and structures with small d -spacing show expanded patterns. It would be more convenient to express a direct relationship between $\sin\theta$ and d -spacing. This is accomplished by construction of a reciprocal lattice in which $1/d$ is directly proportional to $\sin\theta$. The reciprocal lattice can be defined as follows, consider normals to all possible direct lattice planes (h, k, l) to radiate from some lattice point taken as the origin. Terminate each normal at a point at a distance $1/d_{hkl}$ from the origin, where d_{hkl} is the perpendicular distance between planes of set (hkl). The set of points so determined constitutes the reciprocal lattice. Reciprocal lengths and angles are designated by an asterisk appended to the corresponding direct space (crystal lattice) symbols, thus, a^* , b^* , and c^* play the same role in the reciprocal lattice as a , b , and c do in the direct lattice, and α^* , β^* , and γ^* play the same role in the reciprocal lattice as α , β , and γ do in the direct lattice.

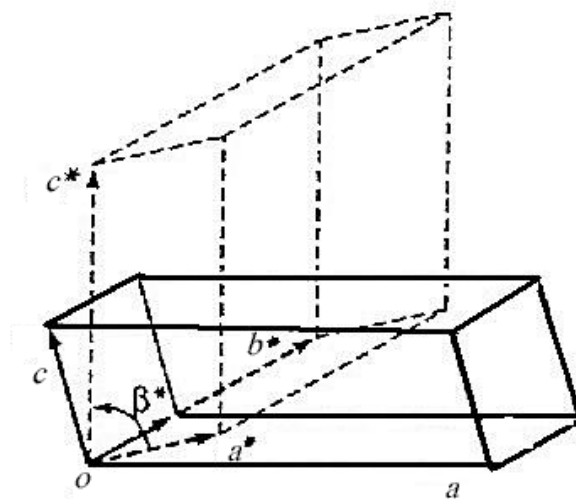


Figure 2.5. The relationship between crystal and reciprocal lattices (redrawn after Glusker and Tureblood, 1985).

The diffraction pattern or x-ray data collected from a single crystal yields an intensity, Miller indices, and the diffraction angle 2θ for each reflection. The intensity of the reflection depends on the nature and arrangement of the atoms in the unit cell and 2θ is dependent only on the dimensions of the crystal lattice. For reflection to occur, Bragg's law must be satisfied, but it must be recognized that atoms are not usually arranged in a unit cell such that all atoms lie directly on lattice planes. The reflections observed are composed of the sum of waves scattered from different atoms at different positions in the unit cell. All atoms (actually, all electrons) contribute to the intensities of all reflections. Superposition of waves is the method of combining different waves to generate the resultant wave observed as the reflection or hkl . The intensity of the reflection is proportional to the square of the amplitude of the diffracted wave (the reflection). Consider a wave with amplitude f and phase angle δ expressed in terms of complex numbers as

$$f(\cos\delta + i\sin\delta) = A + iB$$

$$\delta = \tan^{-1}(B/A)$$

Then

$$|f| = (A^2 + B^2)^{1/2} = [(\sum f_i \cos\delta_i)^2 + (\sum f_i \sin\delta_i)^2]^{1/2}$$

For an atom f is known as the atomic scattering factor. At $2\theta=0$ all electron in atom scatter in phase, and the scattering power of an atom at this angle relative to the scattering power of a free electron, is just equal to the atomic number for neutral atoms.

For the scattering by a unit cell of a structure in which there is a diffraction maximum has a particular combination of amplitude and phase, known as the structure factor and symbolized as F or F_{hkl} for each reflection h, k, l .

$$A_{hkl} = \sum f_i \cos \delta_i$$

$$B_{hkl} = \sum f_i \sin \delta_i$$

$$F_{hkl} = A_{hkl} + iB_{hkl} = |F_{hkl}| \exp[i\delta_{hkl}]$$

In fact the scattering power of a given atom is a function of the atom type, number of electrons associated with the atom or ion or atomic number for a neutral atom, and $(\sin\theta)/\lambda$. The scattering amplitude of an atom is designated as the atomic scattering factor (f). At $2\theta = 0$ or $\sin\theta/\lambda = 0$ the scattering factor is equal to the number of electrons associated with the atom or ion. As $\sin\theta/\lambda$ increases the scattering amplitude falls off as the scattering of x-rays from different electrons in the atom becomes more and more out of phase as shown in Figure 2.6.

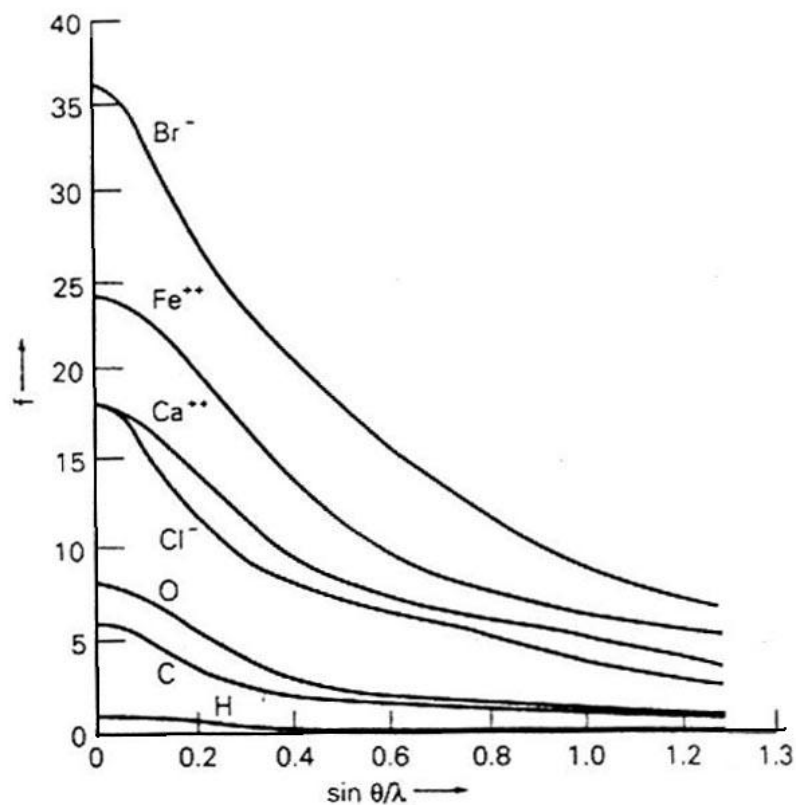


Figure 2.6. The relationship between atomic scattering factors and $\sin\theta/\lambda$ (redrawn after Stout and Jensen, 1989).

The scattering power of an atom is also affected by thermal motion or vibration (or any other phenomena that has the effect of spreading the electrons over a larger volume). Thermal motion causes the electron cloud to be more diffuse. This phenomenon is usually associated with factors such as temperature, how rigid the molecule is, or how rigidly the molecules are packed together in the crystal lattice. The expression of the scattering factor for a spherically (*i.e.*, isotropically) vibrating atom is,

$$|f| = |f_o| \exp\{-B(\sin^2\theta)/\lambda^2\}$$

where B is a temperature parameter related to the mean-square amplitude of vibration (μ^2) by $B = 8\pi^2\mu^2$, μ has unit \AA^2 and extra term has a value > 1 . For larger values of μ the curve falls off more rapidly with increasing Bragg angles.

The quantity measured in the laboratory is intensity rather than the structure factor. The structure factor is proportional to the observed intensity according to equation;

$$I = K|F|^2(Lp)(Abs)$$

K is an initially unknown scale factor (related to the number of scattering units in the crystal selected, the type of radiation, the relative numbers and types of atoms, and other factors; it is determined by refinement), L is the Lorentz factor (related to the geometry of the data collection), p is the polarization factor (related to the orientation of the crystal, the monochromator crystal, and other beam conditioning devices), and Abs is absorption (related to crystal shape, foreign material such as glue in the x-ray beam and other factors). The observed intensities or reflections can be converted into observed structure factors, $|F_{obs}|$ (generally called F observed). These quantities are used to calculate electron density maps from which atomic positions and ultimately the three-dimensional structure are determined (Stout and Jensen, 1989).

The diffraction pattern is the Fourier transform of the electron density. The number of electrons per unit volume or the electron density at any point x, y, z is represented by $\rho(xyz)$ and expressed as

$$\rho(xyz) = 1/V \sum_h \sum_k \sum_l |F_{hkl}| \cdot \exp[i\delta(hkl)] \cdot \exp[-2\pi i(hx+ky+lz)]$$

In practice when an x-ray diffraction pattern is obtained only the amplitudes $|I_{hkl}|$ of the diffraction maxima can be measured and the final exponential term can be calculated for the contribution of each reflection hkl to each position xyz , while the relative phase $[\delta_{(hkl)}]$ relationships are lost, this problem is called the phase problem.

The solution to this problem is finding a suitable trial structure. The term “trial structure” implies that the structure found first is only an approximation to the correct or true structure. The term “suitable” implies that the trial structure is close enough to the true structure that it can be smoothly refined to a good fit to the data set. The trial structure is in $\rho(xyz)$ terms so structure factors (F calculated) and phase angles (δ calculated) for the trial structure can be calculated. The calculated and observed structure factors can be compared.

Direct methods is one analytical technique for deriving an approximate set of phases from which a first approximation to the electron density map can be calculated. Direct methods makes use of the fact that the reflection intensities contain structural information and that the electron density in a real crystal is everywhere positive or zero, it cannot be negative. So the waves must be added together in such a way as to build up and concentrate positive regions of electron density and to cancel out negative regions. Since large numbers of reflections are involved in the complete Fourier transform calculation and then expressed in term probabilities that depend on the relative intensities, direct methods involves selecting the most important reflections (those which contribute most to the Fourier transform), working out the probable relationships among their phases, then trying different possible starting phases to see how well the probability relationships are satisfied. Approximation to

electron density maps can be calculated with the experimental observed values of $|F_o|$ and the calculated values of phase δ derived from the direct methods calculation. The amplitude and phases of the structure factor from this approximation to the structure will be, to some degree, incorrect, the errors increasing with the imperfection of the model as compared with the true structure.

If the trial structure is good enough the maps will be a reasonable representation of the correct electron density maps, and the structure can be refined to give a better fit of the observed structure factors $|F_o|$ and the calculated structure factors $|F_c|$. One commonly used measure for evaluating the correctness of the structure is the crystallographic discrepancy index or residual factor, R-factor (Hamilton, 1964), defined as

$$R = \frac{\sum (|F_o|) - (\sum |F_c|)}{\sum |F_o|}$$

The R-factor is at best a measure of the precision of the fit of the model to the experimental data obtained, not a measure of the accuracy. Some structures have a low R-factor but have been shown to be incorrect. For a correct and complete crystal structure determined from well measured data, R is typically around 0.02–0.07; for an initial model structure it is much higher, possibly as high as 0.4–0.5 depending on the fraction of electron density located in the initial trial structure. The decrease in the R-factor during the next stages in a measure of progress, *i.e.*, as additional atoms are added to the model, occupancies or atom types are adjusted, or numerical parameters describing the model structure are varied the value of the R-factor is the primary criterion to judge if the agreement between the diffraction pattern calculated from the model by a Fourier transform and the observed diffraction pattern is improved or if

one has produced the best agreement possible. The comparison of observed and calculated diffraction patterns is made entirely on their structure factors $|F_o|$ and $|F_c|$ or amplitudes $|F_o^2|$ and $|F_c^2|$. Changing any of the structure parameters modifies the model structure and thus affects the $|F_c|$ values, while the $|F_o|$ values remain fixed. The most common process for refining small molecule structures is least-squares refinement analysis, which defines the best parameters, corresponding to some assumed model of the structure, to be the result of the best fit of two sets of data, $|F_o|$ and $|F_c|$ (or $|F_o^2|$ and $|F_c^2|$), by minimizing the sum of weighted squares of the discrepancies between the observed and calculated structure factors or intensities:

$$\sum w(|F_o| - |F_c|)^2$$

or

$$\sum w(F_o^2 - F_c^2)^2$$

The structure parameters used in routine least squares refinement programs in the minimization process include an overall scale factor for the experimental observations, the atomic position parameters x , y , and z for each atom, and atomic displacement parameters (commonly called vibration parameters) for each atom. A single atomic displacement parameter can be used to define isotropic motion, or six atomic displacement parameters can be used to define anisotropic motion commonly seen in structure diagrams in the chemical literature. If disorder is present, occupancy factors varying from 0 to 1 may be refined for selected atoms, and perhaps correlated with occupancy factors of the other atoms. Thus in the simplest general case there may be as many as $9N+1$ or even a few more parameters to be defined for a structure with N independent atoms. More advanced refinement programs, such as RAELS

(Rae, 1996) include quite complicated group on group constructions to reduce or minimize the number of positional parameters, libration models to reduce the number of displacement parameters, and several advanced capabilities to aid modeling various nonroutine features when required.

There are no certain tests for the correctness of the structure, but all the following criteria are helpful;

1. The agreement of the individual observed structure factor amplitudes with those calculated for the refined model should be consistent with the estimated precision of the experimental measurement of the observations.

2. A difference map phased with the final parameters of the refined structure should reveal no fluctuations in electron density greater than those expected on the basis of the estimated precision of the electron density, ($\pm 1 \text{ e } \text{Å}^{-3}$).

3. Any anomalies in the molecular geometry and packing should be scrutinized with great care and regarded with some skepticism.

The results of an x-ray structure determination are the unit cell parameters, space group (symmetry), the atomic coordinates in the unit cell, and atomic displacement parameters. From this information other parameters that can be used to describe the structure, including bond lengths, bond angles, torsion angles, the shapes and conformation of rings, least-squares planes through groups of atoms, degree of association (monomer, polymer), and intermolecular geometry such as hydrogen bonds, van der Waals contacts, π -interaction stacking, and so forth, can be derived (Glusker and Tureblood, 1985).

2.2 Structure Correlation

Crystal Coordinates

The results of an x-ray crystallographic study are usually expressed as a numerical table of positional coordinates and atomic displacement parameters for the atoms contained in an asymmetric unit of structure. Atomic positions are usually expressed as fractional coordinates x_i, y_i, z_i , fractional scalar components along the length of a, b , and c crystal axes, respectively. The scalar quantities a, b, c are the lengths of a, b, c and the interaxial angles are denoted by Greek letters α (between b and c), β (between c and a) and γ (between a and c). Fractional scalar components can be converted to structure parameters such as bond distances, bond angles, and torsion angles. For example for a triclinic lattice the distance between two points in fractional coordinates (x_1, y_1, z_1) and (x_2, y_2, z_2) is given by the law of cosines in three dimensions as

$$l = \{(\Delta xa)^2 + (\Delta yb)^2 + (\Delta zc)^2 - 2ab\Delta x\Delta y\cos\gamma - 2ac\Delta x\Delta z\cos\beta - 2bc\Delta y\Delta z\cos\alpha\}^{1/2}$$

where $a, b, c, \alpha, \beta, \gamma$ are the unit cell parameter.

The angle between two vectors l_1 and l_2 with components along oblique axes is given by the dot product formula

$$\cos\theta_{l_2} = \frac{|(x_1a + y_1b + z_1c) \cdot (x_2a + y_2b + z_2c)|}{|l_1 l_2|}$$

In similar ways we can calculate other structure parameters; generally these geometric formula are available in the structure refinement program packages.

To compare molecules or molecular fragments from different crystal structures with different unit cells and space groups one generally uses a coordinate system related to the molecule or molecular fragments rather than using the structure in which it is embedded. Then only the relative atomic positions are required. The relative atomic positions may be specified by interatomic vectors. Their lengths and the angles between them are coordinate-system independent.

For describing molecules their lengths are then the bond lengths, the angles between the vectors emanating from the same atom are the bond angles and the angle between two planes defined by three vectors along a chain of four atoms is known as a torsion angle or a dihedral angle. The number of independent parameters, also called the degrees of freedom, for describing a molecule of N atoms is $3N-6$ parameters. In general for a Cartesian coordinate system there are $3N$ parameters, but atom 1 can be assigned at the origin, the x axis can always be chosen along the direction of the vector from atom 1 to atom 2, and the y axis can be chosen to lie in the plane of atoms 1, 2, and 3. Thus, atom 1 has coordinates $(0, 0, 0)$, atom 2 $(x_2, 0, 0)$ and atom 3 $(x_3, y_3, 0)$. The list of coordinates contains six zeros (nonadjustable coordinates). The relative positions of the atoms are then defined by the remaining $3N-6$ degrees of freedom (for a planar molecule only $2N-3$ degrees of freedom are needed).

The description of a molecule in terms of its bond lengths, bond angles, and torsion angles is often convenient because it is usually possible to guess the approximate value of these quantities on the basis of prior chemical knowledge. Thus,

given the constitution of a molecule, the bond lengths can usually be regarded as fixed within narrow limits at standard values that are characteristic of the various bond types. Bond angles are more flexible than bond lengths, but they do not vary much from characteristic values unless forced to do so by ring constraints. Torsion angles can always be translated into information about the interatomic distances in sets of four atoms or about relationships among the edges of tetrahedra for describing the relative arrangement of points in three dimensions such as when examining ring conformations.

Out-of-Plane Deformation of Six-Membered Ring

To consider deformations of a six-membered ring use the concepts of rigidity and flexibility in a mathematical rather than a mechanical sense. Rigidity implies the presence of some functional relationship between torsion angles and other internal structure parameter that remain constant; in the rigid molecule we cannot alter any torsion angles without changing at least one parameter. The six-membered ring has three degrees of freedom referred to the symmetry properties of the out-of-plane distortion of a regular hexagon, that nine may be chosen in the mean plane. The individual z coordinates normal to the plane of the hexagon transform like the $p(z)$ atomic orbitals in a Huckel molecular orbital calculation for benzene. The first three sets of bonding orbitals includes A_{1u} and E_{1g} and do not correspond to deformation of the hexagon; A_{1u} is a translation normal to the plane and the degenerate E_{1g} are rotations about axes that lie in the plane (Burgi and Dunitz, 1994a).

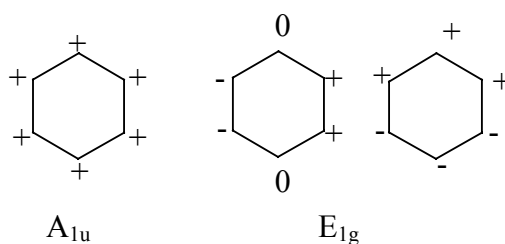


Figure 2.7. In plane bonding orbitals of regular hexagon.

A set of three orthogonal linear combinations of the anti-bonding orbitals corresponded to out-of-plane deformations as shown in the Figure 2.8.

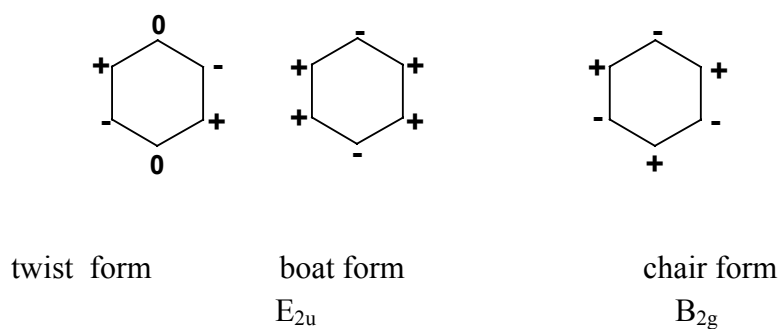


Figure 2.8. Out-of-plane deformations.

The nondegenerate deformation (B_{2g}) can be recognized as the chair form of the hexagon with point group D_{3d} while the pair of generate deformations (E_{2u}) correspond to the twist (D_2) and the boat (C_{2v}) forms. The three symmetry displacement coordinates correspond to out-of-plane deformations that can be described as

$$S(B_{2g}) = (1/6)^{1/2} \sum z_i (-1)^i$$

$$S_1(E_{2u}) = (1/3)^{1/2} \sum z_i \sin(4\pi j/6)$$

$$S_2(E_{2u}) = (1/3)^{1/2} \sum z_i \cos(4\pi j/6)$$

The two deformations E_{2u} can be described by the individual displacements from the mean plane (z axis) as

$$z_j = \delta \sin(4\pi j/6) \quad \text{for twist form}$$

$$z_j = \delta \cos(4\pi j/6) \quad \text{for boat form}$$

and the arbitrary linear combination by

$$z_j = \delta \cos(4\pi j/6 + \alpha) \quad j = 1, 2, \dots, 6$$

whence α is the phase angle as the extra degree of freedom. Values of $\alpha = 0^\circ, 60^\circ, 120^\circ, \dots$ yield the forms with C_{2v} symmetry, while values of $\alpha = 30^\circ, 90^\circ, 150^\circ, \dots$ yield the forms with D_2 symmetry. The nondegenerate deformation B_{2g} is not associated with any phase angle and is therefore rigid, meaning the torsion angles cannot be changed without changing bond angles. Since the presence of such a phase angle in the description of E_{2u} leads to pseudo rotation, at least for infinitesimal deviations from planarity. For finite deviations the bond angle changes are at most second order with respect to changes in torsion angles and allow the ring to be flexible.

The Principle of Structure Correlation

Generally the molecular structure contains considerable information of a compound such as the chemical reactivity of that compound. The structure assigned to

a compound was essentially a kind of summary of the reactions that the compound could undergo. The most characteristic feature of the compound in crystalline state is its three dimensional regularity. The molecules in a given crystal are usually frozen in a definite conformation, and interactions with neighboring molecules are fixed or at least severely restricted by the crystal packing. This means that the observed structures in the solid state tend to concentrate in low lying regions of the potential energy surface. Thus the scatter plot comparisons among the structure parameters such as bond lengths, bond angles, and torsion angles can be used to locate regions with a high density of points, which can be taken as a quantitative measure corresponding to low energy. This relationship is expressed as the principle of structure correlation. In several cases the results of structure correlation have been compared with results of *ab initio* or force-field calculations. Invariably, it is found that the regions in configuration space populated by the concentrations of structure data points coincide, approximately, with calculated regions of low energy. Therefore, it has been concluded that we can learn true information relating to stable structural features from correlation scatter plots (Burgi and Dunitz, 1994a).

In the structure correlation the structure parameters that are used for comparison are those commonly used for certain specific types of analysis. For example a bond length study would have an objective to focus on one particular type of bond in a specific chemical environment. In these studies it is wise to examine structural parameters that are associated with the environment of the bond of interest; *e.g.* lengths of direct substituent bonds, valence angles at the two atoms defining the bond, and so forth. Most importantly, when there is freedom of rotation about the bond, then the relevant torsion angles should also be examined. The conformation

studies are normally carried out using a basis set of torsion angles to define the fragment conformation. If we are only interested in the magnitude of deviations from local symmetry and not in the direction of the deviation the absolute numerical value of a single torsion angles is often sufficient.

Chapter III

Experimental

3.1 Structure Correlation

A search of version 5.21 of the Cambridge Structure Database (CCDC, 2001) reveals 55 x-ray structural characterizations are hits for the search fragment consisting of five fused six-membered rings with all ring carbon-carbon bonds as single bonds. The input instructions and the hit list of internal reference codes and bibliographic information from this search appear in Appendix A. Twenty-five of the hits are for structures of friedelin and its derivatives and an additional nine structures have oxygen bound at C(3). These thirty-four structure entries are used in this study, and are given in Table 3.1. Retrieved compounds include those isolated from nature as well as those resulting from chemical synthesis. No restrictions were made on *R*-factor or other criteria when searching the Cambridge Structure Database.

The crystal data and atomic coordinates were obtained, then reformatted as instruction files and used with a dummy *hkl* file for calculation using the SHELXL 93 (Sheldrick, 1993) structure refinement and analysis package. Structure parameters, the bond distances, bond angles, least squares mean planes and torsion angles, including those involving substituent groups, or suitable combinations of such distances and angles, were calculated. The structure parameters were input into version 8.0 of the EXCEL 97 program (Microsoft, 1997). The correlations were done between bond distances:bond angles, bond distances:torsion angles, bond

angles: torsion angles, and the sum of the three C–C–C and C–C–O bond angles about C3:C–O bond distances. The scatter plots presented throughout this thesis were generated with version 1.2 of the DPLOTT program (USAE, 1999).

The database entries for twenty-three of the twenty-five structures of friedelin and its derivatives include atomic coordinate positions. Four of those twenty-three are for friedelin itself as studies of improved accuracy were reported. One other structure was redetermined once. Three of the friedelin structures have keto- substituents (therefore, sp^2 ring carbons) Thus, fifteen unique structures are all that are known with the same arrangement of substituent groups on the pentacyclic saturated skeleton for which unit cell and coordinate data are available. These fifteen structures were used to calculate structure parameters and generate scatter plots to indicate endocyclic bond angles of carbon atom types in the rings, and to identify ring and ring junction conformations.

Table 3.1. The Compounds for Structure Correlation.

	Compound	Reference Code
1	3-O-Acetyl-16-O-p-bromobenzoyl-pachysandiol B	ABPACH10
2	28,29-Dihydroxy-friedelan-3-one	BITSOM
3	Stictane-3 β ,22 α -diol	BIZKUO
4	5 β ,6 β -Epoxy-alnusan-3 β -yl acetate	BUKKEN10
5	17-Perhydroxy-28-norfriedelan-3-one	CERCEH
6	Orthosphenic acid monohydrate	CEYVAD
7	5 α ,10 α -Epoxyalnusan-3 β -yl acetate	CITFIU10
8	Campanulin	COMPANL01
9	Taraxasterol	DATJOX
10	Echinocystic acid diacetate bromolactone	ECHABL10
11	Epifriedelinol	EPFRED
12	Longan triterpene-A	EPFRED01
13	5 β ,24-Cyclofriedelan-3-one	FADGEW
14	Methyl 3 β ,16 α -dihydroxy-12-oxo-13 α -olenan-28-oate dihydrate	FAWXUM
15	12 α -Hydroxy-3-oxo-oleanano-28,13-lactone	FITVOT
16	3 β -Acetoxy-ursane-28,20 β -olide	FOLVUX
17	Friede-26 β -ol-1,3-dione	FRDLON
18	22 α -Hydroxystictan-3-one	FUYNUI
19	29-Hydroxyfriedelan-3-one acetate	HFRDAC
20	28-Hydroxyfriedelan-3-one	JAMPOC
21	11 α ,12 α -Epoxy-13-hydroxy-3-oxoursan-28-oic acid- γ -lactone	LILDAL
22	Oleanolic acid diacetate bromolactone	OLDABL
23	Methyl 22 β -hydroxy-3,21-dioxo-D:A-friedo-29-norleanan-24-oate	PAPGAO

Table 3.1 (Continued)

24	2 β -Bromo-19 β ,28-epoxy-18 α -oleana-3-one	PIKMAX
25	Platycodigenin bromolactone benzene solvate	PLAGBL10
26	Prionostemmadione	PRISEM
27	6 β -Hydroxyfriedelan-3,16,21-trione	SOXNUA
28	3 β -Hydroxy-D:A-friedo-oleanan-27-oic acid	VAGCUB
29	Methyl 3-oxofriedelan-20 α -oate	VEFNID
30	Allobetulene	VEPBEX
31	Salaspermic acid monohydrate	YACNEV
32	Dimethyl 3 β -hydroxy-D:A-friedo-oleanan-27,29-dicarboxylate	YEGYOY
33	D:A-friedo-oleanan-3-one	ZZZQAI 02
34	Friedelan-3-one	ZZZQAI11

3.2 Isolation

The root bark of *Salacia chinensis* Linn was collected at amphur Jakaraj, Nakhon Ratchasima province, Thailand, in March 2000. Dried root bark powder of *S. chinensis*, 1.0 kg, was extracted with dichloromethane for 48 hour, then concentrated under vacuum to produce a red gummy material; yield 4.8 g. The material was extracted with hot methanol to separate the desired product from the gutta percha (Richard, 1998). The filtrate was dried under vacuum; yield 0.95 g. The extract was subjected to column chromatography over silica gel (#7734), eluted with solvents of gradually increasing polarity from hexane, dichloromethane, ethyl acetate, and methanol, respectively. The fraction of 1:1 CH₂Cl₂:EtOAc was further separated with 7:2:1 hexane:CH₂Cl₂:EtOAc by preparative thin layer chromatography (tlc plate coated with silica gel #7730), and the fraction with the highest R_f value was collected.

The 25,26-oxidofriedel-1,3-dione obtained was crystallized by slow evaporation; yield 5.1 mg.

3.3 Single Crystal X-ray Crystallography

Single crystal x-ray diffraction data were collected on two diffractometer systems. The data for the disordered epifriedelin-3-ol/friedelin-3-one crystal were collected on the Bruker Nonius KappaCCD area detector diffractometer at the Center for Scientific and Technological Instrumentation, Suranaree University of Technology, Nakhon Ratchasima, Thailand. The data for the 25,26-oxidofriedalan-1,3-dione crystal were collected on a Bruker Nonius KappaCCD area detector diffractometer at the Department of Chemistry, University of Utrecht, Utrecht, The Netherlands. Data collected on the Utrecht system was written to CD ROM for transfer to SUT. The two systems used for data collection have similar configurations, so the hardware, data collection, data reduction, and basic solution and refinement methodology will be described, and the details of the data collections and data reductions will be presented in this section. Crystal data, a summary of data collection parameters, and details of the individual refinements are given in the relevant sections of Chapters IV and V.

Both diffractometers were equipped with horizontally mounted highly-oriented pyrolytic graphite crystal incident beam monochromators. The source x-radiation was the $K\alpha$ lines ($\lambda = 0.71073 \text{ \AA}$) from a fine focus sealed molybdenum anode x-ray tube operated at tube power levels of 40 kV and 25 mA, or from a rotating anode x-ray generator operated at power levels of 60 kV and 50 mA,

respectively. The Utrecht diffractometer system uses standard pinhole incident beam collimators while the SUT instrument has *ifg* focusing optic incident beam collimators which focus the x-rays at the crystal position, increasing the x-ray intensity at the sample by approximately 50-80% for molybdenum $K\alpha$ radiation. The diffraction measuring device consists of a 95 mm CCD camera mounted on a Kappa goniostat.

The Utrecht KappaCCD system employed a variable temperature device capable of producing temperatures at the crystal from near liquid nitrogen temperature to near room temperature. The operating temperature was set at 150 K for the 25,26-oxidofriedalan-1,3-dione data set.

Data collection was controlled by the COLLECT routine (Nonius B.V., 2000) and the obtained frame data were reduced with the DENZO/HKL/SCALEPACK package (Otwinowski and Minor, 1997). Due to the specialized nature of area detector diffractometers and to detector specific corrections, the raw frame data must be reduced to structure factors by the software that is delivered with each individual diffractometer. This requirement produces the disadvantage that the data reduction cannot be optimized based on knowledge gained during the structure solution and refinement stages. The structures were solved with the SIR direct methods program (Altomare, Cascarano, Giacovazzo, Guagliardi, Burla, Polidori, and Camalli, 1994). SHELXTL (Sheldrick, 1997) was used for full matrix least-squares structure refinement, electron density difference maps, and table preparation. Distances and angles for the nonbonded interactions, and the perspective drawings were obtained from ORTEP3, Farrugia's (1997) interactive version of Burnett and Johnson's (1996) ORTEP III graphics package.

Chapter IV

X-ray Structural Characterization of Disordered Epifriedelin-3-ol and Friedelin-3-one ^a

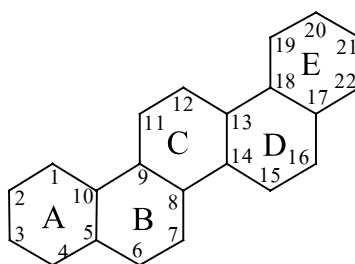
4.1 Introduction

Today about a quarter million structures of organic compounds are stored in the Cambridge Structure Database (CSD). With the assistance of powerful computers and software this resource has been exploited in what has been called data mining. In this enterprise scientists have established favored conformations, intermolecular interactions, and reactivities of classes of compounds or functional groups (Burgi and Dunitz, 1994a, 1994b). Other workers have established the stereochemistry of various supramolecular synthons, weak interaction building blocks for extended solid state structure (*e.g.* Desiraju, 1991). The vast data available on first row transition metal-carbonyl complexes has been analyzed to characterize the structures, and thus help predict reactivities (Braga, Grepioni, Biradha, Pedireddi, and Desiraju, 1995; Paquette, Stepanian, Branan, Edmondson, Bauer, and Rogers, 1996). Additional work to establish the geometrical parameters of C–H···O weak hydrogen bonds in organic compounds has also been reported (Steiner and Desiraju, 1998).

Friedelin and its derivatives are primarily natural products that contain the saturated five fused six-membered ring system with an oxygen functional group at

a. Part of the work in this chapter was presented at the 4th Asian Crystallographic Association Meeting in Bangalore India (Phothikanith and Haller, 2001)

position 3 and substituents at positions 4, 5, 9, 13, 14, 17, and 20 (two substituents at position 20) illustrated in the following schematic diagram:



The conventional numbering system for the pentacyclic skeleton is indicated on the diagram, as is the conventional letter labeling of each of the five rings. Compounds of this family exhibit antileukemic activity (Lee and Nozaki, 1984), cytotoxicity, (Zheng, 1994), and antiviral activity (Chen, Shi, Kashiwada, Zhang, Hu, Jin, Nozaki, Kilkuskie, Tramontano, Cheng, McPhail, McPhail, and Lee, 1992). The oxygen substituent can be either an oxy-functional group such as hydroxyl as in epifriedelin (Laing, Burke-Laing, Bartho, and Weeks, 1977), or a carbonyl as in friedelin (Mo, Winther, and Scrimgeour, 1989). Accurate structural work and *ab initio* molecular orbital calculations in the latter case indicate the molecular packing interactions in friedelin and its derivatives are relatively weak intermolecular forces. The carbonyl and oxy groups contain acceptor oxygen atoms that can form weak C–H \cdots O hydrogen bond interactions, or carbonyl-carbonyl interactions of the $>C(\delta^+) \cdots O(\delta^-)$ type (Allen, Baalham, Lommerse, and Raithby, 1998). The weakness of the intermolecular interactions should make the friedelane system a good candidate for structural correlation to investigate its conformational space.

4.2 Experimental

Structure Correlation: Structure data were retrieved from the Cambridge Structural Database (CCDC, 2001, 233,218 entries) in *cif* form for all 55 triterpene (class No. 56) structures containing the saturated five fused six-member ring search fragment. The 34 entries (Table 4.2) with oxygen bound at C3 were utilized for the structure correlation. Distances, angles, and displacements from the mean plane of six carbon atoms in a ring were derived from the structure data, and the sum of the C2–C3–C4, C2–C3–O3, and C4–C3–O3 angles, $\Sigma\angle C3$, was calculated. The scatterplot of $\Sigma\angle C3$ vs C3–O distance was produced using version 1.2 of the DPLOT program (USAE, 1999).

X-ray Crystallography: The single crystal used for x-ray data collection was selected from an unknown sample isolated from a Thai source (Phaopongthai, 1995), and recrystallized from dichloromethane/hexane. The transparent colorless plate shaped crystal was mounted on a hollow fiber with cyanoacrylate glue. Data were collected using the COLLECT software (Nonius B.V., 2000) on a Bruker Nonius KappaCCD diffractometer equipped with a graphite monochromated fine focus Mo $K\alpha$ x-radiation source and a 0.5 mm *ifg* focusing collimator. Data reduction was carried out with DENZO and scaling and merging with SCALEPACK (Otwinowski and Minor, 1997). The structure was solved by direct methods using SIR (Altomare, Cascarano, Giacovazzo, Guagliard, Burla, Polidori, and Camalli, 1994). SHELXTL (Sheldrick, 1997) was used for full matrix least-squares structure refinement, electron density difference maps, and table preparation. Distances and angles for the nonbonding interactions, and the perspective drawings were obtained from ORTEP III (Farrugia,

2003; Burnett and Johnson, 1996). Details of the crystal data and data collection parameters are given in Table 4.1.

The direct methods solution provided positions for the hydroxy oxygen atom and all 30 carbon atoms. A difference electron density map, calculated after preliminary isotropic refinement of the ordered epifriedelin-3-ol model, clearly revealed a second position about 0.7 Å from the first for the oxygen atom. The two positions were modeled as partial isotropic oxygen atoms assigned O3H (hydroxyl) and O3C (carbonyl) with the single constraint that their occupancies sum to unity. All other nonhydrogen atoms in the refinement model were reasonably well behaved as ordered anisotropic atoms. The hydrogen atoms, including those associated with the partially occupied hydroxyl group, could be located from the electron density difference map calculated at this stage, but were included as geometrically idealized isotropic contributors riding on the atoms to which they are attached. The hydroxy and methyl hydrogen atoms were constrained to the approximate tetrahedral positions as rigid groups allowed to rotate about the C–Me or C–O axis. Each of the three types of carbon bound hydrogen atoms were given a common refined atomic displacement parameter, while that for the hydroxy hydrogen was fixed at 0.06 Å². Occupancies of the partial hydrogen atoms associated with the hydroxy oxygen, O3H, were adjusted to match the oxygen occupancy.

Table 4.1. Crystal Data and Crystallographic Experimental Details.

Crystal data

Disorder component	epifriedelin-3-ol	friedelin-3-one
Chemical formula	C ₃₀ H ₅₂ O	C ₃₀ H ₅₀ O
Chemical formula weight	428.75	426.73
Refined occupancy factor	0.680(5)	0.320(5)
Chemical formula sum	C ₃₀ H _{51.36} O	
Chemical formula weight sum	428.08	
Crystal color and habit	transparent colorless plate	
Crystal size (mm)	0.12 x 0.40 x 0.42	
Crystal system and Space group	monoclinic C2 (No. 5)	
Unit cell	<i>a</i> (Å)	
	13.4372(27)	
	<i>b</i> (Å)	
	6.4300(13)	
	<i>c</i> (Å)	
	29.599(6)	
	β (°)	
	91.97(3)	
	<i>V</i> (Å ³)	
	2552.54	
<i>Z</i>	4	
<i>D</i> _{calc} (Mg m ⁻³)	1.114	
Radiation type	Mo <i>K</i> α	
Wavelength (Å)	0.71073	
Temperature (K)	298	
μ (mm ⁻¹)	0.064	

Data collection

Diffractionmeter	Bruker Nonius KappaCCD
Absorption correction	multiscan
Generator settings (kV/mA)	40 / 25
Data collection method	CCD
No. of integrated reflections	13490
<i>R</i> _{merge} (1 symmetry, 3662 multiples)	0.027
No. of unique reflection	6672

Table 4.1 (Continued)

θ range ($^{\circ}$)	2.75-30.05
Range of h, k, l	$-18 \leq h \leq 18, -8 \leq k \leq 8, -41 \leq l \leq 41$
Refinement	
Refinement on	F^2
No. of unique reflection	6672
R_{sym} (2/m symmetry,)	0.027
No. of observed reflections ($F > 4\sigma F$)	5157
No. of parameters / constraints used	291 / 1
R_1 for 5157 $F > 4\sigma F$	0.0563
wR_2 for 5157 $F > 4\sigma F$	0.1161
R_1 for all 6672	0.0819
wR_2 for all 6672	0.1798
goodness of fit	1.053
Weighting scheme	$w = 1/[\sigma^2(Fo^2) + (0.0358 \times P)^2 + 1.7052 \times P]$ where $P = [\max(Fo^2, 0) + 2 \times F_c^2] / 3$
$\rho_{max}/\rho_{min}/\rho_{err}$ ($e \text{ \AA}^{-3}$)	0.22 / -0.28 / 0.03
Refinement program	SHELXTL v 5.03
Drawing program	ORTEP-III

Refinement converged with $R_1=0.0563$, $wR_2=0.1161$, and estimated error in an observation of unit weight of 1.053. Refined occupancies are 0.680(5) for the hydroxy form and 0.320(5) for the keto form. Refined atomic displacement parameters for the hydrogen atoms are $U_{iso}[\text{H}_{methine}]=0.037(2)$, $U_{iso}[\text{H}_{methylene}]=0.054(2)$, and $U_{iso}[\text{H}_{methyl}]=0.076(2) \text{ \AA}^2$. The highest peak on the final electron density difference map is $0.22(3) e \text{ \AA}^{-3}$. Refinement of the Flack (1983) parameter for determination of absolute configuration was inconclusive. Atomic coordinates (x,y,z) and equivalent

isotropic atomic displacement parameters (U_{eq}) for the nonhydrogen atoms are given in Table 4.4. The coordinates and isotropic atomic displacement parameters are included in Table 4.5, anisotropic atomic displacement parameters in Table 4.6, and torsional angles for all the bonded nonhydrogen atoms in Table 4.7

4.3 Results and Discussion

Structure Correlation: The structure correlation scatterplot of $\Sigma\angle C3$ vs $d[C3-O]$ is given in Figure 4.1 for the 34 polycyclic triterpene molecules with oxygen at position C3 listed in Table 4.2. The oxygen atom should be connected by either a single bond or a double bond as shown in Figure 4.2.

Table 4.2. The Compounds for Structure Correlation.

Compound	Reference Code	Reference
1 3-O-Acetyl-16-O-p-bromobenzoyl-pachysandiol B	ABPACH10	Masaki, N., <i>et al.</i> , (1975)
2 28,29-Dihydroxy-friedelan-3-one	BITSOM	Nozaki, H., <i>et al.</i> , (1982)
3 Stictane-3 β ,22 α -diol	BIZKUO	Corbett, R. E., <i>et al.</i> , (1982)
4 5 β ,6 β -Epoxy-alnusan-3 β -yl acetate	BUKKEN10	Tori, M., <i>et al.</i> , (1984)
5 17-Perhydroxy-28-norfriedelan-3-one	CERCEH	Lee, K.-H., <i>et al.</i> , (1984)
6 Orthosphenic acid monohydrate	CEYVAD	Gonzalez, A. G., <i>et al.</i> , (1983)
7 5 α ,10 α -Epoxyalnusan-3 β -yl acetate	CITFIU10	Takai, M., <i>et al.</i> , (1985)
8 Campanulin	CMPANL01	Mo, F., (1977)
9 Taraxasterol	DATJOX	Reynolds, W. F., <i>et al.</i> , (1985)
10 Echinocystic acid diacetate bromolactone	ECHABL10	Carlisle, C. H., <i>et al.</i> , (1976)
11 Epifriedelinol	EPFRED	Laing, M., <i>et al.</i> , (1977)
12 Longan triterpene-A	EPFRED01	Shi, J-Q., <i>et al.</i> , (1992)
13 5 β ,24-Cyclofriedelan-3-one	FADGEW	Connolly, J. D., <i>et al.</i> , (1986)
14 Methyl 3 β ,16 α -dihydroxy-12-oxo-13 α -oleanan-28-oate dihydrate	FAWXUM	Dhaneshwar, N. N., <i>et al.</i> , (1987)
15 12 α -Hydroxy-3-oxo-oleanano-28,13-lactone	FITVOT	Eggleston, D. S., <i>et al.</i> , (1987)
16 3 β -Acetoxy-ursane-28,20 β -olide	FOLVUX	Druet, D., <i>et al.</i> , (1987)
17 Friede-26 β -ol-1,3-dione	FRDLON	Rogers, D., <i>et al.</i> , (1980)
18 22 α -Hydroxystictan-3-one	FUYNUI	Wilkins, A. L., <i>et al.</i> , (1988)
19 29-Hydroxyfriedelan-3-one acetate	HFRDAC	Betancor, C., <i>et al.</i> , (1980)
20 28-Hydroxyfriedelan-3-one	JAMPOC	Subramanian, K., <i>et al.</i> , (1989)
21 11 α ,12 α -Epoxy-13-hydroxy-3-oxoursan-28-oic acid- γ -lactone	LILDAL	Tkachev, A.V., <i>et al.</i> , (1994)
22 Oleanolic acid diacetate bromolactone	OLDABL	van Schalkwyk, T. G. D., <i>et al.</i> , (1974)
23 Methyl 22 β -hydroxy-3,21-dioxo-D:A-friedo-29-norleanan-24-oate	PAPGAO	Kutney, J. P., <i>et al.</i> , (1992)
24 2 β -Bromo-19 β ,28-epoxy-18 α -oleana-3-one	PIKMAX	Novotny, J., <i>et al.</i> , (1993)
25 Platycodigenin bromolactone benzene solvate	PLAGBL10	Akiyama, T., <i>et al.</i> , (1970)
26 Prionostemma-dione	PRISEM	Monache, F. D., <i>et al.</i> , (1979)
27 6 β -Hydroxyfriedelan-3,16,21-trione	SOXNUA	Nozaki, H., <i>et al.</i> , (1991)
28 3 β -Hydroxy-D:A-friedo-oleanan-27-oic acid	VAGCUB	Tanaka, R., <i>et al.</i> , (1988)
29 Methyl 3-oxofriedelan-20 α -oate	VEFNID	Cota, A. B. <i>et al.</i> , (1990)
30 Allobetulene	VEPBEX	Klinot, J., <i>et al.</i> , (1989)

Table 4.2 (Continued)

31 Salaspermic acid monohydrate	YACNEV	Chen, K., <i>et al.</i> , (1992)
32 Dimethyl 3 β -hydroxy-D:A-friedo-oleanan-27,29-dicarboxylate	YEGYOY	Gibbons, S., <i>et al.</i> , (1993)
33 D:A-friedo-oleanan-3-one	ZZZQAI02	Declercq, J.-P., <i>et al.</i> , (1991)
34 Friedelan-3-one	ZZZQAI11	Mo, F., <i>et al.</i> , (1989)

Table 4.3. Crystal Data for the Different Friedelin Structures.

Compound	Friedelin-3-one	epifriedelin-3-ol	Friedelin-3-one	anomalous	disordered	
CSD Refcode	ZZZQAI11	EPFRED	ZZZQAI02	EPFRED01	freieelin-3-one/epifriedelin-3-ol	
Formula	C ₃₀ H ₅₀ O	C ₃₀ H ₅₂ O	C ₃₀ H ₅₀ O	C ₃₀ H ₅₂ O	C ₃₀ H ₅₀ O	C ₃₀ H ₅₂ O O
Space group	<i>P2₁2₁2₁</i>	<i>C2</i>	<i>P2₁2₁2₁</i>	<i>C2</i>	<i>C2</i>	
Crystal system	Orthorhombic	Monoclinic	Orthorhombic	Monoclinic	Monoclinic	
<i>a</i> (Å)	6.371(1)	13.43(2)	6.362(2)	13.419(4)	13.4372(27)	
<i>b</i> (Å)	13.943(2)	6.35(1)	13.923(2)	6.422(2)	6.4300(13)	
<i>c</i> (Å)	28.456(6)	29.59(3)	28.419(5)	29.586(7)	29.5987(59)	
β	90	92.5(2)	90	91.91(2)	91.97(3)	
<i>Z</i>	4	4	4	4	4	
Volume (Å ³)	2527.8(7)	2521.0(2)	2517.3(3)	2548.2(4)	2555.54(4)	
MW (Dalton)	426.70	427.71	426.70	427.71	428.75	426.73
<i>D_{cal}</i> (Mg m ⁻³)	1.121	1.130	1.126	1.117	1.109	1.116
<i>R</i> -factor	0.133	0.17	0.047	0.068	0.0563	
Reference	Mo, <i>et al.</i> , 1989	Laing, <i>et al.</i> , 1977	Declercq, <i>et al.</i> , 1991	Shi, <i>et al.</i> , 1992	present work	

The scatterplot obviously characterizes the hybridization of the carbon atom for all but one of the compounds (labeled ‘anomalous’ in Figure 4.1). Ideal angles about carbon for sp^2 and sp^3 hybridization are 120° and 109.5°, giving expected values for the sum of the nonhydrogen angles of ~360° and ~329° respectively. Expected $d[C-O]$ for a C₂-CH-OR single bond (hydroxyl or ester) is 1.43 Å and $d[C=O]$ for cyclohexanones is 1.21 Å (Orpen, Brammer, Allen, Kennard, Watson and Taylor, 1994); these two ideal points are represented by hexagonal symbols on Figure 4.3. The average values of the two clusters are 1.445 Å / 331.2° and 1.218 Å / 359.7° for the hydroxyl and carbonyl types, respectively; the small increases in both $d[C-O]$

values and in the hydroxyl $\Sigma\angle C3$ consistent with expectations based on the increased steric volume of ring carbon atoms. The anomalous structure, EPFRED01 (Shi, Wu, Xu, Chen, and Xu, 1992), previously identified as epifriedelin-3-ol and represented by a pentagonal symbol on Figure 4.3, falls on the scatterplot at $d[C-O] = 1.33 \text{ \AA}$ and $\Sigma\angle C3 = 343.1^\circ$, almost at the midpoint between the centroids of the two most probable value clusters. A second, apparently isomorphous, independent determination of epifriedelin-3-ol, EPFRED (Laing, Burke-Laing, Bartho, and Weeks, 1977), while a poor structure based on the high R value, falls within the cluster. Inspection of the crystal data for these and other known related structures given in Table 4.3 show that with the interchange of the a and b axes the cells have the nearly the same metrics, suggesting that the packing of epifriedelin-3-ol and the closely related friedelin-3-one, differing only in the nature of the oxygen functional group at C(3), are apparently the same.

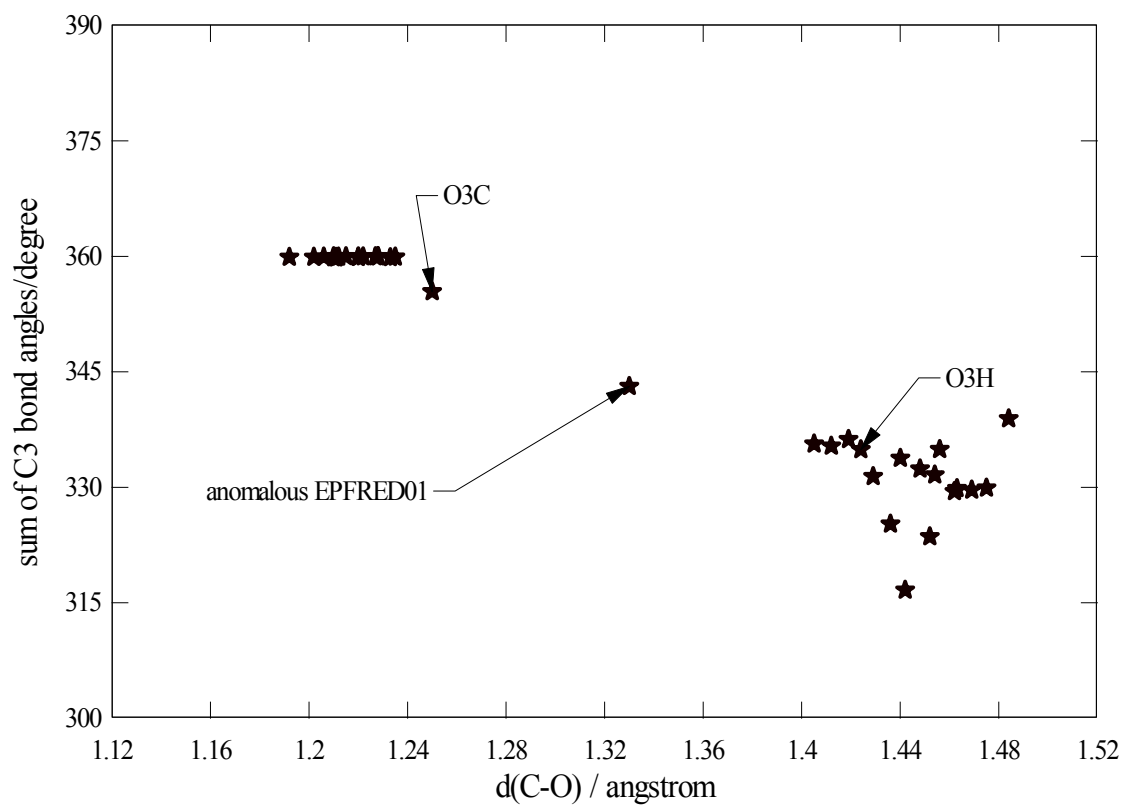
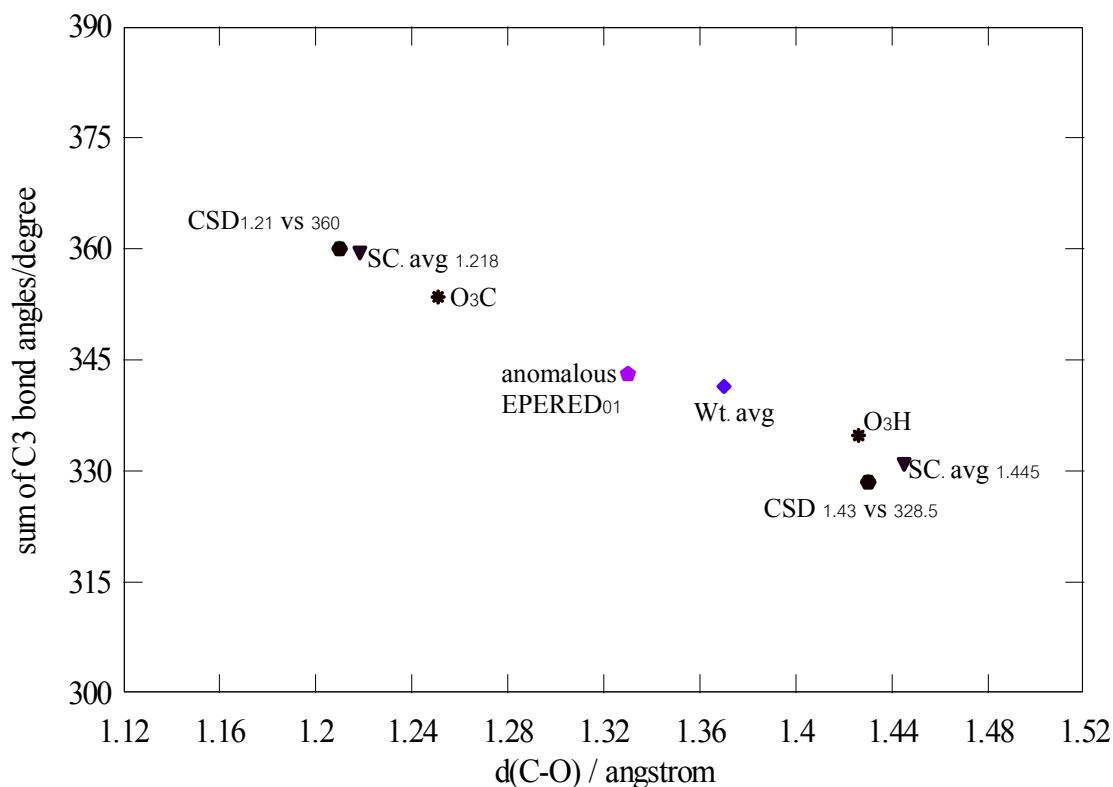


Figure 4.1. Scatterplot of the sum of bond angles about C(3) versus C(3)–O bond distances.



Figure 4.2. Ring A fragment with oxygen bound to sp^2 and sp^3 carbon at C3.



Notation

1. CSD is the values from Cambridge Structure database searched
2. SC. avg is average value of structure correlation related to sp^2 and sp^3 hybridization.
3. Wt. avg is the occupancy weighted average of O₃C and O₃H

Figure 4.3. Distribution of oxygen atoms related to sp^2 and sp^3 hybridization.

Table 4.4. Fractional Monoclinic Coordinates^a and Isotropic Atomic Displacement Parameters^b (\AA^2) for the Nonhydrogen Atoms.

Atom ^c	<i>x</i>	<i>y</i>	<i>z</i>	<i>U</i> _{iso}
C1	0.45627(14)	0.3573(4)	0.37281(7)	0.0441(5)
C2	0.4800(2)	0.1774(5)	0.40485(8)	0.0557(6)
C3	0.4002(2)	0.1422(4)	0.43860(7)	0.0514(6)
O3H	0.4083(2)	0.2979(6)	0.47287(9)	0.0552(6)
O3C	0.4063(4)	0.1903(12)	0.4796(2)	0.0552(6)
C4	0.2961(2)	0.1295(3)	0.41664(7)	0.0406(5)
C5	0.27035(13)	0.3170(3)	0.38477(6)	0.0339(4)
C6	0.17039(14)	0.2712(3)	0.35968(6)	0.0381(5)
C7	0.14812(13)	0.4143(3)	0.31967(7)	0.0381(4)
C8	0.23062(12)	0.3981(3)	0.28541(6)	0.0311(4)
C9	0.33224(13)	0.4716(3)	0.30724(6)	0.0318(4)
C10	0.35340(12)	0.3283(3)	0.34913(6)	0.0329(4)
C11	0.41295(13)	0.4369(3)	0.27211(6)	0.0363(4)

Table 4.4 (Continued)

Atom ^c	<i>x</i>	<i>y</i>	<i>z</i>	<i>U</i> _{iso}
C12	0.38588(13)	0.5267(3)	0.22529(6)	0.0364(4)
C13	0.28770(13)	0.4400(3)	0.20398(6)	0.0315(4)
C14	0.20178(13)	0.4849(3)	0.23743(6)	0.0327(4)
C15	0.10583(14)	0.3742(4)	0.21911(7)	0.0442(5)
C16	0.0957(2)	0.3496(4)	0.16740(7)	0.0503(6)
C17	0.15432(14)	0.4985(4)	0.13743(7)	0.0428(5)
C18	0.26249(13)	0.5478(3)	0.15777(6)	0.0357(4)
C19	0.34283(15)	0.5053(4)	0.12303(7)	0.0436(5)
C20	0.3230(2)	0.5979(4)	0.07558(7)	0.0518(6)
C21	0.2181(2)	0.5290(5)	0.05750(8)	0.0637(7)
C22	0.1627(2)	0.3973(5)	0.09083(8)	0.0563(6)
C23	0.2184(2)	0.0802(4)	0.45168(8)	0.0548(6)
C24	0.2599(2)	0.5176(4)	0.41279(7)	0.0448(5)
C25	0.3377(2)	0.7036(3)	0.32075(7)	0.0436(5)
C26	0.3035(2)	0.2024(3)	0.19726(7)	0.0425(5)
C27	0.1786(2)	0.7197(3)	0.24086(7)	0.0435(5)
C28	0.0921(2)	0.7003(5)	0.13065(8)	0.0581(6)
C29	0.3327(2)	0.8349(5)	0.07717(9)	0.0708(8)
C30	0.4019(2)	0.5134(6)	0.04454(8)	0.0772(9)

- a. The standard deviations of the least significant digits are given in parentheses.
b. Equivalent isotropic atomic displacement parameters for the atoms refined anisotropically. The values for O3H and O3C were refined isotropically and constrained to be equal. U_{eq} or $U_{iso} = \exp(-8\pi^2 U[\sin\theta/\lambda]^2)$
c. Occupancy was refined for O3H/H3H/H3HO and O3C with the constraint that the sum equal 1.0; the occupancy of O3H/H3H/H3HO is 0.680(5).

Table 4.5. Fractional Monoclinic Coordinates^a and Isotropic Atomic Displacement Parameters^b (Å²) for the Hydrogen Atoms.

Atom ^c	<i>x</i>	<i>y</i>	<i>z</i>	<i>U</i> _{iso}
H1A	0.50685(14)	0.3655(4)	0.35029(7)	0.0542(14)
H1B	0.45721(14)	0.4868(4)	0.38965(7)	0.0542(14)
H2A	0.4881(2)	0.0514(5)	0.38731(8)	0.0542(14)
H2B	0.5427(2)	0.2053(5)	0.42101(8)	0.0542(14)
H3H	0.4139(2)	0.0079(4)	0.45319(7)	0.037(2)
H3HO	0.4375(24)	0.3996(23)	0.4631(4)	0.060
H4	0.2972(2)	0.0073(3)	0.39685(7)	0.037(2)
H6A	0.17083(14)	0.1284(3)	0.34904(6)	0.0542(14)
H6B	0.11720(14)	0.2841(3)	0.38084(6)	0.0542(14)
H7A	0.14319(13)	0.5568(3)	0.33017(7)	0.0542(14)
H7B	0.08477(13)	0.3761(3)	0.30523(7)	0.0542(14)
H8	0.23915(12)	0.2483(3)	0.28078(6)	0.037(2)
H10	0.35560(12)	0.1875(3)	0.33645(6)	0.037(2)

Table 4.5 (Continued)

H11A	0.47463(13)	0.5002(3)	0.28325(6)	0.0542(14)
H11B	0.42462(13)	0.2886(3)	0.26915(6)	0.0542(14)
H12A	0.43962(13)	0.4970(3)	0.20521(6)	0.0542(14)
H12B	0.38028(13)	0.6768(3)	0.22778(6)	0.0542(14)
H15A	0.10319(14)	0.2370(4)	0.23266(7)	0.0542(14)
H15B	0.04869(14)	0.4517(4)	0.22914(7)	0.0542(14)
H16A	0.1154(2)	0.2086(4)	0.16007(7)	0.0542(14)
H16B	0.0257(2)	0.3631(4)	0.15876(7)	0.0542(14)
H18	0.26422(13)	0.6979(3)	0.16361(6)	0.037(2)
H19A	0.35032(15)	0.3558(4)	0.12002(7)	0.0542(14)
H19B	0.40575(15)	0.5598(4)	0.13500(7)	0.0542(14)
H21A	0.1789(2)	0.6520(5)	0.05019(8)	0.0542(14)
H21B	0.2252(2)	0.4504(5)	0.02982(8)	0.0542(14)
H22A	0.1966(2)	0.2647(5)	0.09444(8)	0.0542(14)
H22B	0.0962(2)	0.3697(5)	0.07841(8)	0.0542(14)
H23A	0.1548(3)	0.0577(26)	0.43662(9)	0.077(2)
H23B	0.2137(9)	0.1949(12)	0.4723(4)	0.077(2)
H23C	0.2379(7)	-0.0429(16)	0.4681(4)	0.077(2)
H24A	0.3246(2)	0.5634(14)	0.4234(5)	0.077(2)
H24B	0.2193(10)	0.4902(7)	0.4382(3)	0.077(2)
H24C	0.2292(11)	0.6239(8)	0.3943(2)	0.077(2)
H25A	0.3868(9)	0.7216(5)	0.3448(4)	0.077(2)
H25B	0.2739(4)	0.7484(7)	0.3307(5)	0.077(2)
H25C	0.3559(12)	0.7852(4)	0.2951(2)	0.077(2)
H26A	0.2546(8)	0.1504(6)	0.1757(4)	0.077(2)
H26B	0.2967(12)	0.1320(4)	0.22560(13)	0.077(2)
H26C	0.3689(5)	0.1780(4)	0.1864(5)	0.077(2)
H27A	0.1470(11)	0.7664(6)	0.2131(2)	0.077(2)
H27B	0.2394(2)	0.7954(4)	0.2463(5)	0.077(2)
H27C	0.1348(10)	0.7432(5)	0.2653(3)	0.077(2)
H28A	0.1330(4)	0.8068(9)	0.1181(5)	0.077(2)
H28B	0.0686(10)	0.7459(15)	0.15926(12)	0.077(2)
H28C	0.0363(7)	0.6729(8)	0.1104(4)	0.077(2)
H29A	0.2860(8)	0.8905(6)	0.0978(4)	0.077(2)
H29B	0.3190(12)	0.8911(6)	0.04754(14)	0.077(2)
H29C	0.3991(4)	0.8719(5)	0.0871(5)	0.077(2)
H30A	0.3916(8)	0.5709(21)	0.0148(2)	0.077(2)
H30B	0.3969(8)	0.3645(6)	0.0430(4)	0.077(2)
H30C	0.4669(2)	0.5516(23)	0.0563(3)	0.077(2)

- a. The standard deviations of the least significant digits are given in parentheses.
- b. Three isotropic atomic displacement parameters were refined, one for each hydrogen type; *i.e.* one for primary, one for secondary, and one for tertiary hydrogens; $U[\text{H3OH}]$ was fixed at 0.06. $U_{iso} = \exp(-8\pi^2 U[\sin\theta\lambda]^2)$
- c. Occupancy was refined for O₃H/H₃H/H₃HO and O₃C with the constraint that the sum equal 1.0; the occupancy of O₃H/H₃H/H₃HO is 0.680(5).

Table 4.6. Anisotropic Atomic Displacement Parameters^a (Å²).

Atom	U_{11}	U_{22}	U_{33}	U_{23}	U_{13}	U_{12}
C1	0.0312(9)	0.0590(14)	0.0418(11)	-0.0031(10)	-0.0014(8)	0.0002(9)
C2	0.0413(11)	0.076(2)	0.0497(12)	0.0021(12)	-0.0043(9)	0.0180(12)
C3	0.0530(12)	0.063(2)	0.0379(11)	0.0006(11)	-0.0030(9)	0.0122(11)
C4	0.0478(11)	0.0383(11)	0.0358(10)	-0.0022(9)	0.0032(8)	0.0019(9)
C5	0.0329(9)	0.0361(10)	0.0329(9)	-0.0027(9)	0.0026(7)	-0.0009(8)
C6	0.0307(9)	0.0461(12)	0.0378(10)	0.0012(9)	0.0051(7)	-0.0044(8)
C7	0.0262(8)	0.0473(12)	0.0410(10)	0.0027(9)	0.0033(7)	-0.0009(8)
C8	0.0268(8)	0.0299(9)	0.0367(10)	0.0003(8)	0.0023(7)	-0.0022(7)
C9	0.0268(8)	0.0340(10)	0.0345(9)	-0.0012(8)	0.0019(7)	-0.0027(7)
C10	0.0293(8)	0.0349(10)	0.0344(9)	-0.0046(8)	0.0010(7)	0.0019(8)
C11	0.0245(8)	0.0483(12)	0.0361(10)	-0.0005(9)	0.0008(7)	-0.0032(8)
C12	0.0282(8)	0.0459(12)	0.0352(10)	-0.0013(9)	0.0036(7)	-0.0051(8)
C13	0.0283(8)	0.0336(10)	0.0327(9)	-0.0004(8)	0.0012(7)	-0.0022(7)
C14	0.0257(8)	0.0371(10)	0.0354(10)	0.0012(8)	0.0023(7)	-0.0014(7)
C15	0.0301(9)	0.0578(15)	0.0446(11)	0.0060(10)	-0.0025(8)	-0.0101(9)
C16	0.0394(11)	0.063(2)	0.0480(12)	0.0016(12)	-0.0069(9)	-0.0122(10)
C17	0.0337(9)	0.0555(13)	0.0387(10)	0.0031(10)	-0.0041(8)	-0.0044(9)
C18	0.0342(9)	0.0381(11)	0.0346(9)	-0.0003(8)	-0.0020(7)	-0.0032(8)
C19	0.0388(10)	0.0568(13)	0.0353(10)	0.0033(10)	0.0033(8)	-0.0017(10)
C20	0.0502(12)	0.072(2)	0.0334(11)	0.0040(11)	0.0012(9)	-0.0031(11)
C21	0.0589(14)	0.096(2)	0.0360(11)	0.0012(13)	-0.0073(10)	-0.007(2)
C22	0.0485(12)	0.075(2)	0.0453(12)	-0.0067(12)	-0.0075(10)	-0.0099(12)
C23	0.0617(14)	0.061(2)	0.0417(12)	0.0085(11)	0.0057(10)	-0.0051(12)
C24	0.0486(11)	0.0435(12)	0.0426(11)	-0.0087(10)	0.0059(9)	0.0042(10)
C25	0.0503(12)	0.0354(11)	0.0448(11)	-0.0057(9)	0.0001(9)	-0.0082(9)
C26	0.0475(11)	0.0354(11)	0.0447(11)	-0.0003(9)	0.0043(9)	0.0016(9)
C27	0.0446(11)	0.0406(12)	0.0455(11)	0.0023(10)	0.0027(9)	0.0095(9)
C28	0.0439(12)	0.074(2)	0.0554(13)	0.0080(13)	-0.0076(10)	0.0098(12)
C29	0.082(2)	0.082(2)	0.0482(14)	0.018(2)	-0.0041(13)	-0.012(2)
C30	0.072(2)	0.120(3)	0.0398(13)	0.003(2)	0.0121(12)	0.001(2)

a. The standard deviations of the least significant digits are given in parentheses.

b. The form of the anisotropic atomic displacement parameters is:

$$U = \exp(-2\pi^2[h^2(a^*)^2U_{11} + k^2(b^*)^2U_{22} + \dots + 2hka^*b^*U_{12}])$$

Table 4.7. Selected Torsional Angles^a (deg).

C10-C1-C2-C3	-54.2(3)	C11-C12-C13-C14	57.2(2)
C1-C2-C3-O3C ^b	-105.1(5)	C7-C8-C14-C27	62.1(2)
C1-C2-C3-O3H ^b	-76.2(3)	C9-C8-C14-C27	-69.3(2)
C1-C2-C3-C4	50.1(3)	C7-C8-C14-C15	-55.5(2)
O3C-C3-C4-C23 ^b	-26.1(5)	C9-C8-C14-C15	173.1(2)
O3H-C3-C4-C23 ^b	-59.3(3)	C7-C8-C14-C13	-174.4(2)
C2-C3-C4-C23	176.5(2)	C9-C8-C14-C13	54.2(2)
O3C-C3-C4-C5 ^b	105.6(5)	C12-C13-C14-C27	68.4(2)
O3H-C3-C4-C5 ^b	72.4(3)	C26-C13-C14-C27	-174.5(2)
C2-C3-C4-C5	-51.8(3)	C18-C13-C14-C27	-52.1(2)
C3-C4-C5-C6	172.1(2)	C12-C13-C14-C15	-173.0(2)
C23-C4-C5-C6	-58.3(2)	C26-C13-C14-C15	-56.0(2)
C3-C4-C5-C24	-68.9(2)	C18-C13-C14-C15	66.4(2)
C23-C4-C5-C24	60.7(2)	C12-C13-C14-C8	-53.6(2)
C3-C4-C5-C10	55.4(2)	C26-C13-C14-C8	63.5(2)
C23-C4-C5-C10	-175.0(2)	C18-C13-C14-C8	-174.14(15)
C24-C5-C6-C7	74.1(2)	C27-C14-C15-C16	91.5(2)
C4-C5-C6-C7	-166.2(2)	C8-C14-C15-C16	-149.7(2)
C10-C5-C6-C7	-50.3(2)	C13-C14-C15-C16	-29.8(2)
C5-C6-C7-C8	58.6(2)	C14-C15-C16-C17	-22.8(3)
C6-C7-C8-C14	162.9(2)	C15-C16-C17-C22	159.8(2)
C6-C7-C8-C9	-62.6(2)	C15-C16-C17-C28	-84.6(2)
C7-C8-C9-C25	-65.0(2)	C15-C16-C17-C18	38.9(3)
C14-C8-C9-C25	68.3(2)	C12-C13-C18-C19	62.4(2)
C7-C8-C9-C11	176.1(2)	C26-C13-C18-C19	-55.6(2)
C14-C8-C9-C11	-50.6(2)	C14-C13-C18-C19	-178.7(2)
C7-C8-C9-C10	58.7(2)	C12-C13-C18-C17	-169.8(2)
C14-C8-C9-C10	-168.02(15)	C26-C13-C18-C17	72.2(2)
C2-C1-C10-C5	59.7(2)	C14-C13-C18-C17	-50.9(2)
C2-C1-C10-C9	-165.5(2)	C22-C17-C18-C19	6.9(3)
C6-C5-C10-C1	-175.7(2)	C16-C17-C18-C19	127.1(2)
C24-C5-C10-C1	62.9(2)	C28-C17-C18-C19	-111.3(2)
C4-C5-C10-C1	-59.0(2)	C22-C17-C18-C13	-121.1(2)
C6-C5-C10-C9	50.3(2)	C16-C17-C18-C13	-0.9(3)
C24-C5-C10-C9	-71.1(2)	C28-C17-C18-C13	120.7(2)
C4-C5-C10-C9	167.0(2)	C13-C18-C19-C20	177.7(2)
C25-C9-C10-C1	-60.1(2)	C17-C18-C19-C20	48.4(3)
C11-C9-C10-C1	57.4(2)	C18-C19-C20-C30	-171.8(2)
C8-C9-C10-C1	173.4(2)	C18-C19-C20-C29	70.1(3)
C25-C9-C10-C5	71.7(2)	C18-C19-C20-C21	-52.9(3)
C11-C9-C10-C5	-170.8(2)	C30-C20-C21-C22	119.7(3)
C8-C9-C10-C5	-54.7(2)	C29-C20-C21-C22	-120.5(3)
C25-C9-C11-C12	-74.3(2)	C19-C20-C21-C22	1.6(3)
C10-C9-C11-C12	165.5(2)	C20-C21-C22-C17	53.9(3)
C8-C9-C11-C12	50.2(2)	C16-C17-C22-C21	179.4(2)
C9-C11-C12-C13	-57.7(2)	C28-C17-C22-C21	63.2(3)
C11-C12-C13-C26	-62.8(2)	C18-C17-C22-C21	-57.6(3)
C11-C12-C13-C18	176.9(2)		

a. The standard deviations of the least significant digits are given in parentheses.

b. O3H and O3C are the alternate positions for the disordered -C-OH and -C=O oxygens.

Structure Description: A new sample of epifriedelin-3-ol, isolated from a Thai source (Phaopongthai, 1995), was available for redetermination of the single crystal x-ray structure. The redetermined structure of the anomalous compound is illustrated in Figure 4.4 with the major occupancy O3H hydroxyl group represented as a dark ellipsoid and the minor occupancy O3C carbonyl group as a light ellipsoid. It should be noted that for any given molecule in the lattice it is either the hydroxyl form or the carbonyl form. The refined occupancy indicates that 68% of the molecules are hydroxyl form and 32% are carbonyl form. Interatomic bond distances and angles are given in Tables 4.8 and 4.9, mean planes and atomic displacements from the planes in Table 4.10, and selected torsional angles in Table 4.11.

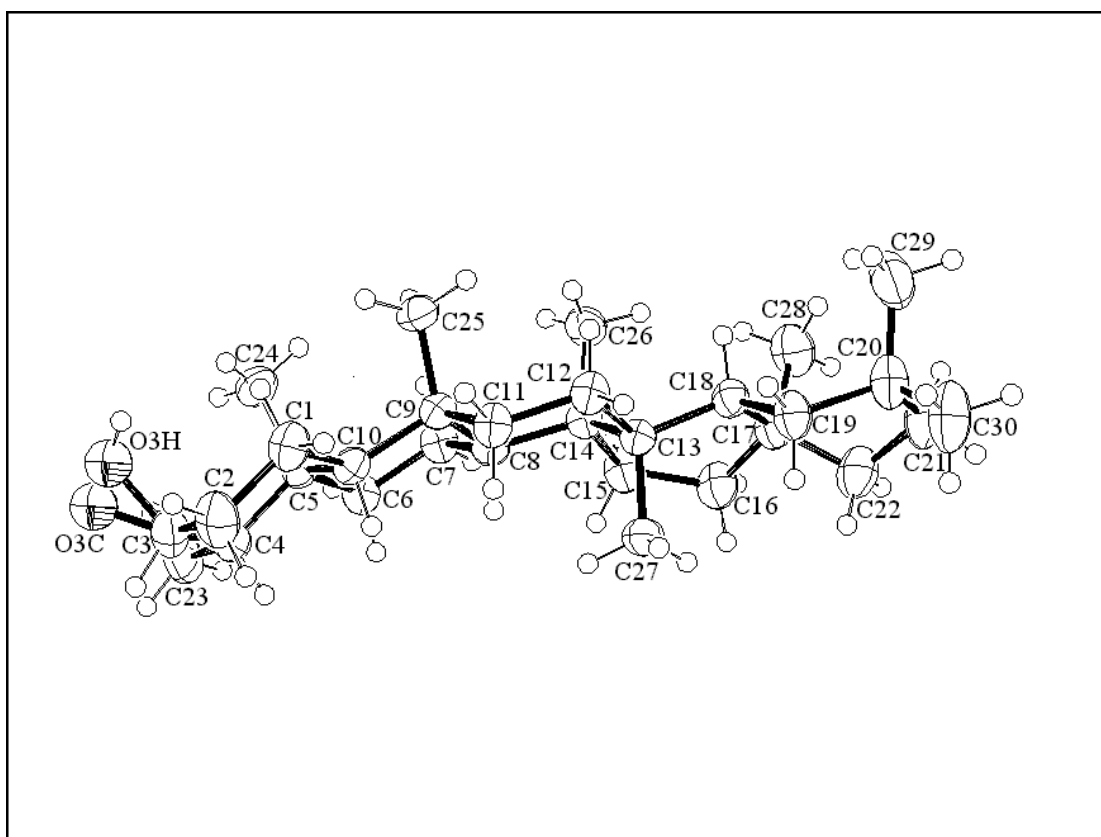


Figure 4.4. The structure of disordered epifriedelin-3-ol and friedelin-3-one.

Table 4.8. Selected Interatomic Distances^a.

C1–C2	1.521(3)
C1–C10	1.538(2)
C2–C3	1.508(3)
C3–O3H ^b	1.426(4)
C3–O3C ^b	1.251(6)
C3–C4	1.523(3)
C4–C23	1.531(3)
C4–C5	1.562(3)
C5–C6	1.539(3)
C5–C24	1.542(3)
C5–C10 *	1.564(2)
C6–C7	1.521(3)
C7–C8	1.532(2)
C8–C14	1.561(3)
C8–C9 *	1.562(2)
C9–C25	1.545(3)
C9–C11	1.545(2)
C9–C10	1.562(3)
C11–C12	1.533(3)
C12–C13	1.545(2)
C13–C26	1.555(3)
C13–C18	1.559(3)
C13–C14 *	1.574(2)
C14–C27	1.545(3)
C14–C15	1.553(3)
C15–C16	1.540(3)
C16–C17	1.540(3)
C17–C22	1.533(3)
C17–C28	1.551(3)
C17–C18 *	1.585(3)
C18–C19	1.541(3)
C19–C20	1.540(3)
C20–C30	1.527(3)
C20–C29	1.529(4)
C20–C21	1.553(3)
C21–C22	1.515(4)
O3H–O3C ^b	0.720

- a. The standard deviations of the least significant digits are given in parentheses.
 b. O3H and O3C are the alternate positions for the disordered –C–OH and –C=O oxygen atom. O3H–O3C is the apparent separation of the disordered positions. Ring junction bonds are denoted by *.

Table 4.9. Selected Bond Angles (deg)

C2–C1–C10	110.9(2)	C12–C13–C26	106.7(2)
C3–C2–C1	112.9(2)	C12–C13–C18	110.70(15)
O3C–C3–C2 ^b	125.6(3)	C26–C13–C18	110.5(2)
O3H–C3–C2 ^b	109.1(2)	C12–C13–C14	108.14(14)
O3C–C3–C4 ^b	117.0(3)	C26–C13–C14	111.50(15)
O3H–C3–C4 ^b	112.8(2)	C18–C13–C14	109.22(14)
C2–C3–C4	112.9(2)	C27–C14–C15	107.7(2)
C3–C4–C23	111.1(2)	C27–C14–C8	109.5(2)
C3–C4–C5	113.4(2)	C15–C14–C8	109.27(15)
C23–C4–C5	115.3(2)	C27–C14–C13	111.99(15)
C6–C5–C24	108.9(2)	C15–C14–C13	108.3(2)
C6–C5–C4	108.3(2)	C8–C14–C13	110.06(14)
C24–C5–C4	110.0(2)	C16–C15–C14	115.9(2)
C6–C5–C10	108.32(14)	C17–C16–C15	118.7(2)
C24–C5–C10	113.9(2)	C22–C17–C16	108.0(2)
C4–C5–C10	107.2(2)	C22–C17–C28	107.1(2)
C7–C6–C5	113.8(2)	C16–C17–C28	108.1(2)
C6–C7–C8	110.3(2)	C22–C17–C18	109.3(2)
C7–C8–C14	114.57(14)	C16–C17–C18	112.7(2)
C7–C8–C9	110.35(15)	C28–C17–C18	111.4(2)
C14–C8–C9	116.94(14)	C19–C18–C13	111.8(2)
C25–C9–C11	106.6(2)	C19–C18–C17	111.4(2)
C25–C9–C10	111.0(2)	C13–C18–C17	114.3(2)
C11–C9–C10	109.69(15)	C18–C19–C20	115.9(2)
C25–C9–C8	115.6(2)	C30–C20–C29	108.2(2)
C11–C9–C8	107.57(14)	C30–C20–C19	108.1(2)
C10–C9–C8	106.36(14)	C29–C20–C19	110.2(2)
C1–C10–C5	110.42(15)	C30–C20–C21	109.4(2)
C1–C10–C9	115.2(2)	C29–C20–C21	111.7(2)
C5–C10–C9	116.66(15)	C19–C20–C21	109.2(2)
C12–C11–C9	113.86(15)	C22–C21–C20	113.3(2)
C11–C12–C13	113.9(2)	C21–C22–C17	113.7(2)

a. The standard deviations of the least significant digits are given in parentheses.

b. O3H and O3C are the alternate positions for the disordered –C–OH and –C=O oxygen atom.

Table 4.10. Least-Squares Mean Planes^a and Atomic Deviations (Å) from the Planes.

Plane 1. Carbonyl Atoms (RMSD of fitted atoms = 0.075 Å)					
1.805(19) x + 6.337(3) y - 2.72(12) z = 0.89(5)					
defining atoms	hydroxyl group atoms		bonded atoms		
* -0.041(1)	C2	-0.749(5)	O3H	-1.311(6)	C1
* 0.130(3)	C3	-1.367(21)	H3HO	-1.359(5)	C5
* -0.037(1)	C4	-0.749(5)	O3H	0.230(5)	C23
* -0.052(1)	O3C				
Plane 2. Ring A Atoms (RMSD of fitted atoms = 0.234 Å)					
- 0.198(13) x + 5.344(3) y + 16.432(24) z = 7.700(10)					
defining atoms	equatorially bound atoms		axially bound atoms		
* 0.245(2)	C1	-0.092(2)	H1A	1.213(2)	H1B
* -0.195(2)	C2	0.207(2)	H2B	-1.158(2)	H2A
* 0.188(2)	C3	0.116(7)	O3C	0.581(4)	O3H
* -0.221(2)	C4	0.107(4)	C23	-1.199(2)	H4
* 0.263(1)	C5	-0.374(3)	C6	1.797(3)	C24
* -0.279(2)	C10		C9		H10
Plane 3. Ring B Atoms (RMSD of fitted atoms = 0.238 Å)					
- 1.274(12) x + 6.013(2) y + 10.145(22) z = 5.277(8)					
defining atoms	equatorially bound atoms		axially bound atoms		
* 0.252(1)	C9	-0.416(3)	C11	1.777(3)	C25
* -0.212(1)	C10	0.072(4)	C1	-1.189(1)	H10
* 0.188(1)	C5	-0.649(3)	C4	1.691(3)	C24
* -0.215(2)	C6	0.145(2)	H6B	-1.182(2)	H6A
* 0.268(2)	C7	-0.027(2)	H7B	1.238(2)	H7A
* -0.282(1)	C8	-0.210(3)	C14	-1.241(1)	H8
Plane 4. Ring C Atoms (RMSD of fitted atoms = 0.228 Å)					
- 1.170(11) x + 6.373(1) y + 2.852(23) z = 3.297(7)					
defining atoms	equatorially bound atoms		axially bound atoms		
* 0.251(2)	C12	-0.058(2)	H12A	1.221(2)	H12B
* -0.219(2)	C11	0.143(2)	H11A	-1.186(2)	H11B
* 0.196(1)	C9	-0.622(3)	C10	1.707(3)	C25
* -0.215(1)	C8	0.082(3)	C7	-1.194(1)	H8
* 0.235(1)	C14	-0.411(4)	C15	-1.799(3)	C26
* -0.247(1)	C13	0.337(3)	C18		C27
Plane 5. Ring D Atoms (RMSD of fitted atoms = 0.278 Å)					
- 4.359(13) x + 6.020(2) y + 4.173(29) z = 2.680(6)					
defining atoms	equatorially bound atoms		axially bound atoms		
* 0.131(2)	C18	-0.619(4)	C19	1.052(2)	H18
* -0.434(1)	C13	-0.252(4)	C12	1.879(3)	C27
* 0.350(2)	C14	-0.098(4)	C8	-1.962(3)	C26
* 0.026(2)	C15	-0.733(2)	H15A	0.783(2)	H15B
* -0.295(2)	C16	0.056(2)	H16B	-1.259(2)	H16A
* 0.222(2)	C17	-0.619(4)	C22		C28
Plane 6. Ring E Atoms (RMSD of fitted atoms = 0.293 Å)					
- 3.622(16) x + 6.187(2) y + 0.275(36) z = 2.318(7)					
defining atoms	equatorially bound atoms		axially bound atoms		
* 0.232(2)	C20	-0.585(5)	C30	1.664(4)	C29
* -0.399(2)	C19	-0.287(2)	H19B	-1.352(2)	H19A
* 0.164(2)	C18	-0.581(4)	C13	-0.456(4)	C16
* 0.246(2)	C17	1.088(2)	H18	1.717(4)	C28
* -0.424(2)	C22	-0.357(3)	H22B	-1.366(2)	H22A
* 0.181(2)	C21		H21A		H21B

a. Coordinates (x, y, z) are in crystal coordinates. Interplanar angles:
 Carbonyl-A=39.79(18), A-B=14.49(9), B-C=14.52(5), C-D=14.15(6), D-E=8.22(9).

The bond distances and endocyclic bond angles for the five ring skeleton are normal for a friedelin system. The ring junction bonds, identified by * in Table 4.8, $d[\text{C5-C10}] = 1.564(2)$, $d[\text{C8-C9}] = 1.562(2)$, $d[\text{C13-C14}] = 1.574(2)$, and $d[\text{C17-C18}] = 1.583(3)\text{\AA}$ are long for C–C single bonds due to steric effects from the predominance of axial substituents on one side of the skeleton. These axial groups cause the pentacyclic ring skeleton to be significantly bowed (as seen from the dihedral angles of $14.49(9)$, $14.52(5)$, $14.15(6)$, and $8.22(9)^\circ$ between planes A and B, B and C, C and D, and D and E, respectively) due to the repulsive interactions between the axial methyl groups. This can also be seen in the positioning of the methyl groups where the position of the C24 methyl group is determined by a C–H \cdots O interaction to the hydroxy oxygen ($d[\text{C24-O3H}] = 2.979(4)$; $d[\text{O3H}\cdots\text{H24a}] = 2.490(14)\text{\AA}$), the C25 methyl group is ‘gearing’ to the C24 methyl group ($d[\text{C24-C25}] = 3.185\text{\AA}$), and the C27 methyl group is ‘gearing’ to the C25 methyl group ($d[\text{C25-C27}] = 3.133\text{\AA}$).

Examination of the displacements from the respective least squares mean planes given in Table 4.10 shows the conformations of rings A, B, and C are chair forms (displacement pattern + – + – + –) and rings D and E are boat forms (+ – + + – +) (Masaki, Niwa and Kikuchi, 1975; Rogers, Philips, Joshi and Viswanathan, 1980). The values of the displacements are similar to those previously reported for friedelin structures.

Torsion angles across the ring junctions (*trans* positions) in Table 4.11 illustrate the difference between chair/chair and boat/boat junctions for which the ideal values are 180° and 120° , respectively. The average deviation of 8.3° for the

chair/chair junction is due to the steric interactions discussed above. The boat/boat junction only deviates 4.1° from the ideal value due to greater distances between the axial ligands of rings E and F. The chair/boat ring junction between C and D includes trans methyl substituents and exhibits torsion angles about C13–C14 of 174° , corresponding to a 6° rotation from an ideal *trans*-geometry.

Table 4.11. Torsion Angles Across Ring Junctions.

Junction	Atoms	Torsion Angles
A–B	C6–C5–C10–C1	$-175.7(2)$
A–B	C4–C5–C10–C9	$167.0(2)$
B–C	C7–C8–C9–C11	$176.1(2)$
B–C	C14–C8–C9–C10	$-168.0(2)$
C–D	C12–C13–C14–C15	$-173.0(2)$
C–D	C18–C13–C14–C8	$-174.1(2)$
	C26–C13–C14–C27	$-174.5(2)$
D–E	C16–C17–C18–C19	$127.1(2)$
D–E	C22–C17–C18–C13	$-121.1(2)$

The present sample, as well as the anomalous compound, crystallize in space group *C2* and are isomorphous with the authentic sample of epifriedelin-3-ol previously reported (Laing, Burke-Laing, Bartho, and Weeks, 1977). The O3 sites on adjacent molecules are related pairwise across the 2-fold axis. The major component is present in more than 50% of the sites and does hydrogen bond across the 2-fold,

$d[\text{O3H}\cdots\text{O3H}] = 2.895 \text{ \AA}$. Similarly, the major and minor occupancy components can also hydrogen bond across the 2-fold, $d[\text{O3H}\cdots\text{O3C}] = 2.902 \text{ \AA}$. However, $d[\text{O3C}\cdots\text{O3C}] = 2.760 \text{ \AA}$, without an intervening hydrogen precludes the possibility of two minor component molecules coexisting across this 2-fold. The shortest C–H \cdots O contact of 3.41 \AA , shows no C–H \cdots O hydrogen bond interactions.

Comparing the anomalous structure identified in Figure 1 with the current structure shows a strong similarity. In the anomalous compound, $d[\text{C}–\text{O}] = 1.33 \text{ \AA}$ and the sum of the nonhydrogen angles about C(3) = 343.1° . The refinement of the disordered model reported herein has occupancies of 0.680 for the hydroxy form and 0.320 for the keto form. If it were refined modeling the oxygen atom as a single anisotropic atom, the atomic displacement parameters of the oxygen will extend in the direction of the two positions given here as O3H and O3C and the apparent atomic position should lie quite close to the occupancy weighted center between the two peaks, *i.e.* mathematically,

$$d[\text{C3}–\text{O}] = (\alpha)(d[\text{C3}–\text{O3H}]) + (1 - \alpha)(d[\text{C3}–\text{O3C}]) = 1.370 \text{ \AA}$$

$$\sum\angle[\text{C}(3)] = (\alpha)(\sum\angle[\text{C}(3–\text{OH})]) + (1 - \alpha)(\sum\angle[\text{C}(3=\text{O})]) = 341.4^\circ$$

where α is the occupancy of hydroxy atoms, and $(1 - \alpha)$ is the occupancy of the keto atom. The good agreement between the values for the anomalous structure and the occupancy weighted averages in the current structure strongly indicate that the structures are the same and the reason for the anomalous value in the literature is the failure to model the disorder.

4.4. Conclusion

Structure correlation, examining the hybridization of the oxygen atom attached to C3 of ring A of all known friedelane structures, showed the expected bimodal distribution for carbon-oxygen bond length versus bond angles about C3, except for one structure. Redetermination and correction of the anomalous structure shows it contains two different friedelane species, epifriedelin-3-ol and friedelin-3-one, demonstrating the ability of structure correlation methods to identify an incorrect structure entry in the crystallographic database.

Chapter V

25,26-Oxidofriedel-1,3-dione

5.1 Introduction

Structural information is essential in chemistry, not only for determining the geometrical arrangement of atoms within a molecule or a crystal, but also because each structure may tell something about the electron distribution, the type and properties of bonds connecting the atoms in their potential energy minimum, and to some extent, about their reactivity. X-ray diffraction techniques that are able to determine this information for virtually all atoms in the molecule are now the most popular and reliable methods of solid state structure analysis. The analysis is carried out on crystalline solids, preferably, on single crystals. Nowadays, the structure determination of small and medium sized organic molecules, including biologically important polymers, is readily achieved. The number of structures already determined by x-ray crystallography is such that computer-assisted systematic searches in databases such as the Cambridge Structure Database, presently containing more than 270,000 organic structures (CCDC, 2002), permits a new approach to structure analysis. Chemical information may be extracted from these data through extensive comparisons between large numbers of related molecules.

Generally, molecular packing of organic compounds are held together by attractive electrostatic forces based on charge localization in the molecule (the strongest of which are hydrogen bonds), and/or van der Waals interactions (also

called dispersion bonds). van der Waals interactions occur when equal atoms are in contact and induced dipoles interact to give small short-term attractive forces.

Taylor and Kennard (1982) established that weak C–H···O, C–H···N, and C–H···Cl interactions are important in describing the packing of molecular compounds into crystals. Sarma and Desiraju (1986) extended this concept to include motifs such as Cl···Cl which do not include hydrogen. This interaction of groups of atoms interacting in the same way (such a grouping is often called a supramolecular synthon) throughout a large range of dissimilar compounds led to the idea of crystal engineering. Since then, many additional interactions have been demonstrated using the technique of structure correlation based on the large and growing structural databases (Burgi and Dunitz, 1994a, 1994b). Furthermore, several types of interactions such as C–H···O interactions have been refined into subtypes of interactions. Of particular relevance to the work presented in this chapter are the two C–H···O interactions where the acceptor is a carbonyl group or a hydroxy group, as illustrated in Figure 5.1.

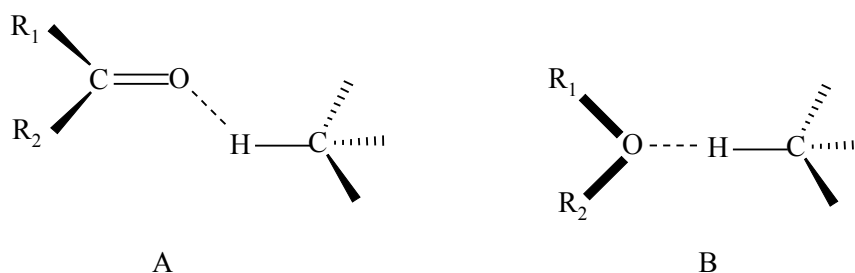


Figure 5.1. Carbonyl (A) and ethereal (B) acceptor motifs of C–H···O interactions.

These interactions can be characterized by the carbon to acceptor oxygen distance, $d[\text{C}\cdots\text{O}]$, or the hydrogen to acceptor oxygen distance, $d[\text{H}\cdots\text{O}]$, and the

interaction angles θ and ϕ at the donor hydrogen and acceptor oxygen atoms as shown in Figure 5.2. The two motifs are quite different; C–H \cdots O contacts for carbonyl acceptors tend to lie in the plane defined by the sp^2 oxygen atom and its lone pairs, resulting in H \cdots O=C angles close to 120° , while C–H \cdots O contacts for ethereal acceptors tend to lie in the plane of the sp^3 oxygen atom and its lone pairs, which bisects the R₁OR₂ angle. Desiraju (1991) elucidated the significance of C–H \cdots O hydrogen bonds in organic crystals by considering C–H \cdots O lengths, angles, and associated spectroscopic data.

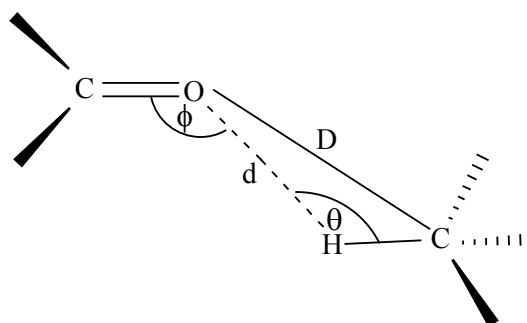


Figure 5.2. Geometry of the C–H \cdots O hydrogen bond.

Steiner and Desiraju (1998) described the fundamental difference between C–H \cdots O hydrogen bonds and van der Waals interactions in terms of the different bond length and angle directionality characteristics of these interactions. They established the angular distribution of C–H \cdots O interactions for different types of C–H groups and showed that the directionality decreases with decreasing C–H polarization. For the acidic ethynyl donors C \equiv C–H, the mean C–H \cdots O angle θ was $152(2)^\circ$, for vinyl donors C=CH₂ \cdots O the mean angle θ falls to $143(1)^\circ$, and for the weakly polarized methyl donors of the ethyl group the mean angle θ falls further to

The anti-parallel motif involves two short C \cdots O interactions and is the most common of the three. While the perpendicular motif and the parallel motif both involve a single short C \cdots O interaction, the anti-parallel motif involves a pair of short C \cdots O interactions. Assuming a perfect rectangular anti-parallel dimer having both $d[\text{C}\cdots\text{O}] = 3.02 \text{ \AA}$ gave an attractive energy of $-22.3 \text{ kJ mol}^{-1}$ and attractive energies less than -20 kJ mol^{-1} over the $d[\text{C}\cdots\text{O}]$ range 2.92-3.32 \AA . Intermolecular perturbation theory calculated an attractive interaction energy of -7.6 kJ mol^{-1} for the single $d[\text{C}\cdots\text{O}]$ again at 3.02 \AA in the perpendicular motif.

Several structures of friedelane type triterpenes have been studied by single crystal x-ray crystallography which gives conformations of the saturated five fused six-membered ring systems. Masaki, Niwa, and Kikuchi (1975) suggested that the extended S form, *i.e.* the chair-chair-chair-boat-boat form is favored for friedelane skeleton systems. Additional support for the S form conformation as the preferred form appeared in the work of Laing, Burke-Laing, Bartho, and Weeks (1977) and Rogers, Philips, Joshi, and Viswanathan (1980). The importance of van der Waals forces to stabilize the solid state packing of the molecules was studied by Rogers, Philips, Joshi, and Viswanathan (1980), and Subramaniun, Selladurai, Sivakumar, Ponnuswany, and Sukumar (1989), while Eggleston (1987) established that the lactone carbonyl oxygen of 12 α -hydroxy-30-oxooleanano-28,31-lactone acts as a hydrogen bond acceptor. Hambley, Lewis, Tucker, and Turner (1998) studied the stereochemistry of 3 β -acetoxy-12 α -bromo-13 β ,28-epoxyoleana-16 α -ol, establishing the presence of a hydrogen bond in the lattice with $d[\text{O}16\cdots\text{O}31]$ less than 3.0 \AA .

Rogers, Williams, Joshi, Kamat, and Viswanathan (1974) first isolated 25,26-oxidofriedel-1,3-dione from *Salacia prinoides* DS and established its structure by an

x-ray study of the dibromo derivative. This compound contains three acceptor oxygen atoms that can form weak C–H \cdots O hydrogen bonds, or noncovalent >C(δ^+) \cdots O(δ^-) dipole-dipole interactions. This chapter reports the single crystal x-ray crystallographic structure investigation of 25,26-oxidofriedel-1,3-dione isolated from *Salacia chinensis* Linn.

5.2 Experimental

Crystal material

Root bark of *S. chinensis* Linn was collected at amphor Jakaraj, Nakorn Ratchasima province, Thailand, in March 2000. Dried powdered root bark of *Salacia chinensis* (1.0 kg) was extracted with dichloromethane for 48 hours, then concentrated under vacuum to yield 4.8 g of red gummy material. Gutta percha was removed by hot methanol extraction, and the filtrate dried under vacuum to yield 0.95 g of product. The extract was subjected to column chromatography over silica gel, eluted with gradually increasing polarity of solvent from hexane to dichloromethane to ethyl acetate, and finally to methanol. The CH₂Cl₂:EtOAc (1:1) fraction was further purified by preparative tlc; the compound with the highest R_f value (0.65) for hexane:CH₂Cl₂:EtOAc (7:2:1) was collected and crystallized by slow evaporation to yield 5.1 mg of 25,26-oxidofriedel-1,3-dione.

Data Collection

A single crystal was selected and mounted on a glass capillary with cyanoacrylate glue and data collection carried out on a KappaCCD diffractometer. Details of the data collection, structure solution, and least squares refinement of 25,26-oxidofriedel-1,3-dione are given in Table 5.1.

Table 5.1. Experimental Details for 25,26-oxidofriedel-1,3-dione.

Crystal data

Chemical formula	$C_{30}H_{46}O_3$
Chemical formula weight (Dalton)	454.67
Crystal habit	equant
Crystal size (mm)	0.27×0.30×0.36
Crystal color	transparent colorless
Crystal system	monoclinic
Space group	$P2_1$
a (Å)	7.6688(1)
b (Å)	16.1829(2)
c (Å)	10.7132(2)
β (°)	109.861(1)
V (Å ³)	1250.46(3)
Z	2
D_{calc} (Mg m ⁻³)	1.208
Radiation type	Mo $K\alpha$
Wavelength (Å)	0.71073
θ range (°)	2.02 - 27.37
μ (mm ⁻¹)	0.075
Temperature (K)	150(2)
Data collection	
Diffractometer	Bruker Nonius KappaCCD

Table 5.1 (Continued)

Data collection method	ω scans plus ϕ scans
Total No. of integrated reflections	15037
$\sin\theta/\lambda_{\max}$ (\AA^{-1})	0.647
Generator setting (kV/mA)	60 / 50
Refinement	
Refinement on	F^2
No. of observed reflections ($F_o > 4\sigma F_o$)	2622
No. of unique reflection	2903
No. of parameters refined	304
R_{sym}	0.055
R_I for 2622 $F_o > 4\sigma F_o$	0.036
wR for 2622 ($F_o > 4\sigma F_o$)	0.096
R_I for 2903	0.042
wR_2 for 2903	0.100
S	1.048
Weighting scheme	$w = 1/[\sigma^2 (F_o^2) + (0.0698 \times P)^2 + 0.0111 \times P]$ Where $P = [\max(F_o^2, 0) + 2 F_c^2] / 3$
$\rho_{\max} / \rho_{\min} / \rho_{\text{err}}$ (e \AA^3)	0.27 / -0.18 / 0.04
Refinement program	SHELXL-97
Drawing program	ORTEP3

5.3 Results and Discussion

The structure of 25,26-oxidofriedel-1,3-dione was solved by direct methods and refined with SHELXTL (Sheldrick, 1997) as described in Table 5.1. The fractional atomic coordinates and equivalent isotropic displacement parameters are given in Table 5.2, selected bond distances in Table 5.3, and selected bond angles in Table 5.4. A perspective view of 25,26-oxidofriedel-1,3-dione is shown in Figure 5.4.

The average C–C bond distance is 1.514(3) Å, with longer bonds at the ring junctions C5–C10, C8–C9, C13–C14, and C17–C18, as required to relieve the repulsive forces of the methyl substituent groups at the ring junctions and the constraints added by the ether ring. The bond angles are characterized as three types based on the secondary, tertiary, and quaternary carbon atoms. The C–C–C angles at secondary carbon are larger than ideal tetrahedral angles, average = 113.9(16)°, those at tertiary carbon atoms are close to tetrahedral angles, average = 109.9(19)°, and those at quaternary carbon atoms are less than tetrahedral angles, average = 108.6(10)°.

Table 5.2. Fractional Monoclinic Coordinates and Equivalent Isotropic Displacement

Parameters (Å ²).				
Atom ^a	<i>x</i>	<i>y</i>	<i>z</i>	<i>U</i> _{eq} ^b (Å ²)
O1	1.2162(29)	0.2841(2)	-0.0548(1)	0.0287(4)
O3	0.8767(31)	0.1071(2)	-0.3289(1)	0.0347(4)
O25	0.9820(27)	0.4457(2)	0.1535(1)	0.0235(3)
C1	1.1186(38)	0.2258(3)	-0.0519(1)	0.0212(4)
C2	1.1190(42)	0.1487(3)	-0.1334(2)	0.0291(5)
C3	0.9249(40)	0.1195(3)	-0.2109(1)	0.0248(4)
C4	0.7977(38)	0.1128(3)	-0.1301(1)	0.0227(4)
C5	0.7864(36)	0.2006(3)	-0.0709(1)	0.0185(4)
C6	0.6540(36)	0.1959(3)	0.0091(1)	0.0204(4)
C7	0.6644(36)	0.2707(2)	0.0975(1)	0.0198(4)
C8	0.8611(36)	0.2818(3)	0.1986(1)	0.0174(4)
C9	1.0051(36)	0.2951(2)	0.1272(1)	0.0184(4)
C10	0.9863(37)	0.2227(3)	0.0272(1)	0.0185(4)
C11	1.1999(38)	0.2900(3)	0.2350(2)	0.0231(4)

Table 5.2 (Continued)

C12	1.2314(37)	0.3484(2)	0.3538(1)	0.0217(4)
C13	1.0746(36)	0.3463(3)	0.4148(1)	0.0169(4)
C14	0.8802(36)	0.3517(2)	0.3010(1)	0.0169(4)
C15	0.7242(39)	0.3470(3)	0.3636(1)	0.0227(4)
C16	0.7813(41)	0.3701(3)	0.5110(2)	0.0270(4)
C17	0.9277(39)	0.4389(3)	0.5579(1)	0.0212(4)
C18	1.0970(36)	0.4232(3)	0.5085(1)	0.0176(4)
C19	1.2832(39)	0.4219(3)	0.6255(1)	0.0244(4)
C20	1.3149(39)	0.4957(3)	0.7220(1)	0.0229(4)
C21	1.1451(41)	0.5059(3)	0.7695(1)	0.0270(5)
C22	0.9958(41)	0.4402(3)	0.7105(2)	0.0269(4)
C23	0.6126(42)	0.0733(3)	-0.2093(2)	0.0339(5)
C24	0.7134(40)	0.2628(3)	-0.1862(1)	0.0245(4)
C25	0.9756(40)	0.3807(3)	0.0608(1)	0.0225(4)
C26	0.8548(39)	0.4339(3)	0.2230(1)	0.0202(4)
C27	1.0925(41)	0.2628(3)	0.4901(1)	0.0253(4)
C28	0.8317(46)	0.5226(3)	0.5084(2)	0.0295(4)
C29	1.3509(43)	0.5752(3)	0.6576(1)	0.0291(5)
C30	1.4880(45)	0.4772(3)	0.8429(2)	0.0357(5)

a. Estimated standard deviations in the least significant digits are given in parentheses.

b. The form of the equivalent isotropic displacement parameter is

$$U_{eq} = \exp(-2\pi^2[h^2(a^*)^2 U_{11} + k^2(b^*)^2 U_{22} + \dots + 2hka^*b^* U_{12}])$$

Table 5.3. Selected Bond Distances (Å) for 25,26-oxidofriedel-1,3-dione.

Bond	distances	Bond	distances	Bond	distances
C1–C2	1.523(3)	C9–C25	1.538(3)	C13–C18	1.572(3)
C2–C3	1.513(3)	C9–C11	1.550(3)	C18–C19	1.547(3)
C3–C4	1.512(3)	C11–C12	1.537(3)	C19–C20	1.543(3)
C4–C5	1.570(3)	C12–C13	1.551(3)	C20–C21	1.559(3)
C4–C23	1.525(3)	C13–C14*	1.576(3)	C20–C29	1.529(3)
C5–C24	1.543(3)	C13–C27	1.557(3)	C20–C30	1.536(3)
C5–C10*	1.578(3)	C14–C26	1.547(3)	C21–C22	1.532(3)
C5–C6	1.538(3)	C14–C15	1.559(3)	C22–C17	1.538(3)
C6–C7	1.522(3)	C15–C16	1.535(3)	C1–O1	1.210(3)
C7–C8	1.540(3)	C16–C17	1.539(3)	C3–O3	1.208(3)
C8–C9*	1.558(3)	C17–C18*	1.585(3)	C1–C10	1.529(3)
C8–C14	1.547(3)	C9–C10	1.560(3)	C17–C28	1.547(3)

a. Estimated standard deviations in the least significant digits are given in parentheses.

b. * as C–C at ring junction.

Table 5.4. Selected Bond Angles (°) for 25,26-oxidofriedel-1,3-dione.

C10–C1–C2	114.94(2)	C11–C12–C13	114.11(2)
C10–C1–O1	124.96(2)	C12–C13–C14	109.77(2)
C2–C1–O1	120.09(2)	C12–C13–C18	108.62(2)
C1–C2–C3	112.21(2)	C13–C14–C15	109.09(2)
C2–C3–C4	114.46(2)	C13–C14–C8	110.14(2)
C2–C3–O3	121.37(2)	C13–C14–C26	112.19(2)
C3–C4–C5	107.08(2)	C8–C14–C26	106.35(2)
C3–C4–C23	111.77(2)	C15–C14–C26	107.46(2)
C5–C4–C23	115.84(2)	C14–C15–C16	116.02(2)
C4–C5–C6	108.54(2)	C15–C16–C17	115.68(2)
C4–C5–C10	107.42(2)	C16–C17–C18	111.45(2)
C4–C5–C24	110.53(2)	C16–C17–C22	107.67(2)
C6–C5–C24	110.53(2)	C16–C17–C28	108.16(2)

Table 5.4 (Continued)

C6–C5–C10	108.39(2)	C22–C17–C28	107.67(2)
C5–C6–C7	113.71(2)	C18–C17–C28	112.02(2)
C6–C7–C8	111.22(2)	C17–C18–C13	114.67 (2)
C7–C8–C9	111.03(2)	C17–C18–C19	111.60(2)
C7–C8–C14	114.69(2)	C13–C18–C19	112.15(2)
C9–C8–C14	109.61(2)	C18–C19–C20	115.07(2)
C8–C9–C10	108.53(2)	C19–C20–C21	109.97(2)
C8–C9–C25	109.49(2)	C19–C20–C29	111.12(2)
C8–C9–C11	106.89(2)	C19–C20–C30	107.98(2)
C10–C9–C25	113.25(2)	C21–C20–C29	110.92(2)
C9–C10–C5	118.01(2)	C21–C20–C30	108.91(2)
C5–C10–C1	108.39(2)	C29–C20–C30	107.85(2)
C10–C9–C11	108.26(2)	C20–C21–C22	112.45(2)
C9–C11–C12	115.20(2)	C21–C22–C17	112.57(2)
C9–C25–O25	112.08(2)	C14–C26–O25	114.50(2)
C25–O25–C26	113.15(2)	C4–C3–O3	124.06(2)

a. Estimated standard deviations in the least significant digits are given in parentheses.

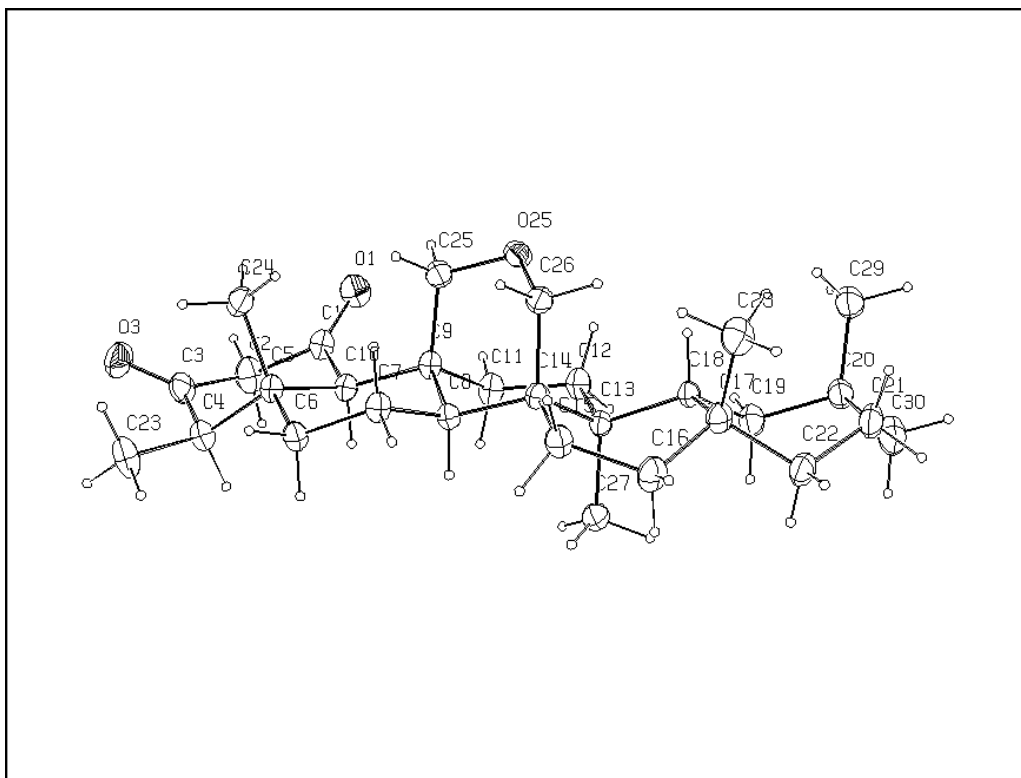


Figure 5.4. The structure of 25,26-oxidofriedel-1,3-dione.

The conformation of the ring system can be seen from the atom displacements from the mean plane of each ring given in Table 5.5. The conformations are chair chair chair boat boat or S forms corresponding to the prediction of Masaki and coworkers (1975) for a friedelane skeleton. The dihedral angles between the least squares planes of the five fused six-membered rings are 10.23° , 13.53° , 11.52° , and 5.52° for rings A/B, B/C, C/D, and D/E, respectively, showing the skeleton to be more nearly planar because of the ether ring connecting C9 to C14 across the B/C ring junction.

Table 5.5. Least-Squares Mean Planes for 25,26-oxidofriedel-1,3-dione.

Ring A		Ring B		Ring C		Ring D		Ring E	
Atom	z								
C1	0.181	C9	0.218	C12	0.167	C18	0.145	C20	0.220
C2	-0.151	C10	-0.185	C11	-0.193	C13	-0.443	C19	-0.407
C3	0.207	C5	0.185	C9	0.259	C14	0.329	C18	0.183
C4	-0.293	C6	-0.230	C8	-0.313	C15	0.079	C17	0.238
C5	0.319	C7	0.271	C14	0.282	C16	-0.360	C22	-0.439
C10	-0.264	C8	-0.257	C13	-0.201	C17	0.249	C21	0.205

The crystal packing is considered on the basis of C–H···O weak hydrogen bonds and noncovalent $>C(\delta^+) \cdots O(\delta^-)$ dipole-dipole interactions. The geometries of contacts for $>C(\delta^+) \cdots O(\delta^-)$ dipole-dipole interaction were examined using ORTEP3 for distance and angle calculations with noncovalent contact criteria of less than the sum of the van der Waals radii plus a tolerance value (van der Waals radii for C, O, and H are 1.70, 1.52, and 1.06 Å, respectively) (Bondi, 1964). The noncovalent distances at C3=O3···H18(2)–C18(2) and C3=O3···H29b(2)–C29(2) lie on the sum of the van der Waals radii between hydrogen and oxygen at 2.56 Å. For O3···H18(2) the C=O···H angle is 129.03° placing H18(2) directly in contact with the plane of the sp² lone pair electrons of the $>C3=O3$ carbonyl group. While O3···H29b(2) is a short distance contact, the C=O···H angle is 176.12° placing H29b(2) in the plane of the lone pairs of the $>C3=O3$ carbonyl group between the two lone pairs. Thus, this is more likely a chance contact rather than a weak C=O···H hydrogen bond. Table 5.6 lists the characteristics of C–H···O hydrogen bonds at C3 that the perspective view shows in Figure 5.5.

Table 5.6. The Characteristics of C–H···O Weak Hydrogen Bonds at O3.

	d[H···O] Å	d[C···O] Å	>C–H···O θ (degree)	>C=O···H φ (degree)
C=O···H Intermolecular interaction at O3				
C3=O3···H18(2)–C18(2)	2.589	3.586	175.45	129.03
C3=O3···H29b(2)–C29(2)	2.553	3.397	144.21	176.12

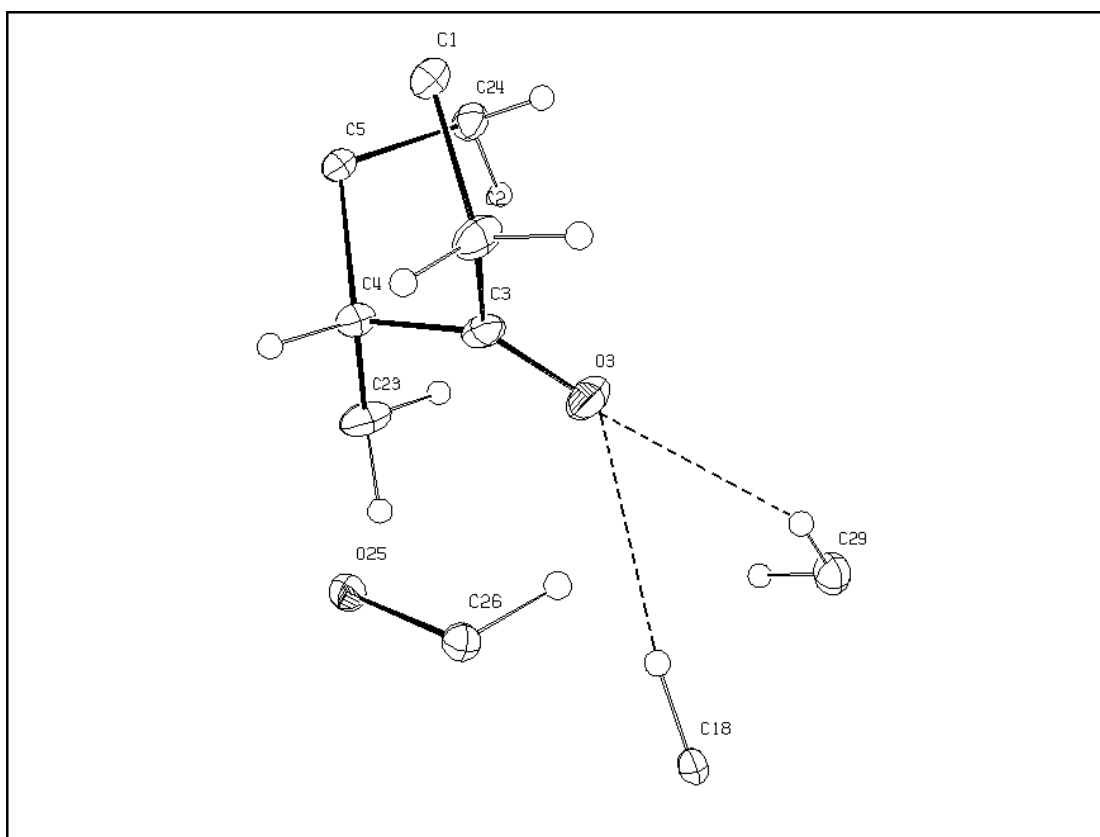


Figure 5.5. Perspective view showing the weak intermolecular C–H···O hydrogen bond at O3.

The $>C(\delta^+) \cdots O(\delta^-)$ dipole-dipole interaction is a noncovalent contact between the carbon atom of the carbonyl group on one molecule and the ether oxygen atom of another molecule in the crystal. The $C(\delta^+) \cdots O(\delta^-)$ noncovalent distance is 2.915 Å and

the angles $\text{O}=\text{C}(\delta^+)\cdots\text{O}(\delta^-)$, $\text{C4}-\text{C3}(\delta^+)\cdots\text{O}(\delta^-)$ and $\text{C2}-\text{C3}(\delta^+)\cdots\text{O}(\delta^-)$ are 91.55° , 88.29° , and 93.54° , respectively. A perspective view of the interaction is shown in Figure 5.6.

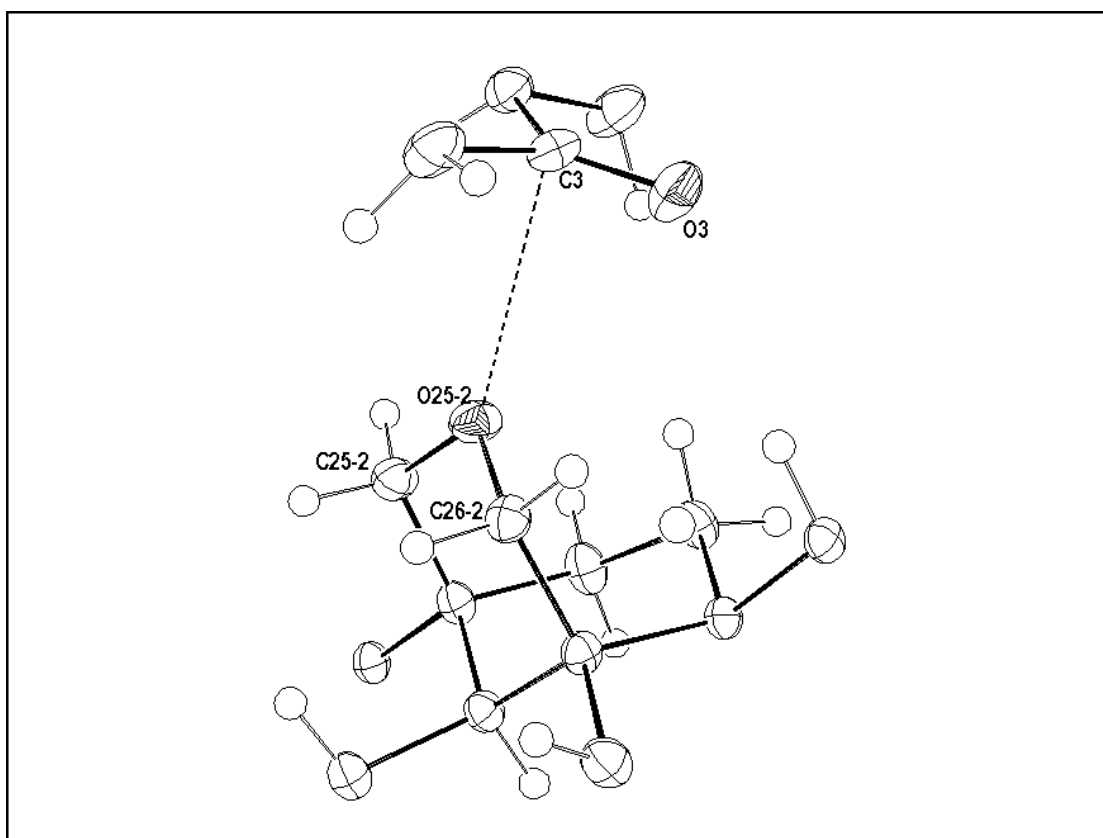


Figure 5.6. Perspective view of the $>\text{C}(\delta^+)\cdots\text{O}(\delta^-)$ dipole-dipole interaction.

The geometry of this carbonyl-ether dipole-dipole interaction is similar to the perpendicular motif of the carbonyl-carbonyl dipole-dipole interaction shown in Figure 1.6 (Allen, Baalham, Lommerse, and Raithby, 1998). The lone pairs of the ether oxygen atom function in the same way as the lone pairs of the electron donor oxygen of one carbonyl group. The lone pairs donate electron density to the positively

polar carbon atom of the acceptor carbonyl group in a kind of bifurcated dipole-dipole bond. Thus the crystal packing of 25,26-oxidofriedel-1,3-dione utilizes C–H···O weak hydrogen bonds and $>C(\delta^+) \cdots O(\delta^-)$ carbonyl-ether dipole-dipole interactions as shown in Figure 5.7.

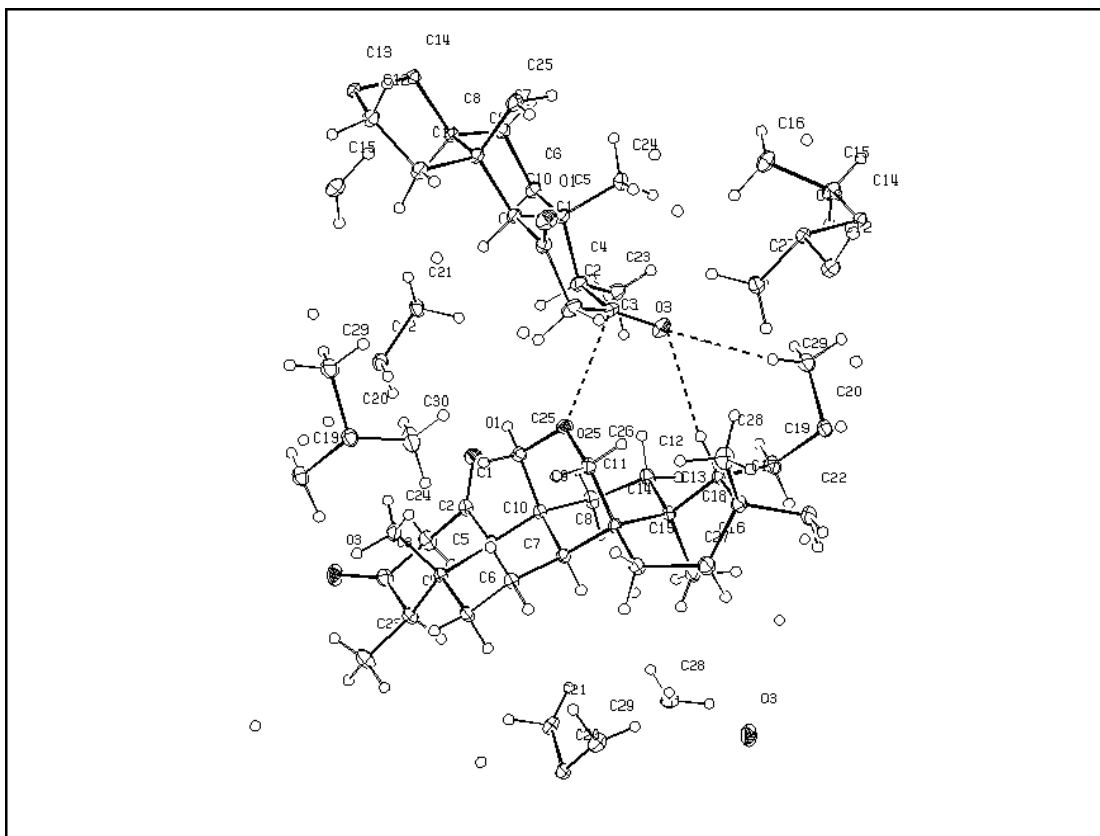


Figure 5.7. The weak C–H···O hydrogen bonds and noncovalent $>C(\delta^+) \cdots O(\delta^-)$ carbonyl-ether dipole-dipole interaction in the 25,26-oxidofriedel-1,3-dione crystal structure.

5.4 The Geometry of the Carbonyl Ether Intermolecular Interaction

The carbonyl-ether dipole-dipole interaction was defined by $C_2C=O$ and $C-O-C$ molecular fragments with an interaction distance $B1$ between the central atoms of the fragments as illustrated in Figure 5.8. The Cambridge Structural Database (CCDC, 2002) was searched for all occurrences of these two fragments where the interaction distance was between 2.0 and 3.3 Å. The lower limit was chosen to exclude normal covalent bonds and the upper limit was chosen as the sum of the van der Waals radii of carbon and oxygen as determined by Bondi (1964) plus a small tolerance value. For each of the 629 structure hits the interaction distance, $B1$, the carbonyl bond length, $B2$, and the angles $A1$, $A2$, and $A3$ characterizing the relationship between the carbonyl fragment and the ether oxygen atom were saved to a file for further analysis. The search was conducted using the ConQuest program provided with the Cambridge Structural Database (CCDC, 2002) and histograms for data analysis were generated using the DPLOT program (USAE, 1999). Histograms are given in Figure 5.9.

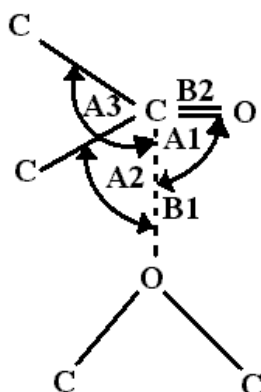
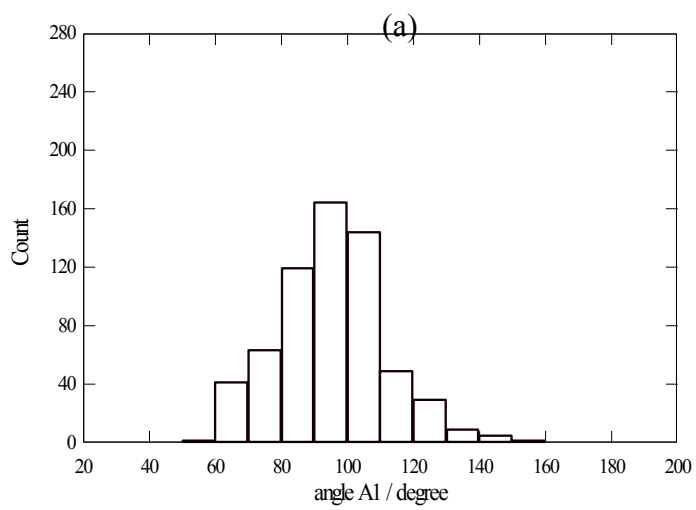
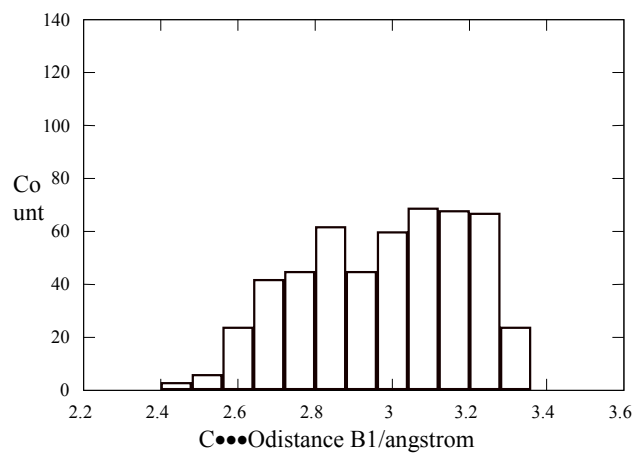
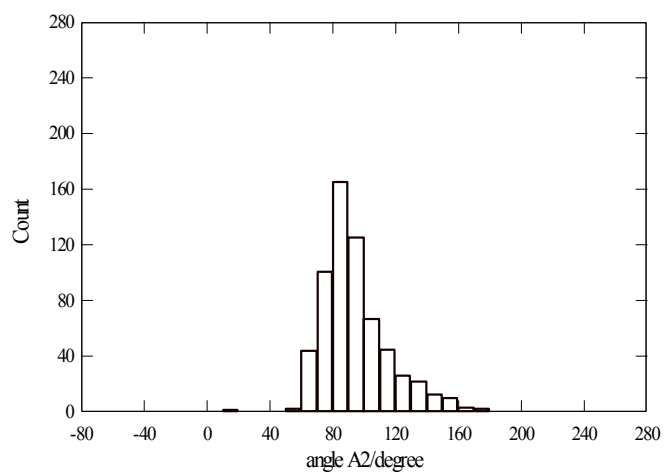


Figure 5.8. The geometric parameters of the carbonyl-ether dipole-dipole interaction.



(b)



(c)

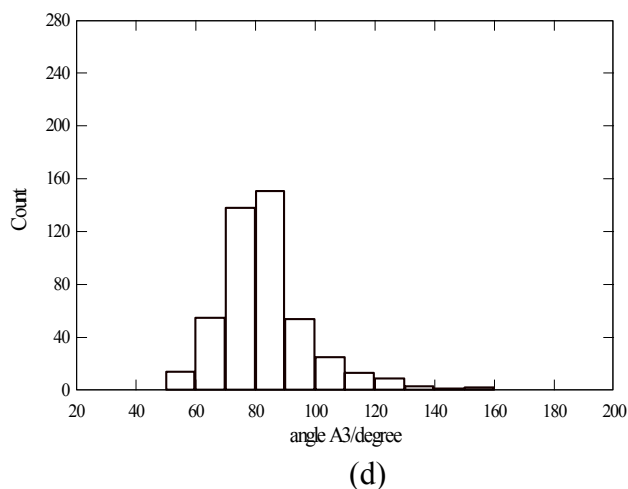


Figure 5.9. Histograms of the $>C(\delta^+)\cdots O(\delta^-)$ carbonyl-ether dipole-dipole interaction; (a) histogram of noncovalent $>C(\delta^+)\cdots O(\delta^-)$ distances defined as B1 (Å) (b) - (d) histograms of the angles between $C\cdots O$ to the plane of the carbonyl group defined as A1, A2, and A3 (°).

The distance histogram shows a peak in the distribution for the $C\cdots O$ distances of $>C(\delta^+)\cdots O(\delta^-)$ carbonyl-ether interaction within the range 2.3 to 3.3 Å, below the sum of the van der Waals radii, indicating an attractive interaction. The peak maximum is at 2.84 Å, followed by a decrease in frequency to 2.92 Å. At larger distances the frequency increases continuously consistent with larger volume elements, and therefore, higher probability of chance encounters in each constant change in radius shell. The mean value of the three angles are 95.37°, 94.42°, and 83.35° for A1, A2, and A3, respectively. These establish the geometry of the $>C(\delta^+)\cdots O(\delta^-)$ carbonyl-ether intermolecular interaction between the carbonyl carbon atom and the ether oxygen atom in the perpendicular contact to the lone pairs of the sp^2 ether oxygen atom.

5.5 Conclusion

25,26-oxidofriedel-1,3-dione (C₃₀H₄₆O₃) was separated from *S. chinensis* Linn and the single crystal x-ray structure determined (monoclinic $P2_1$, $a = 7.6688(1)$, $b = 16.1829(2)$, $c = 10.7132(2)$ Å, $V = 1250.46(3)$ Å³, T 150 K, $Z = 2$, $D_x = 1.208$ g cm⁻³, $\mu = 0.075$ (mm⁻¹), $\lambda(\text{MoK}\alpha) = 0.71073$ Å, and $R_I = 0.042$ for 2903 reflections). The molecular structure exhibits the chair-chair-chair-boat-boat conformation as expected. The crystal packing includes weak C–H \cdots O hydrogen bonds at O3 and a $>\text{C}(\delta^+) \cdots \text{O}(\delta^-)$ carbonyl-ether dipole-dipole interaction *via* the O25 ether oxygen atom and the C3 carbon of the C3=O carbonyl group.

Chapter VI

Conclusions

6.1 Conclusions

The structure correlation method was used to explore the character of five fused six-membered ring friedelane skeletons. The favored conformation of friedelane skeletons is chair-chair-chair-boat-boat or S form which has an average bond distance 1.548(19) Å. The average endocyclic bond angles at secondary and tertiary carbon atoms are larger than 109.4°, as 114.1(20)° and 113(3)°, respectively, while quaternary carbon atoms are less than 109.4° as 108.3(10)°. The average torsion angles for rings A-E are 54(6)°, 54(6)°, 54.3(21)°, 39(7)° and 41(6)°, respectively, which can confirm the ring conformation of friedelane skeletons. The torsion angles across the ring junctions between chair-chair forms are close to 180° while the ring junction between boat-boat forms is close to 120°, which deviates from the normal value because of substituent groups at the ring junction and terminal positions.

The structure correlation method can also indicate anomalous structures in the structure database for which the values of structure parameters deviate from normal values. The method was used to identify a disordered structure in the database by structure correlation of the 34 compounds that contain saturated five fused six-membered rings with the oxygen atom attached to C3 of ring A. The expected bimodal distribution for carbon-oxygen bond length versus bond angles about C3 is

observed in the scatterplot. There was also one point between the two expected positions which was shown to be due to disorder of the oxygen position as a result of the crystal containing two different friedelane species, epifriedelin-3-ol and friedelin-3-one. The structure of the anomalous compound was reinvestigated with single crystal x-ray crystallographic methods (monoclinic $C2$, $a = 13.4372(27)$ Å, $b = 6.4300(13)$ Å, $c = 29.599(6)$ Å, $\beta = 91.97(3)^\circ$, $V = 2552.54$ Å³, $Z = 4$, and $R_I = 0.0563$). The crystal packing includes one weak C–H \cdots O hydrogen bond and a carbonyl-carbonyl interaction. The anomalous structure was resolved into disorder of the oxygen atom corresponding to a mixture of the epifriedelin-3-ol and friedelin-3-one structures in the solid state with occupancies of 0.680(5) for friedelin-3-ol and 0.320(5) for friedelin-3-one.

The structural investigation of 25,26-oxidofriedelan-1,3-dione, $C_{30}H_{46}O_3$, $M_r = 454.67$ separated from *Salacia chinensis* Linn was also carried out (monoclinic $P2_1$, $a = 7.6688(1)$, $b = 16.1829(2)$, $c = 10.7132(2)$ Å, $\beta = 109.861(1)$, $V = 1250.46(3)$ Å³, $Z = 2$, $T = 150$ K, and $R_I = 0.0365$). The conformation of the ring system is S form agreeing with the structure correlation results for the friedelin skeleton. The crystal packing includes C–H \cdots O weak hydrogen bonds and a noncovalent carbonyl-ether interaction between the positive polarity carbon atom of carbonyl group and the negative polarity oxygen atom of the ether linkage C(δ^+) \cdots O(δ^-).

6.2 Suggestions for Further Study

The previously undescribed $>C(\delta^+)\cdots O(\delta^-)$ supramolecular carbonyl-ether intermolecular interaction synthon can be added to the library of synthons available to enable the design and manipulation of molecular systems such as those found in the field of rational drug design, crystal engineering, supramolecular chemistry and physical organic chemistry. Additional studies of spectroscopy such as infrared spectroscopy, and *ab initio* molecular orbital calculations should be used to provide a better understanding of this interaction.

References

References

- Akiyama, T., Tanaka, O. & Iitaka, Y., (1970). **Acta Crystallogr., Sect. B**, 26, 163.
- Allen F. H., Baalham C. A., Lommerse J. P. M., and Raithby P. R., (1998). **Acta Crystallogr., Sect. B**, 54, 320-329.
- Altomare, A., Cascarano, G., Giacovazzo, G., Guagliardi, A., Burla, M. C., Polidori, G. & Camalli, M. (1994). **J. Appl. Cryst.** 27: 435-436.
- Betancor, A., Freire, R., Gonzalez, A. G., Salazar, J. A., Pascard, C. & Prange, T., (1980). **Phytochemistry**, 19, 1989.
- Bondi, A., (1964). **J. Phys. Chem.**, 68:3 441-451.
- Braga, D., Grepioni, F., Biradha, K., Pedireddi R. V. & Desiraju, G. R., (1995). **J. Am. Chem. Soc.**, 117, 3156.
- Burgi, H. B. & Dunitz, J. D., (1994a). **Structure Correlation**, Vol. 1, VCH., New York.
- Burgi, H. B. & Dunitz, J. D., (1994b). **Structure Correlation**, Vol. 2, VCH., New York.
- Burgi, H. B., Dunitz, J. D., & Shefter, E., (1974). **Acta Crystallogr., Sect. B**, 30 1517.
- Burnett, M. N. & Johnson, C. K., (1996). **ORTEP-III; Oak Ridge Thermal Ellipsoid Plot Program For Crystal Structure Illustrations**, Report ORNL-6895, Oak Ridge National Laboratory, Tennessee.

- CCDC, (2001). April 2001 CSD Release Notes, Cambridge Crystallographic Data Center, Cambridge, U.K. (233,218 entries).
- CCDC, (2002). November 2002 CSD Release Notes, version 5.2 Cambridge Crystallographic Data Center, Cambridge, U.K. (272,066 entries).
- Carlisle, C. H., Lindley, P. F. & Parales, A., (1976). **Acta Crystallogr., Sect. B**, 32, 3053.
- Chen, K., Shi, Q., Kashiwada, Y., Zhang D.-C., Hu, C.-Q., Jin, J.-Q., Nozaki, H., Kilkuskie, R. E., Tramontano, E., Cheng, Y.-C., McPhail, D. R., McPhail, A. T. & Lee, K.-H., (1992). **J. Nat. Prod.**, 55, 340-346.
- Clegg, W., (1998), **Crystal Structure Determination**, Oxford University Press.
- Connolly, J. D., Freer, A. A., Anjaneyulu, V., Ravi, K. & Sambasivarao, G., (1986). **Acta Crystallogr., Sect. C (Cr. Str. Comm.)**, 42, 1352.
- Corbett, R. E., Simpson, J., Goh, E. M., Nicholson, B. K., Wilkins, A. L., & Robinson, W.T., (1982). **J. Chem. Soc., Perkin Trans. 2**, 1339.
- Cota, A. B., Mascarenhas, Y. P., Silva, G. D. F. & de Souza, J. R., (1990). **Acta Crystallogr., Sect. C (Cr. Str. Comm.)**, 46, 326.
- Declercq, J-P., van Puyvelde, L., de Kimpe, N., Nagy, M., Verhegge, G. & de Vierman, R., (1991). **Acta Crystallogr., Sect. C (Cr. Str. Comm.)**, 47, 209-211.
- Desiraju, G. R., (1991). **Acc. Chem. Res.**, 24, 290-296
- Dhaneshwar, N. N., Sawaikar, D. D., Narayanan, C. R., Tarale, S. S. & Guru Row, T. N., (1987). **Acta Crystallogr., Sect. C (Cr. Str. Comm.)**, 43, 66.

- Domenicano, A. & Hargittai, I., (1992). **Accurate Molecular Structures: Their Determination and Importance**, International Union of Crystallography, Oxford University Press.
- Douglas, E. B., McDaniel, H. D., and Alexander, J. J., (1993), **Concepts and Models of Inorganic Chemistry**, John Wiley & Sons, Inc., New York
- Druet, D., Comeau, L. C., Viani, R., Baldy, A., Estienne, J. & Pieerrot, M., (1987). **Can. J. Chem.**, 65, 851.
- Dunitz, J. D. & Waser, J., (1972). **J. Am. Chem. Soc.**, 94, 5645
- Eggleston, D. S., (1987). **Acta Crystallogr., Sect. C (Cr. Str. Comm.)**, 43, 1229.
- Farrugia, L. J., (1997). **J. Appl. Crystallogr.** 30: 565.
- Flack, H. D. (1983). **Acta Crystallogr., Sect. A** 39, 876-881.
- Giacovazzo, C., Monaco, H. L., Viterbo, D., Scordari, F., Gilli, G., Zanotti, G. & Catti, M. (1992). "**Fundamentals of Crystallography**", Oxford University Press Inc.:New York.
- Gibbons, S., Gray, A. I., Hockless, D. C. R., Lavaud, C., Nuzillard, J.-M., Massiot, G., Waterman, P. G. & White, A. H., (1993). **Phytochemistry**, 34, 273.
- Glusker, J. P. & Trueblood, K. N. (1985). "**Crystal Structure Analysis: A Primer**", 2nd Edition, Oxford University Press Inc.:New York.
- Gonzalez, A. G., Fraga, B. M., Gonzalez, P., Gonzalez, C. M., Ravelo, A. G., Ferro, E., Dominguez, X. A., Martinez, M. A., Perales, A. & Fayos, J., (1983). **J. Org. Chem.**, 48, 3759.

- Hahn, T. (1992). "International Tables for Crystallography, Volume A, Space Group Symmetry", 3rd Revised Edition, International Union of Crystallography/Kluwer Academic:Dordrecht.
- Hambley, T. W., Lewis, K. G., Tucker, D. J. & Turner, P., (1998). **Aust. J. Chem.**, 51, 343.
- Hamilton, W. C. (1964). "**Statistics in Physical Science**", Ronald:New York.
- Kikuchi, T., Niwa, M. & Masaki, N., (1972). **Tetrahedron Letters**, 5249.
- Klinot, J., Podlaha, J., Podlahova, J., Hilgard, S. & Klinotova, E., (1989). **Collect. Czech. Chem. Commun.**, 54, 737.
- Kutney, J. P., Hewitt, G. M., Lee, G., Piotrowska, K., Roberts, M. & Rettig, S. J., (1992). **Can. J. Chem.**, 70, 1455.
- Laing, M., Burke-Laing, M. E., Bartho, R. & Weeks, C. M., (1977). **Tetrahedron Letters**, 18:43 3039-3842.
- Lee, K.-H. & Nozaki, H., (1984). **Tetrahedron Letters**, 25:7 707.
- Lee, K.-H., Nozaki, H. & McPhail, A. T., (1984). **Tetrahedron Letters**, 25:7 710.
- Mackay, S., Gilmore, C. J., Edwards, C., Tremayne, M., Stuart, N. & Shankland, K. (1998). "maXus: a computer program for the solution and refinement of crystal structure from diffraction data", U. of Glasgow, Scotland, UK, Nonius BV, Delft, and MacScience Co. Ltd., Yokohama.
- Masaki, N., Niwa, M. & Kikuchi, T., (1975), **J. Chem. Soc., Perkin Trans. 2** 610-618.

- Microsoft, (1997). Microsoft Excel 97, Thai version 8.0, Microsoft Corporation:Redlands, Washington.
- Mo, F., (1977). **Acta Crystallogr., Sect. B**, 33, 641.
- Mo, F., Winther, S. & Scrimgeour, S. N., (1989). **Acta Crystallogr., Sect. B**, 45, 261-271.
- Monache, F. D., Marini-Bettolo, G. B., Pomponi, M., de Mello, J. F., King, T. J. & Thomson, R. H., (1979). **J. Chem. Soc., Perkin Trans. 1**, 2649.
- Nonius B.V. (2000). **Collect Data Collection Software**, Nonius B.V.:Delft.
- Novotny, J., Podlaha, J. & Klinot, J., (1993). **Collect. Czech. Chem. Commun.**, 58, 2737.
- Nozaki, H., Matsuura, Y., Hirono, S., Kasai, R., Tada, T., Nakayama, M. & Lee, K.-H., (1991). **Phytochemistry**, 30, 3819.
- Nozaki, H., Suzuki, H., Lee, K.-H. & McPhail, A. T., (1982). **J. Chem. Soc., Chem. Comm.**, 1048.
- Orpen, A. G., Brammer, L., Allen, F. H., Kennard, O., Watson, D. G. & Taylor, R. (1994). "Typical Interatomic Distances" in Burgi, H. B. & Dunitz, J. D., **Structure Correlation**, Vol. 2, VCH., New York, pp 751-858.
- Otwinowski, Z. & Minor, W. (1997). "Processing of X-ray Diffraction Data Collected in Oscillation Mode", in **Methods in Enzymology**, Vol. 276: Macromolecular Crystallography, part A, C. W. Carter & R. M. Sweet, Eds., pp 307-326.

- Paquette, L. A., Stepanian, M., Branan, B. M., Edmondson, S. D., Bauer, C. B. & Rogers, R. D., (1996). **J. Am. Chem. Soc.**, 118, 4504-4505.
- Phaopongthai, J., (1995). MS Thesis, Chulalongkorn University.
- Phothikanith, A. & Haller, K. J., (1999). **Identification of a Disordered Friedelin Structure by Structure Correlation**, 25th Congress on Science and Technology in Thailand, Pitsanulok. Abstract A100.
- Phothikanith, A. & Haller, K. J., (2001). **X-Ray Structure Characterization of Disordered Friedelin-3-one and Epifriedelin-3-ol**. AsCA'01, 4th Asian Crystallographic Association Meeting, Bangalore, India: Abstract A4-9.
- Pickett, M. H. & Strauss, L. H., (1970). **J. Am. Chem. Soc.**, 92, 7281.
- Prakash, O., Roy, R., Garg, S. H. & Bhakuni, S. D., (1987). **J. Am. Chem. Soc.**, 118, 4504.
- Rae, A. D., (1996) **RAELS96. A Comprehensive Constrained Least Squares Refinement Program**, The Australian National University, Australia.
- Reynolds, W. F., Sawyer, J. F., Enriquez, R. G., Escobar, L. I., Chavez, M. A. & Shoolery, J. N., (1985). **Can. J. Chem.**, 63, 1048.
- Richard, J. P. Cannell (1998). **Natural Products Isolation**, Humana Press, Totowa, NJ.
- Rogers, D., Phillips, F. L., Joshi, B. S. & Viswanathan, N., (1980). **J. Chem. Soc., Chem. Comm.** 1048.
- Rogers, D; Williams, D. J.; Joshi, B. S.; Kamat, V. N. & Viswanathan, N. (1974). **Tetrahedron Letters.** 63.

- San-oon, S., Nivesanond, K., Prasithichokekul, S., Pungpo, P. & Hangnongbua, S., (1999). **Computational Calculations of Conformational Analysis of HIV-1 Reverse Transcriptase inhibitor 4,5,6,7-tetrahydroimidazo-8-chloro-5-methyl-(3-methyl-2-buthenyl) imidazo [4,5,1-jk][1,4]-benzodiazepin-2(1H)-thione(8-chloro-TIBO)**, 25th Congress on Science and Technology in Thailand, Pitsanulok.
- Sarma J. A. R. P. & Desiraju G. R., (1986). **Acc. Chem. Res.**, 19, 222-228.
- Sheldrick, G. M. (1993). **Program for the Refinement of Crystal Structure**. University of Goettingen, Germany.
- Sheldrick, G. M. (1997). **SHELXTL Reference Manual**, Ver. 5.1, Bruker AXS, Inc., Madison.
- Shi, J.-Q., Wu, Q.-J., Xu, B.-J., Chen, Y.-Z. & Xu, J., (1992). **Youji Huaxue (J. Org. Chem.)**, 12, 301-309.
- Sieskind, O., Kintzinger, J. P., Metz, B. & Albrecht, P., (1995). **Tetrahedron**, 51, 2009.
- Steed, J. W. & Atwood, J. L. (2000). **Supramolecular Chemistry**, Wiley, England, pp 392-397.
- Steiner, T. & Desiraju, G. R., (1998). **Chem. Commun.**, 891-392
- Stout, G. H. & Jensen, L. H. (1989). **X-Ray Structure Determination: A Practical Guide**, 2nd Edition, John Wiley & Sons, Inc., New York.
- Subramanian, K., Selladurai, S., Sivakumar, K., Ponnuswamy, M. N., & Sukumar, E., (1989). **Acta Crystallogr., Sect. C (Cr. Str. Comm.)**, 45, 921.

- Takai, M., Tori, M., Tsuyuki, T., Takahashi, T., Itai, A. & Iitaka, Y., (1985). **Bull. Chem. Soc. Jpn.**, 58, 185.
- Tanaka, R., Matsunaga, S. & Ishida, T., (1988). **Tetrahedron Letters**, 29:37 4751.
- Taylor, R. & Kennard, O. (1982). **J. Am. Chem. Soc.** 104: 5063-5070.
- Tkachev, A.V., Denisov, A. Y., Gatilov, V., Bagryanskaya, I. Y., Shevtsov, S. A. & Rybalova, T. V., (1994). **Tetrahedron**, 50, 11459.
- Tori, M., Takai, M., Matsumoto, Y., Moriyama, Y., Tsuyuki, T., Takahashi, T., Ohnishi, H., Itai, A. & Iitaka, Y., (1984). **Bull. Chem. Soc. Jpn.**, 57, 2498.
- USAE (1999). Attributed to the USAE Waterway Station, obtained from the **Xtal Nexus**, Ver. 8.56, Nov. 2002, CD-ROM resource compiled by Lachlan M. D. Cranswick, CCP14, Birkbeck University.
- van Schalkwyk, T. G. D. & Kruger, G. J., (1974). **Acta Crystallogr., Sect. B** 30, 2261.
- White, J. D., Fayos, J. & Clardy, J., (1973). **Chem. Commun.**, 357.
- Wilkins, A. L. & Goh, E.-M., (1988). **Aust. J. Chem.**, 41, 143.
- Zheng, G.-Q., (1994). **Planta Med.**, 60, 54.

Appendices

Appendix A

Search of the Cambridge Structure Database

April 2001 release 233,218 entries

FRIED Search: Five Fused 6-member saturated carbon ring system (Figure 1.1)

```
T1 *CONN
NFRAG 1
AT1 C 2           :XY 238 248
AT2 C 2           :XY 151 298
AT3 C 2           :XY 151 399
AT4 C 2           :XY 238 449
AT5 C 3           :XY 325 398
AT6 C 3           :XY 325 298
AT7 C 2           :XY 412 247
AT8 C 2           :XY 499 297
AT9 C 3           :XY 500 397
AT10 C 3          :XY 413 448
AT11 C 2          :XY 412 549
AT12 C 2          :XY 499 600
AT13 C 3          :XY 587 550
AT14 C 3          :XY 587 448
AT15 C 2          :XY 675 398
AT16 C 2          :XY 763 450
AT17 C 3          :XY 762 551
AT18 C 3          :XY 674 601
AT19 C 2          :XY 674 702
AT20 C 2          :XY 761 753
AT21 C 2          :XY 849 703
AT22 C 2          :XY 850 602
BO 1 2 1
BO 2 3 1
BO 3 4 1
BO 4 5 1
BO 5 6 1
BO 1 6 1
BO 6 7 1
BO 7 8 1
BO 8 9 1
BO 9 10 1
BO 5 10 1
BO 10 11 1
BO 11 12 1
BO 12 13 1
BO 13 14 1
```

BO 9 14 1
 BO 14 15 1
 BO 15 16 1
 BO 16 17 1
 BO 17 18 1
 BO 13 18 1
 BO 18 19 1
 BO 19 20 1
 BO 20 21 1
 BO 21 22 1
 BO 17 22 1

END

SAVE 0 REFC FBIB FDAT CIF

QUES T1

ABPACH10

3-O-Acetyl-16-O-p-bromobenzoyl-pachysandiol B
 absolute configuration

C39 H57 Br1 O4

N.Masaki,M.Niwa,T.Kikuchi, J.Chem.Soc.,Perkin Trans.2, , 610,1975

-----+-----+-----+-----+-----+-----+-----+
 BITSOM

28,29-Dihydroxy-friedelan-3-one

Maytenfoliol

antileukaemic activity

C30 H50 O3

H.Nozaki,H.Suzuki,K.-H.Lee,A.T.McPhail, J.Chem.Soc.,Chem.Comm., , 1048,1982

-----+-----+-----+-----+-----+-----+-----+
 BIZKUO

Stictane-3beta,22alpha-diol

C30 H52 O2

R.E.Corbett,J.Simpson,E.M.Goh,B.K.Nicholson,A.L.Wilkins,W.T.Robinson

J.Chem.Soc.,Perkin Trans.2, , 1339,1982

-----+-----+-----+-----+-----+-----+-----+
 BUKKEX

5beta,6beta-Epoxy-alnusan-3beta-yl acetate

C32 H52 O3

M.Tori,M.Takai,Y.Matsumoto,Y.Moriyama,T.Tsuyuki,T.Takahashi,A.Itai,Y.Iitaka

Chem.Lett., , 527,1983

-----+-----+-----+-----+-----+-----+-----+
 BUKKEX10

5beta,6beta-Epoxy-alnusan-3beta-yl acetate Sengupta's epoxide

C32 H52 O3

M.Tori,M.Takai,Y.Matsumoto,Y.Moriyama,T.Tsuyuki,T.Takahashi,H.Ohnishi,A.Itai,

Y.Iitaka, Bull.Chem.Soc.Jpn., 57, 2490,1984

-----+-----+-----+-----+-----+-----+-----+
 BXFRED

2,2-Dibromo-25,26-oxido-friedel-1,3-dione

C30 H44 Br2 O3

D.Rogers,D.J.Williams,B.S.Joshi,V.N.Kamat,N.Viswanathan, Tetrahedron Lett., , 63,1974

-----+-----+-----+-----+-----+-----+-----+
 CERCEH

17-Perhydroxy-28-norfriedelan-3-one

Maytensifolin A

C29 H48 O3

K.-H.Lee,H.Nozaki,A.T.McPhail, Tetrahedron Lett., 25, 707,1984

-----+-----+-----+-----+-----+-----+-----+

CEYVAD

(2R,3R,4R,5S,8S,9R,10S,13S,14R,17R,18R,20R)-2,24-Dihydroxy-3-oxo-friedelan-29-oic acid hemiketal monohydrate

Orthosphenic acid monohydrate absolute configuration

C30 H48 O5, H2 O1

A.G.Gonzalez, B.M.Fraga, P.Gonzalez, C.M.Gonzalez, A.G.Ravelo, E.Ferro, X.A.Dominguez, M.A.Martinez, A.Perales, J.Fayos, *J.Org.Chem.*, 48, 3759, 1983

CITFIU

5alpha,10alpha-Epoxyalnusan-3beta-yl acetate

C32 H52 O3

M.Takai, M.Tori, T.Tsuyuki, T.Takahashi, A.Itai, Y.Iitaka, *Chem.Pharm.Bull.*, 32, 2464, 1984

CITFIU10

5alpha,10alpha-Epoxyalnusan-3beta-yl acetate

C32 H52 O3

M.Takai, M.Tori, T.Tsuyuki, T.Takahashi, A.Itai, Y.Iitaka, *Bull.Chem.Soc.Jpn.*, 58, 185, 1985

CMPANL

Campanulin

C30 H50 O1

J.D.White, J.Fayos, J.Clardy, *J.Chem.Soc., Chem.Comm.*, , 357, 1973

CMPANL01

Campanulin

C30 H50 O1

F.Mo, *Acta Crystallogr., Sect.B*, 33, 641, 1977

DATJOX

Taraxasterol

C30 H50 O1, C2 H6 O1

W.F.Reynolds, J.F.Sawyer, R.G.Enriquez, L.I.Escobar, M.A.Chavez, J.N.Shoolery *Can.J.Chem.*, 63, 1048, 1985

ECHABL10

Echinocystic acid diacetate bromolactone

C34 H51 Br1 O6

C.H.Carlsle, P.F.Lindley, A.Perales. *Acta Crystallogr., Sect.B*, 32, 3053, 1976

EPFRED

Epifriedelinol

C30 H52 O1

M.Laing, M.E.Burke-Laing, R.Bartho, C.M.Weeks. *Tetrahedron Lett.*, , 3839, 1977

EPFRED01

Longan triterpane-A

C30 H52 O1

Jian-Qiu Shi, Qiang-Jin Wu, Ben-Jie Xu, Yuan-Zhu Chen, Jian Xu.

Youji Huaxue (J.Org.Chem.), 12, 301, 1992

EUPTIA

Eupteleogenin iodoacetate

C31 H43 I1 O5

M.Nishikawa, K.Kamiya, T.Murata, Y.Tomiie, I.Nitta. *Tetrahedron Lett.*, , 3223, 1965

FADGEW

5beta,24-Cyclofriedelan-3-one

C30 H48 O1

J.D.Connolly, A.A.Freer, V.Anjaneyulu, K.Ravi, G.Sambasivarao

Acta Crystallogr., Sect.C (Cr.Str.Comm.), 42, 1352, 1986

-----+-----+-----+-----+-----+-----+-----+-----+
FAGRAG
 Avenesterenin A-2 deuteriochloroform solvate deuterium oxide antifungal agent
 C37 H52 O7,C1 D1 Cl3,D2 O1
 M.J.Begley,L.Crombie,W.M.L.Crombie,D.A.Whiting.
 J.Chem.Soc.,Perkin Trans.1, , 1905,1986
 -----+-----+-----+-----+-----+-----+-----+-----+

FAWXUW
 Methyl 3beta,16alpha-dihydroxy-12-oxo-13alpha-oleanan-28-oate dihydrate
 C31 H50 O5,2(H2 O1)
 N.N.Dhaneshwar,D.D.Sawaikar,C.R.Narayanan,S.S.Tavale,T.N.G.Row
 Acta Crystallogr.,Sect.C (Cr.Str.Comm.), 43, 66,1987
 -----+-----+-----+-----+-----+-----+-----+-----+

FITVOT
 12alpha-Hydroxy-3-oxo-oleanano-28,13-lactone
 C30 H46 O4
 D.S.Eggleston. Acta Crystallogr.,Sect.C (Cr.Str.Comm.), 43, 1229,1987
 -----+-----+-----+-----+-----+-----+-----+-----+

FOLVUX
 3beta-Acetoxy-ursane-28,20beta-olide
 C32 H50 O4
 D.Druet,L.C.Comeau,R.Viani,A.Baldy,J.Estienne,M.Pierrot. Can.J.Chem., 65, 851,1987
 -----+-----+-----+-----+-----+-----+-----+-----+

FRDLON
 Friedel-26beta-ol-1,3-dione
 C30 H48 O3
 D.Rogers,F.L.Phillips,B.S.Joshi,N.Viswanathan. J.Chem.Soc.,Chem.Comm., , 1048,1980
 -----+-----+-----+-----+-----+-----+-----+-----+

FUYNUI
 22alpha-Hydroxystictan-3-one
 C30 H50 O2
 A.L.Wilkins,E.M.Goh. Aust.J.Chem., 41, 143,1988
 -----+-----+-----+-----+-----+-----+-----+-----+

HFRDAC
 29-Hydroxy-friedelan-3-one acetate
 C32 H52 O3
 C.Betancor,R.Freire,A.G.Gonzalez,J.A.Salazar,C.Pascard,T.Prange
 Phytochemistry, 19, 1989,1980
 -----+-----+-----+-----+-----+-----+-----+-----+

JAMPOC
 28-Hydroxyfriedelan-3-one
 anticancer drug,insect repellent and antimicrobial activity
 C30 H50 O2
 K.Subramanian,S.Selladurai,K.Sivakumar,M.N.Ponnuswamy,E.Sukumar
 Acta Crystallogr.,Sect.C (Cr.Str.Comm.), 45, 921,1989
 -----+-----+-----+-----+-----+-----+-----+-----+

JIBBOL
 3beta-Hydroxy-2-oxofriedelan-20alpha-carboxylic acid
 C30 H48 O4
 J.R.De Sousa,G.D.F.Silva,J.L.Pedersoli,R.J.Alves, Phytochemistry, 29, 3259,1990
 -----+-----+-----+-----+-----+-----+-----+-----+

JUWDIO
 13,28-Epoxyolean-3,24,28-triyl tris(p-iodobenzoate)
 antiviral activity against herpes simplex and polio viruses, also antifungal activity against
 some phytopathogenic fungi
 C51 H59 I3 O8
 G.Aliotta,L.De Napoli,F.Giordano,G.Piccialli,V.Piccialli,C.Santacroce
 Phytochemistry, 31, 929,1992
 -----+-----+-----+-----+-----+-----+-----+-----+

KASZOT

3beta-Acetoxyoleanane-13beta,15alpha-diol-12-one

Rubioprasin A

C32 H52 O5

H.Itokawa,Y.-F.Qiao,K.Takeya,Y.Iitaka, Chem.Pharm.Bull., 37, 1670,1989

LIKUD

7beta,8beta-Epoxyfriedelane possible antitumour activity

C30 H50 O1

I.Dey,A.Banerjee, Acta Crystallogr.,Sect.C (Cr.Str.Comm.), 51, 119,1995

LIKJOE

22-(1-Chloroethylidene)-13-fluoro-4-(4-hydroxypentan-2-olato)-4,4-dinoroleanane

C35 H58 Cl1 F1 O2

P.V.Fish,W.S.Johnson,G.S.Jones,F.S.Tham,R.K.Kullnig, J.Org.Chem., 59, 6150,1994

LILDAL

11alpha,12alpha-Epoxy-13-hydroxy-3-oxoursan-28-oic acid gamma-lactone

possible biological activity

C30 H44 O4

A.V.Tkachev,A.Yu.Denisov,Yu.V.Gatilov,I.Yu.Bagryanskaya,S.A.Shevtsov,T.V.Rybalova

Tetrahedron, 50, 11459,1994

LILDEP

3beta-Acetyloxy-11alpha,12alpha-epoxy-14alpha-hydroxyisoursan-28-oic acid delta-lactone

possible biological activity

C32 H48 O5

A.V.Tkachev,A.Yu.Denisov,Yu.V.Gatilov,I.Yu.Bagryanskaya,S.A.Shevtsov,T.V.Rybalova

Tetrahedron, 50, 11459,1994

NAGHEI

Angeloyloxy-oleanolic acid

Reduced Lantadene-A 22a

C35 H54 O5

V.Kabaleeswaran,S.S.Rajan,V.Pattabhi,O.P.Sharma, Z.Kristallogr., 211, 411,1996

OLDABL

Oleanolic acid diacetate bromolactone absolute configuration

C34 H51 Br1 O6

T.G.D.van Schalkwyk,G.J.Kruger, Acta Crystallogr.,Sect.B, 30, 2261,1974

OLENAN11

18-alpha(H)-Oleanane triclinic form

C30 H52

D.T.Fowell,B.G.Melsom,G.W.Smith, Acta Crystallogr.,Sect.B, 34, 2244,1978

OLENAN20

18-alpha(H)-Oleanane orthorhombic form

C30 H52

D.T.Fowell,B.G.Melsom,G.W.Smith, Acta Crystallogr.,Sect.B, 34, 2244,1978

PAPGAO

Methyl 22beta-hydroxy-3,21-dioxo-D:A-friedo-29-noroleanan-24-oate

absolute configuration

C30 H46 O5

J.P.Kutney,G.M.Hewitt,Gin Lee,K.Piotrowska,M.Roberts,S.J.Rettig

Can.J.Chem., 70, 1455,1992

PEYVAQ

3beta-Acetoxy-12alpha-bromo-13beta,28-epoxyoleanan-16alpha-ol
absolute configuration determined by refinement of the Flack parameter to 0.01(2)

C32 H51 Br1 O4

T.W.Hambley,K.G.Lewis,D.J.Tucker,P.Turner, Aust.J.Chem., 51, 343,1998

PIKMAX

2beta-Bromo-19beta,28-epoxy-18alpha-oleanan-3-one

C30 H47 Br1 O2

J.Novotny,J.Podlaha,J.Klinot, Collect.Czech.Chem.Comm., 58, 2737,1993

PLAGBL10

Platycodigenin bromolactone benzene solvate absolute configuration

C30 H47 Br1 O7,C6 H6

T.Akiyama,O.Tanaka,Y.Iitaka, Acta Crystallogr.,Sect.B, 26, 163,1970

PRISEM

Prionostemmadiene

C30 H48 O2

F.D.Monache,G.B.Marini-Bettolo,M.Pomponi,J.F.de Mello,T.J.King,R.H.Thomson

J.Chem.Soc.,Perkin Trans.1, , 2649,1979

PUTNOH

1,2,6,6,10,17,17,20-Octamethyl-7-acetoxypentacyclo(12.8.0.0\$2, 11!.0\$5,10!.0\$15,
20!)docosane

C32 H51 O2

Lu Yang,Wang Shu-Chun,Zheng Qi-Tai,Liu Wei,Li Fang-Hua

Gaodeng Xuexiao Huaxue Xuebao(Chem.J.Chin.Uni.), 18, 1978,1997

SOXNAU

6beta-Hydroxyfriedelan-3,16,21-trione Maytensifolin-C

C30 H46 O4

H.Nozaki,Y.Matsuura,S.Hirono,R.Kasai,T.Tada,M.Nakayama,K.-H.Lee

Phytochemistry, 30, 3819,1991

THYMAH10

Tetrahymanol hemihydrate

C30 H52 O1,0.5(H2 O1)

D.A.Langs,W.L.Duax,H.L.Carrell,H.Berman,E.Caspi, J.Org.Chem., 42, 2134,1977

THYMAN

Tetrahymanone

C30 H50 O1

J.T.Gordon,T.H.Doyne, Acta Crystallogr., 21, A113,1966

VAGCUB

3beta-Hydroxy-D:A-friedo-oleanan-27-oic acid Trichadenic acid B

C30 H50 O3

R.Tanaka,S.Matsunaga,T.Ishida, Tetrahedron Lett., 29, 4751,1988

VEFNID

Methyl 3-oxofriedelan-20alpha-oate

C31 H50 O3

A.B.Cota,Y.P.Mascarenhas,G.D.F.Silva,J.R.de Souza

Acta Crystallogr.,Sect.C (Cr.Str.Comm.), 46, 326,1990

VEPBEX

Allobetulone

C30 H48 O2

J.Klinot,J.Podlaha,J.Podlahova,S.Hilgard,E.Klinotova,
Collect.Czech.Chem.Comm., 54, 737,1989

YACNEV

Salaspermic acid monohydrate

antiHIV activity

C30 H48 O4,H2 O1

Ke Chen,Qian Shi,Y.Kashiwada,De-Cheng Zhang,Chang-Qi Hu, Ji-Qin Jin,H.Nozaki,
R.E.Kilkuskie,E.Tramontano,Yung-Chi Cheng,D.R.McPhail,A.T.McPhail,Kuo-Hsiung Lee
J.Nat.Prod., 55, 340,1992

YEGYOY

Dimethyl 3beta-hydroxy-D:A-friedo-oleanan-27,29-dicarboxylate

C32 H52 O5

S.Gibbons,A.I.Gray,D.C.R.Hockless,C.Lavaud,J.-M.Nuzillard,G.Massiot,P.G.Waterman,
A.H.White, Phytochemistry, 34, 273,1993

ZZZQAI

Friedelin

C30 H50 O1

Rogers,Thomas, Bull.Soc.Chim.Fr., , 361,1956

ZZZQAI01

Friedelin

Friedelan-3-one

C30 H50 O1

F.Mo,S.Winther,S.N.Scrimgeour, Eur.Cryst.Meeting, 7, 180,1982

ZZZQAI02

D:A-Friedo-oleanan-3-one

Friedelin

C30 H50 O1

J.-P.Declercq,L.Van Puyvelde,N.De Kimpe,M.Nagy,G.Verhegge,R.De Vierman
Acta Crystallogr.,Sect.C (Cr.Str.Comm.), 47, 209,1991

ZZZQAI11

Friedelan-3-one

Friedelin

C30 H50 O1

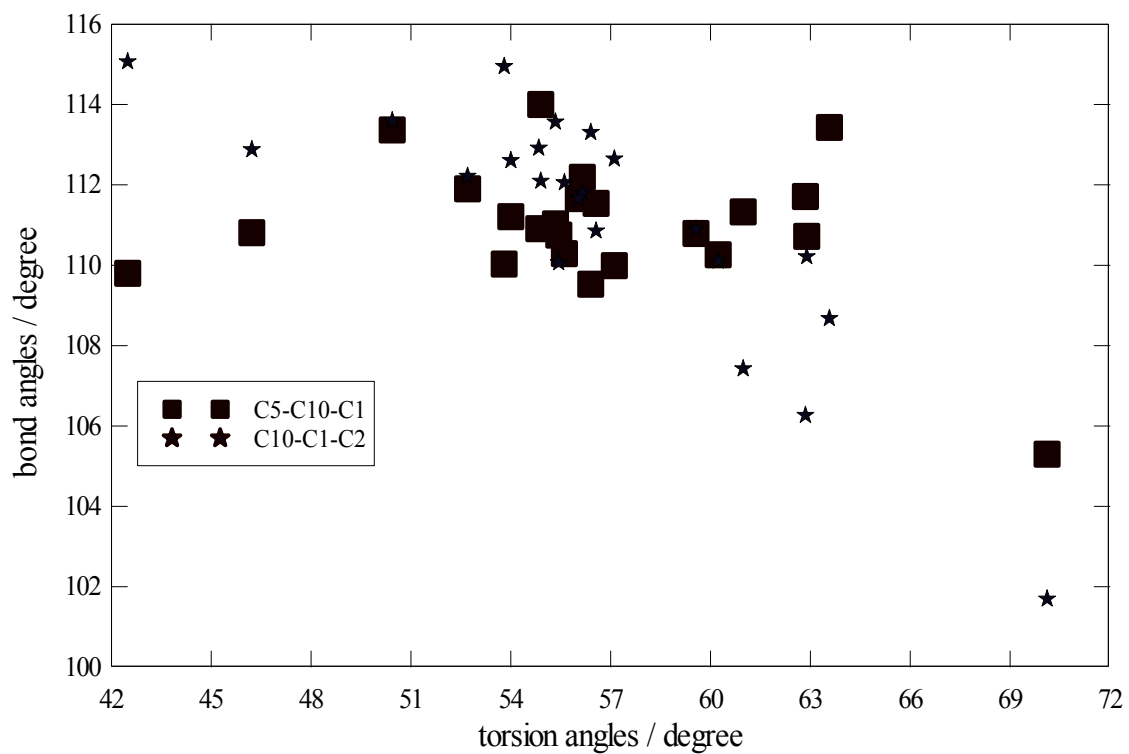
F.Mo,S.Winther,S.N.Scrimgeour, Acta Crystallogr.,Sect.B (Str.Sci.), 45, 261,1989

Appendix B1

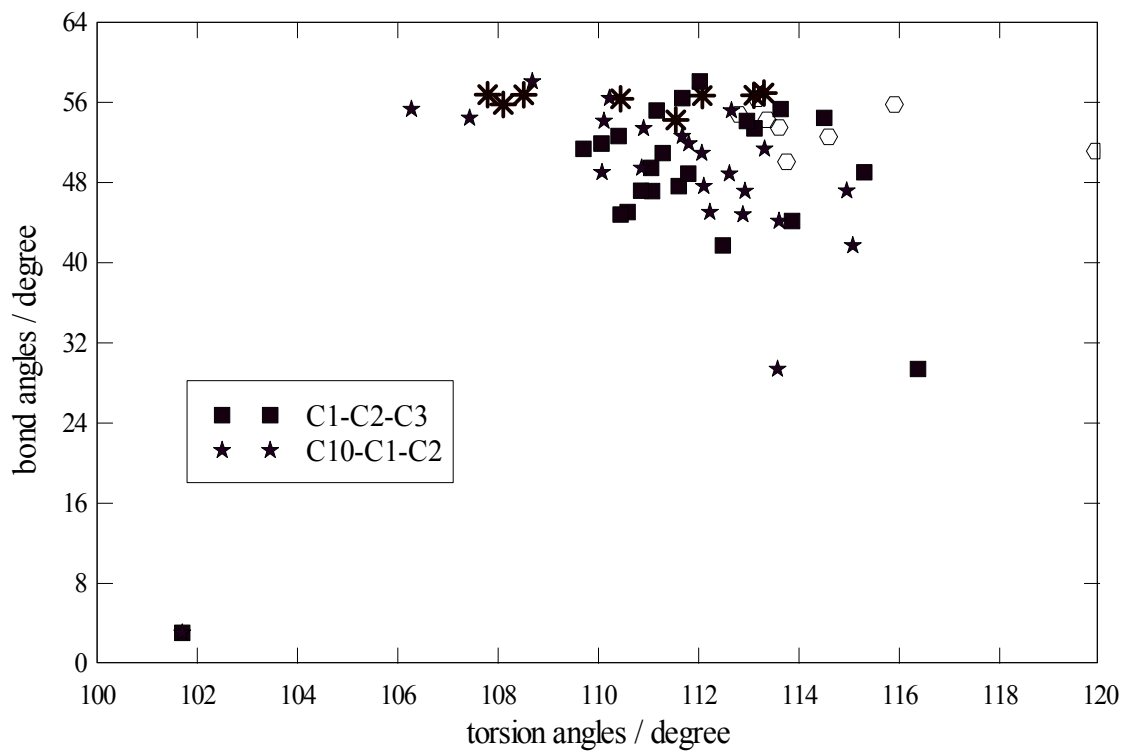
The scatterpot Part 1

The scatterplot between bond angles and torsion angles at bonds angles correspond to that torsion angle of rings A - E for friedelane skeleton

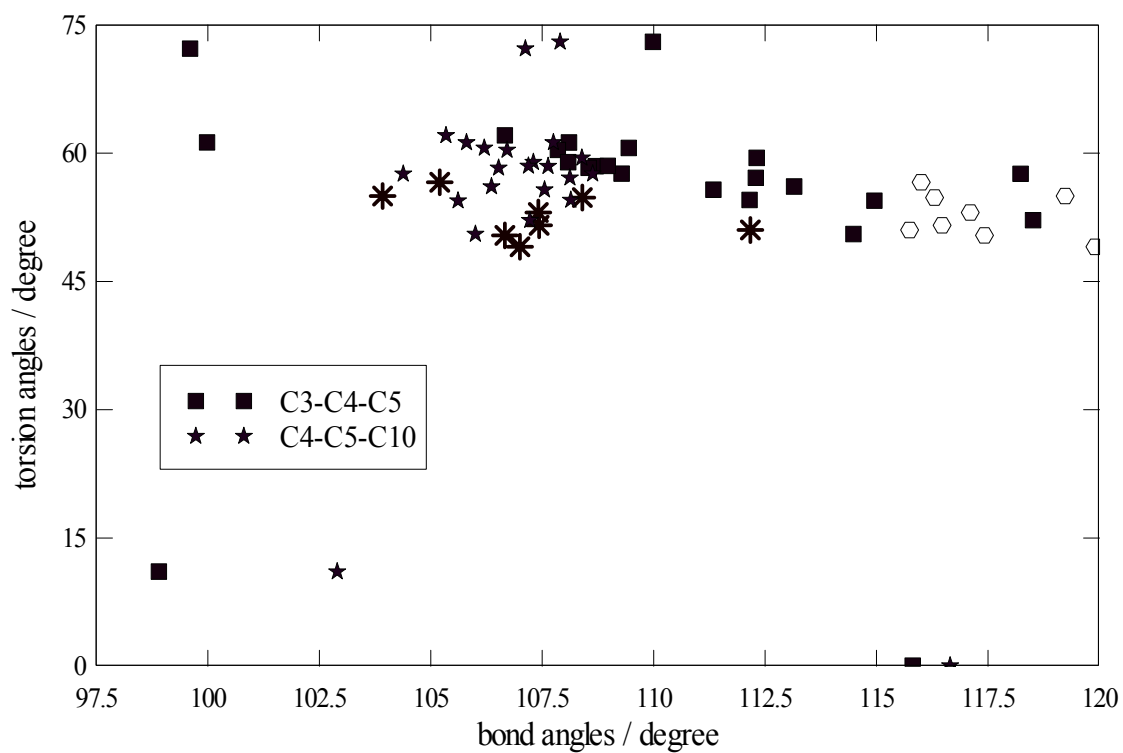
scatterplot of bond angles versus torsion angles (C5-C10-C1-C2) on ring A at C10 for friedelane skeleton



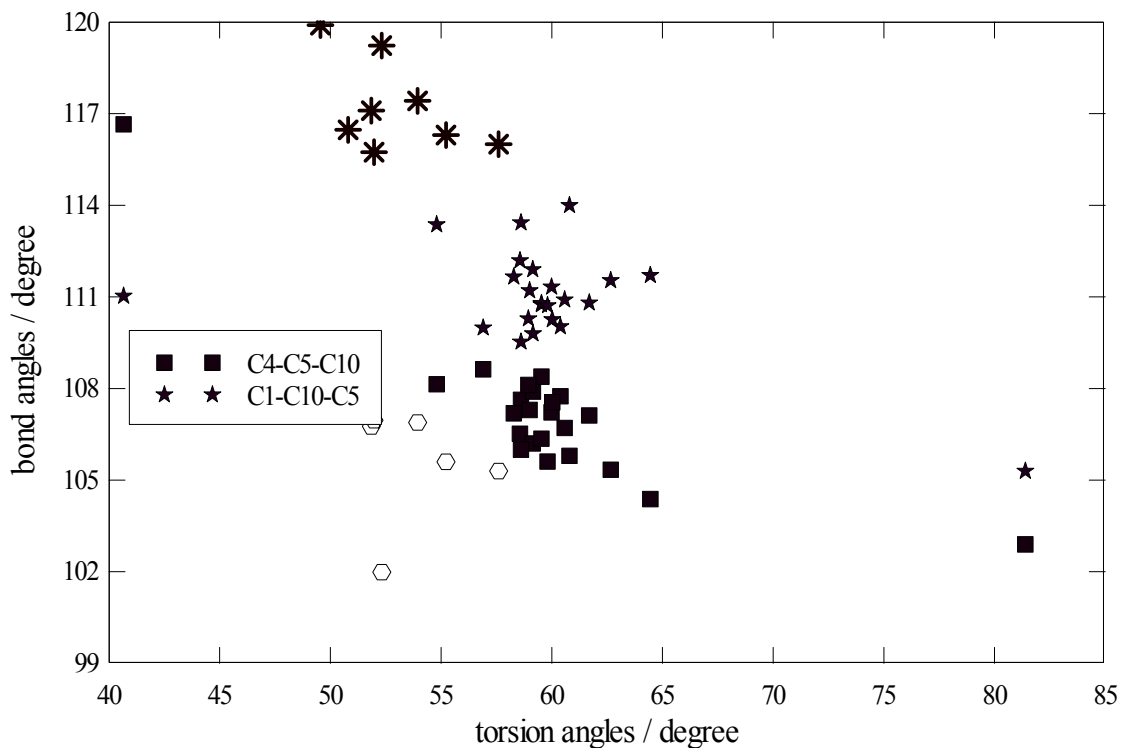
scatterplot of bond angles at C1 and C2 versus torsion angles (C10-C1-C2-C3)
on ring A compare between friedelane and olenane skeletons



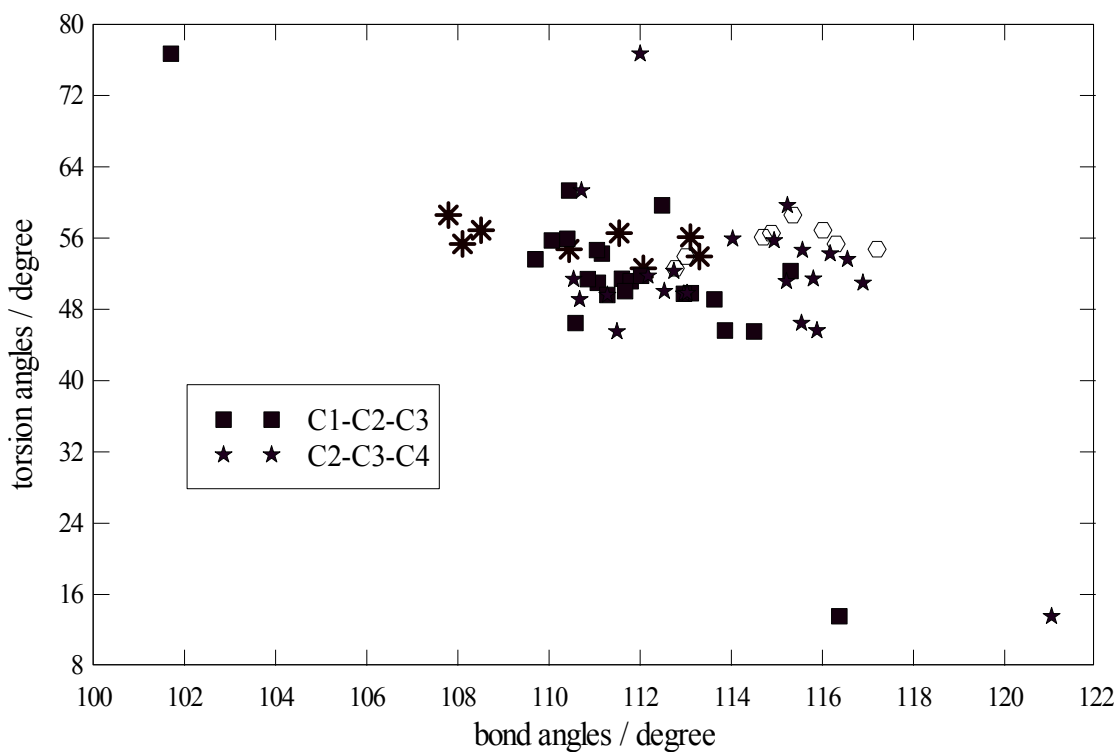
scatterplot of bond angles versus torsion angles (C3-C4-C5-C10) on ring A
compare between friedelane and olenane skeleton



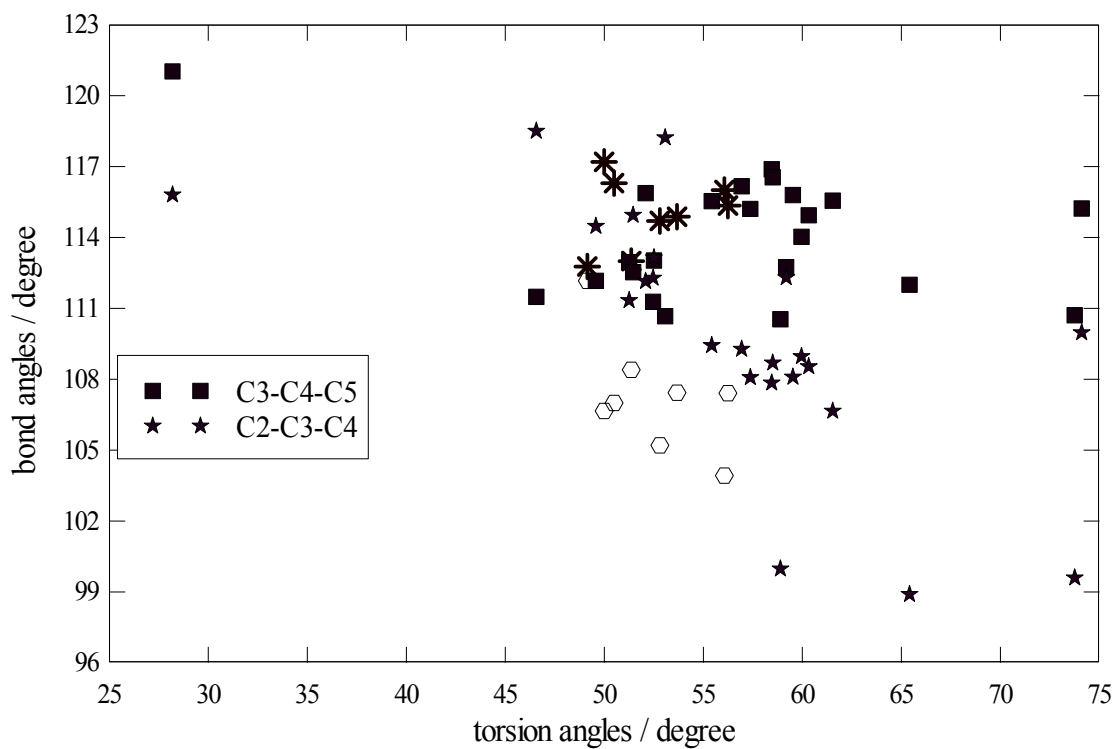
scatterplot of bond angles versus torsion angles (C1-C10-C5-C4) on ring A
at C5 (dark square) compare between friedelane and olenane skeleton



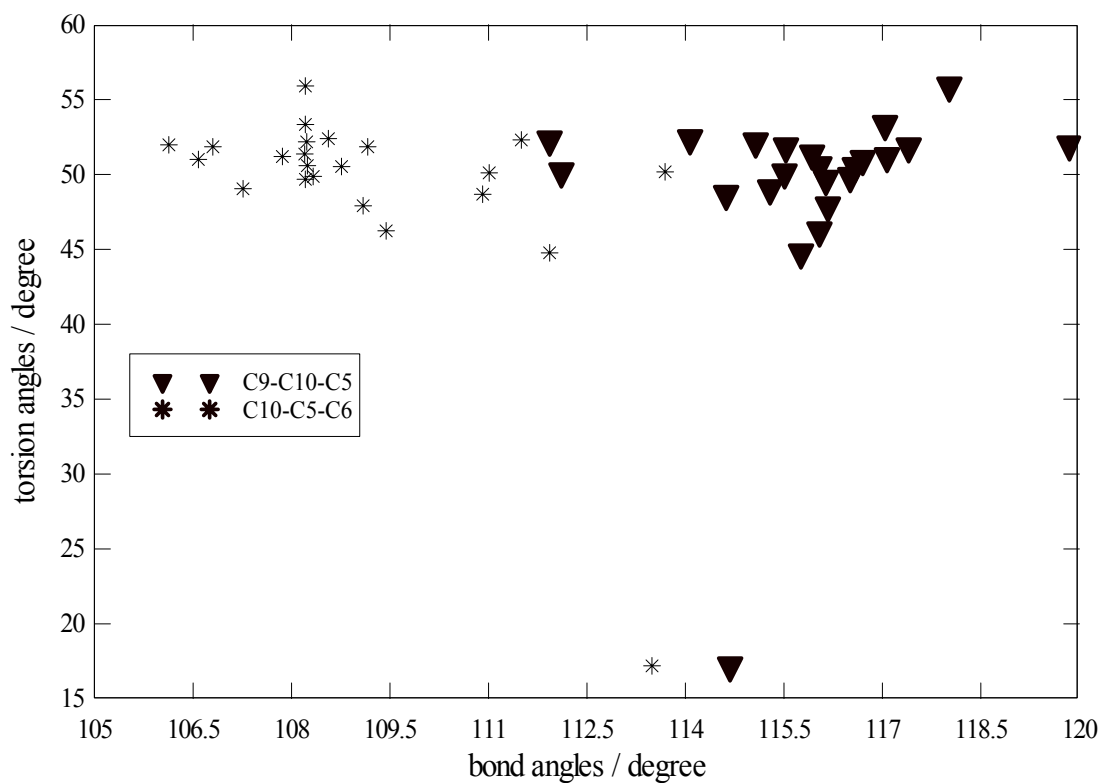
scatterplot of bond angles versus torsion angles (C1-C2-C3-C4) on ring A
compare between friedelane and olenane skeleton



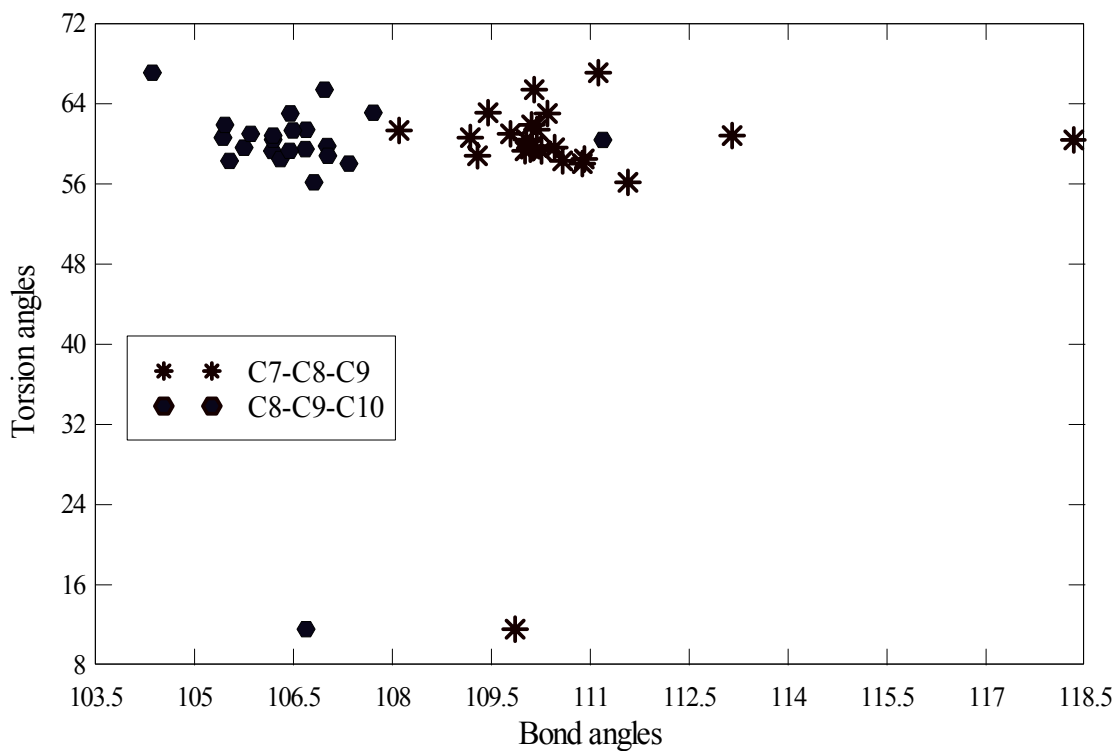
scatterplot of bond angles versus torsion angles (C2-C3-C4-C5) on ring A
at C4(square) compare between friedelane and olenane skeletons



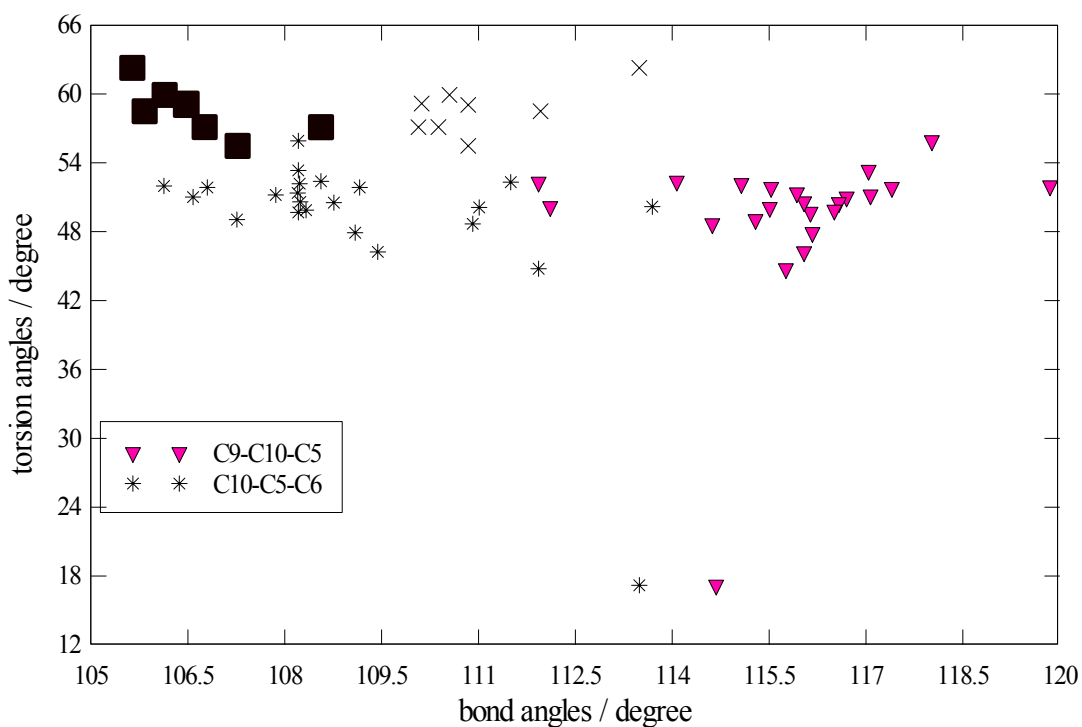
scatterplot of torsion angles(C9-C10-C5-C6) versus bond angles on ring B



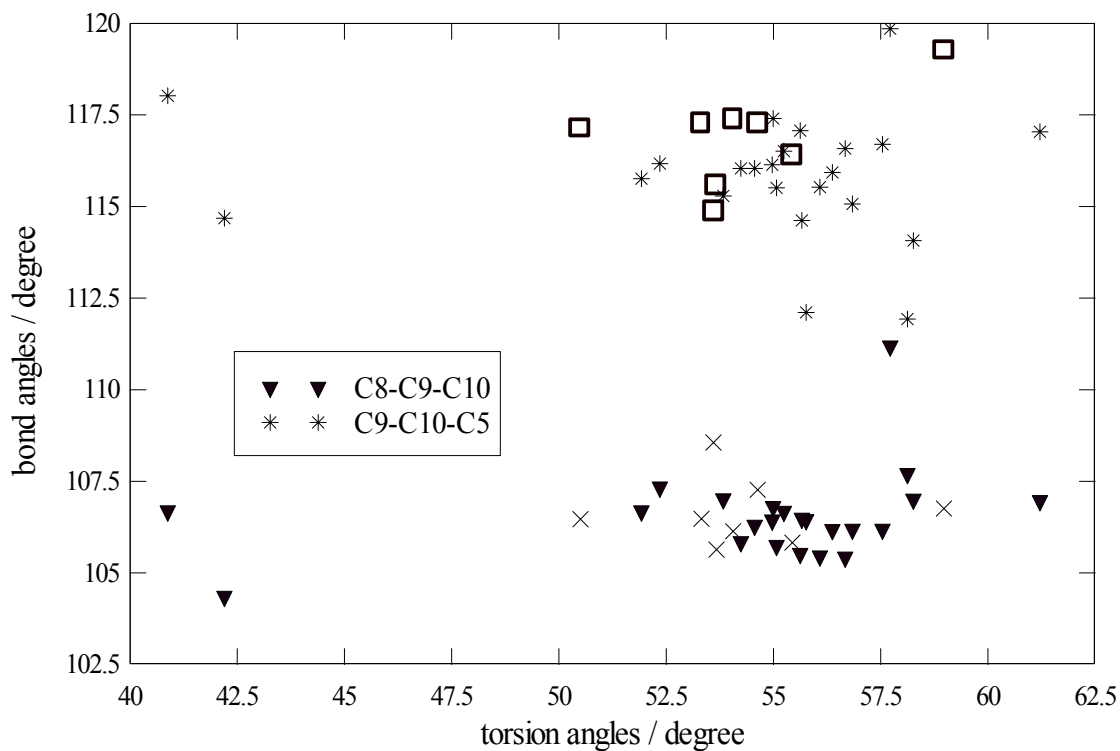
scatterplot between torsion angles versus bond angles related to torsion angles
only junction of ring B-C on ring B



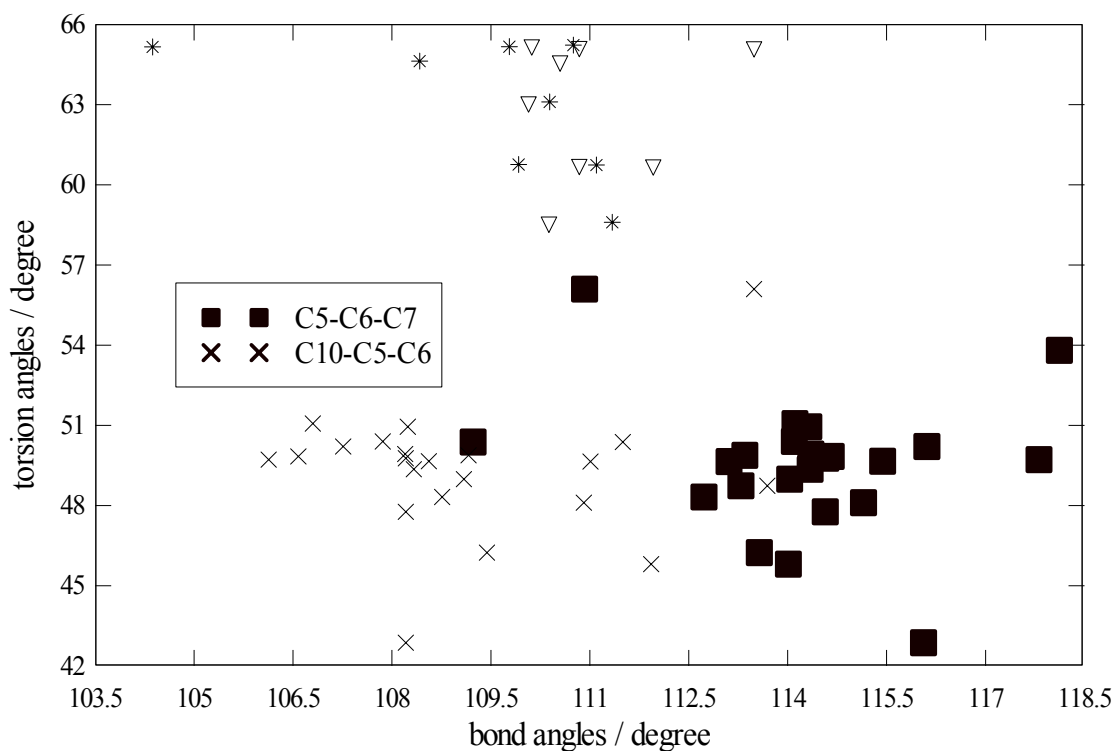
scatterplot of torsion angles(C9-C10-C5-C6) versus bond angles on ring B
compare between friedelane and olenane skeletons



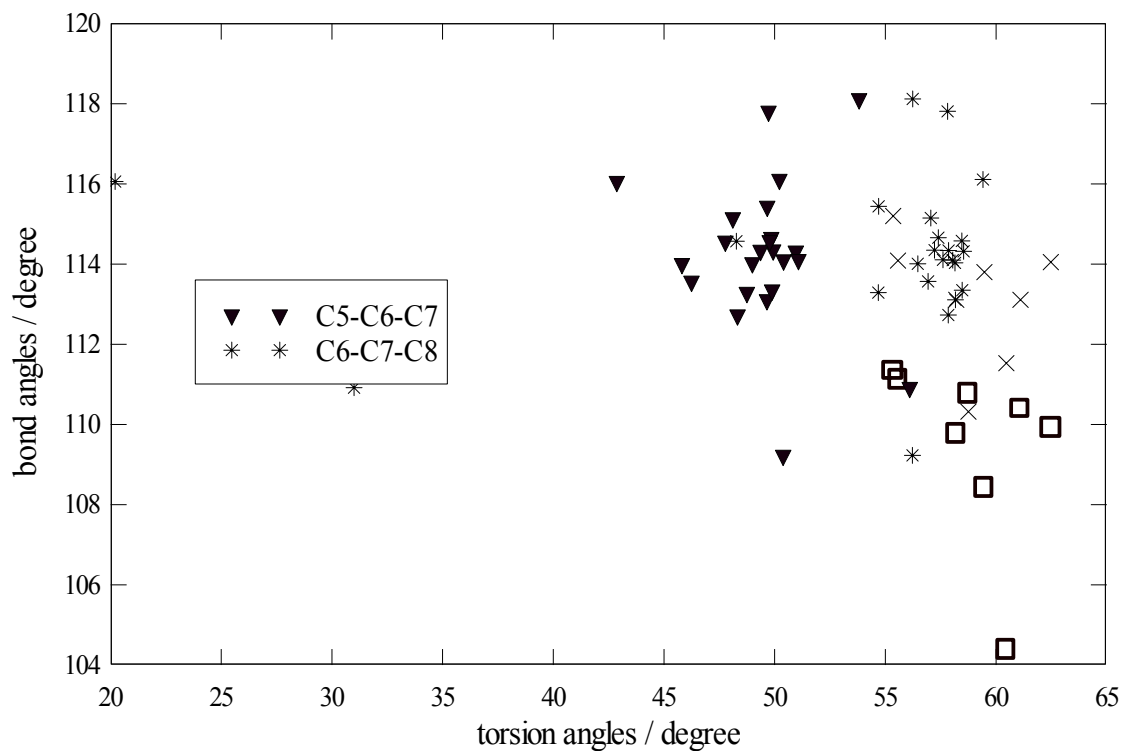
scatterplot of torsion angles(C8-C9-C10-C5) versus bond angles on ring B at C9(dark triangle) compare between friedelane and olenane skeletons



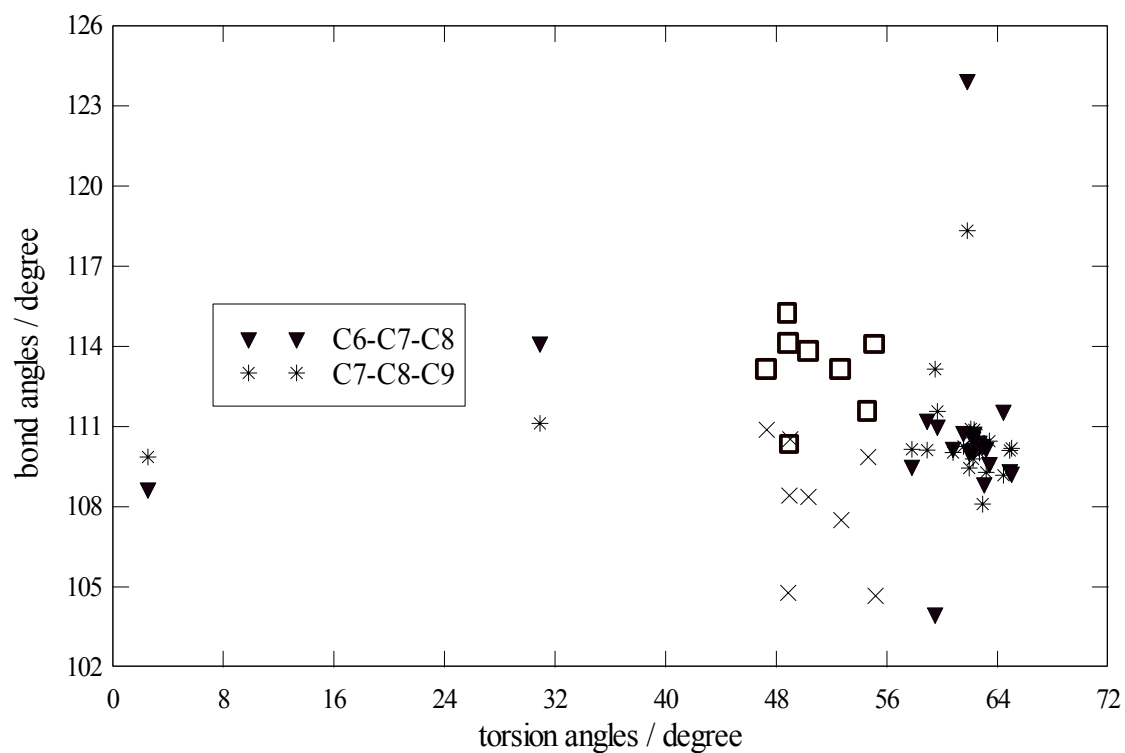
scatterplot of bond angles versus torsion angles(C10-C5-C6-7) related that bond on ring B compare between friedelane and olenane



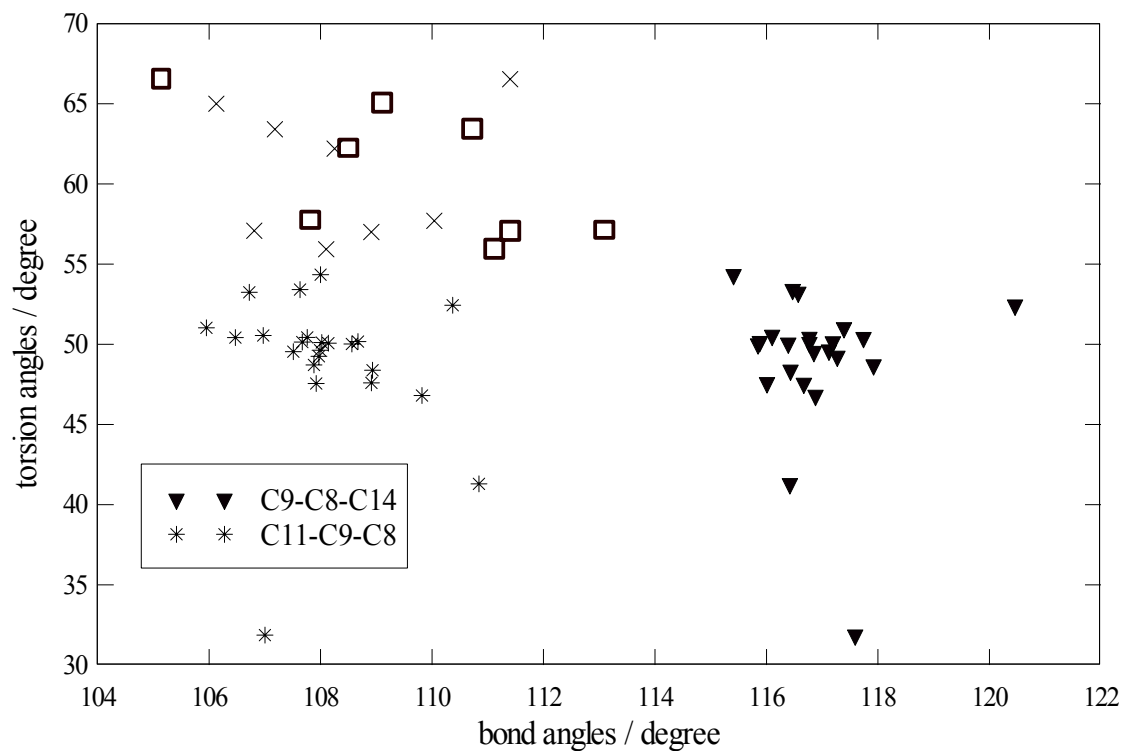
scatterplot of torsion angles(C5-C6-C7-C8) versus bond angles at C6 and C7
on ring B compare between friedelane and olenane skeletons



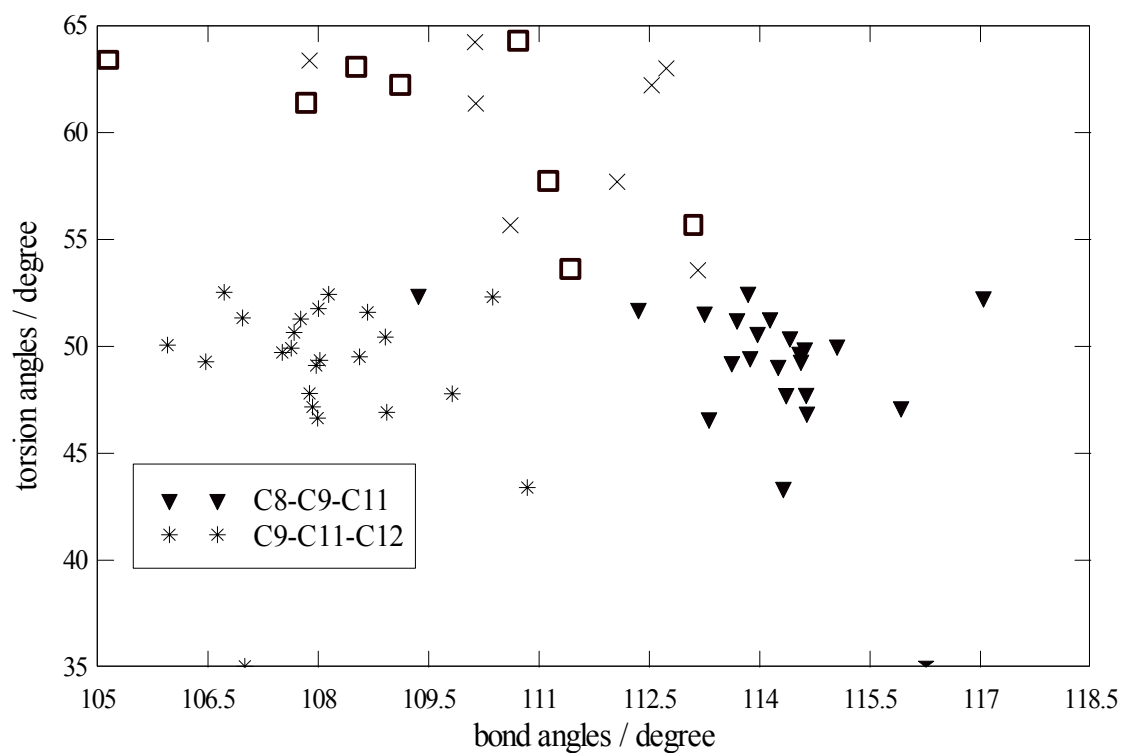
scatterplot of torsion angles(C6-C7-C8-C9) versus bond angles on ring B
at C8 compare between friedelane and olenane skeletons



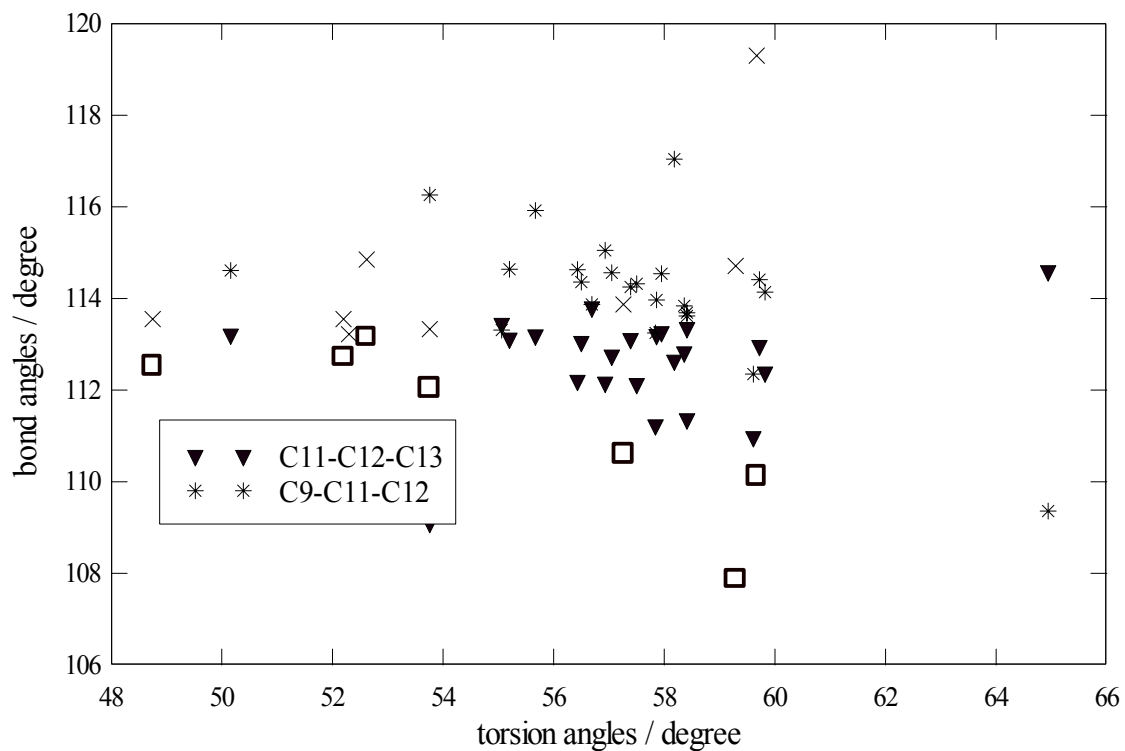
scatterplot of torsion angles(C11-C9-C8-C14) versus bond angles on ring C
compare between friedelane and olenane skeleton



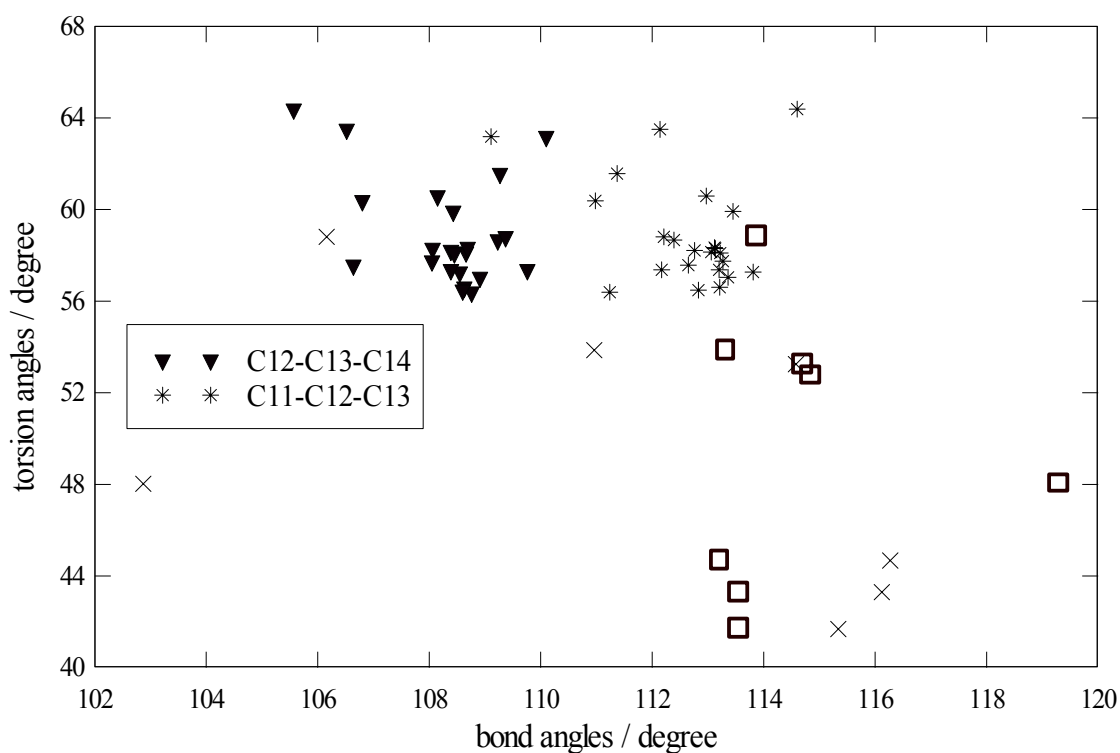
scatterplot of torsion angles(C8-C9-C11-C12) versus bond angles on ring C
compare between friedelane and olenane skeletons



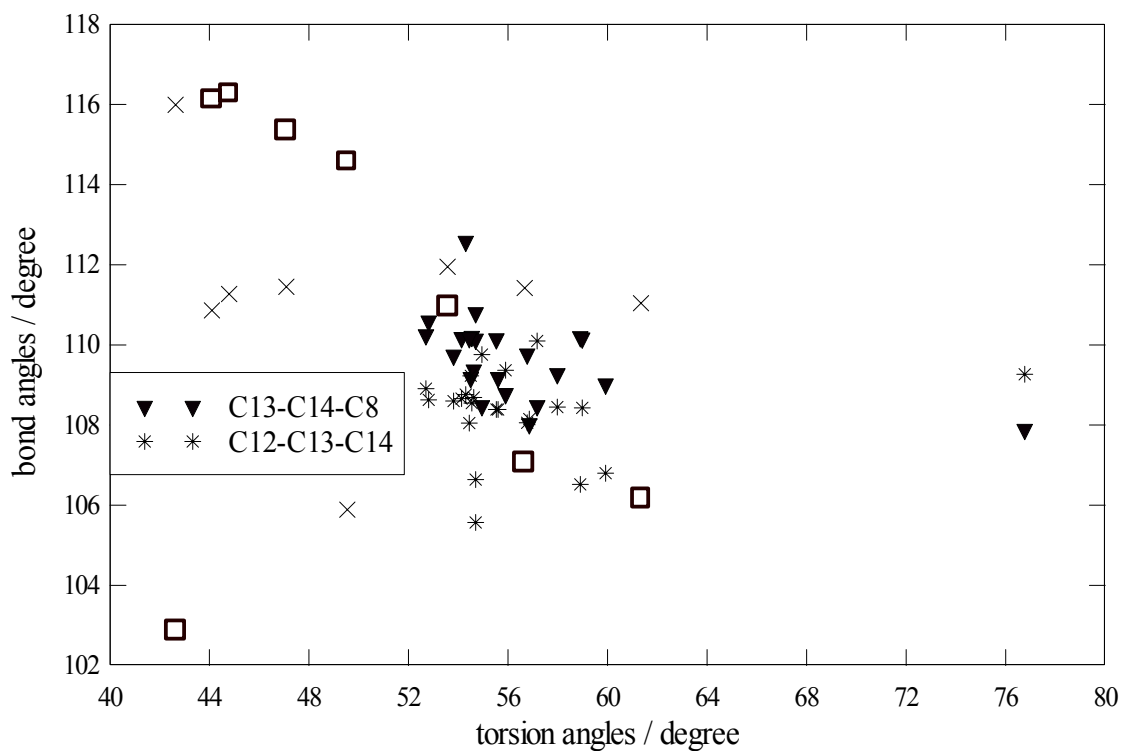
scatterplot of torsion angles(C9-C11-C12-C13) versus bond angles at C11 and C12 on ring C compare between friedelane and olenane skeletons



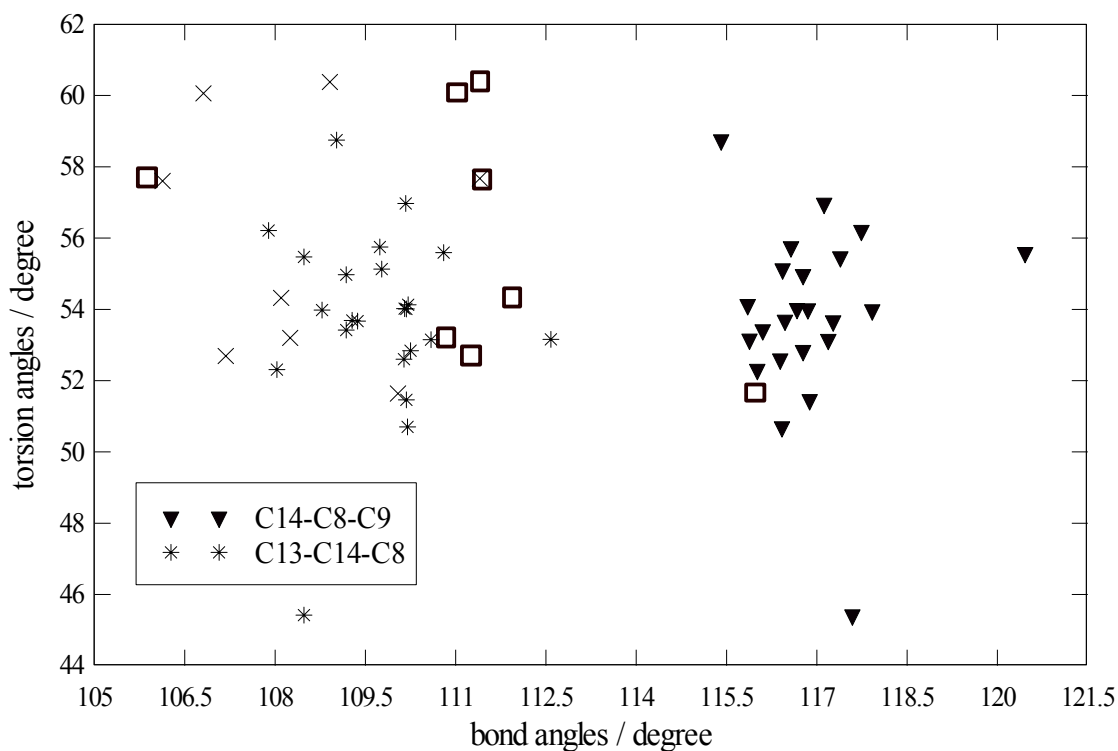
scatterplot of torsion angles(C11-C12-C13-C14) versus bond angles on ring C compare between friedelane and olenane skeletons



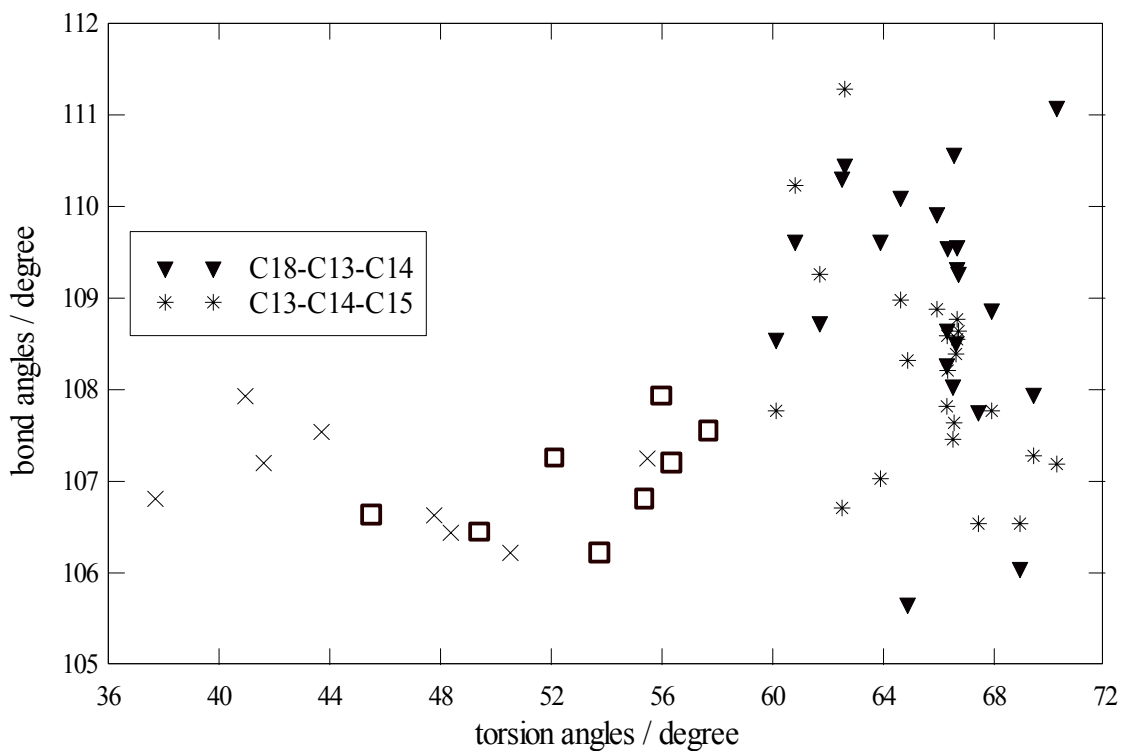
scatterplot of torsion angles(C12-C13-C14-C8) versus bond angles on ring C
at C13 and C14 compare between friedelane and olenane skeletons



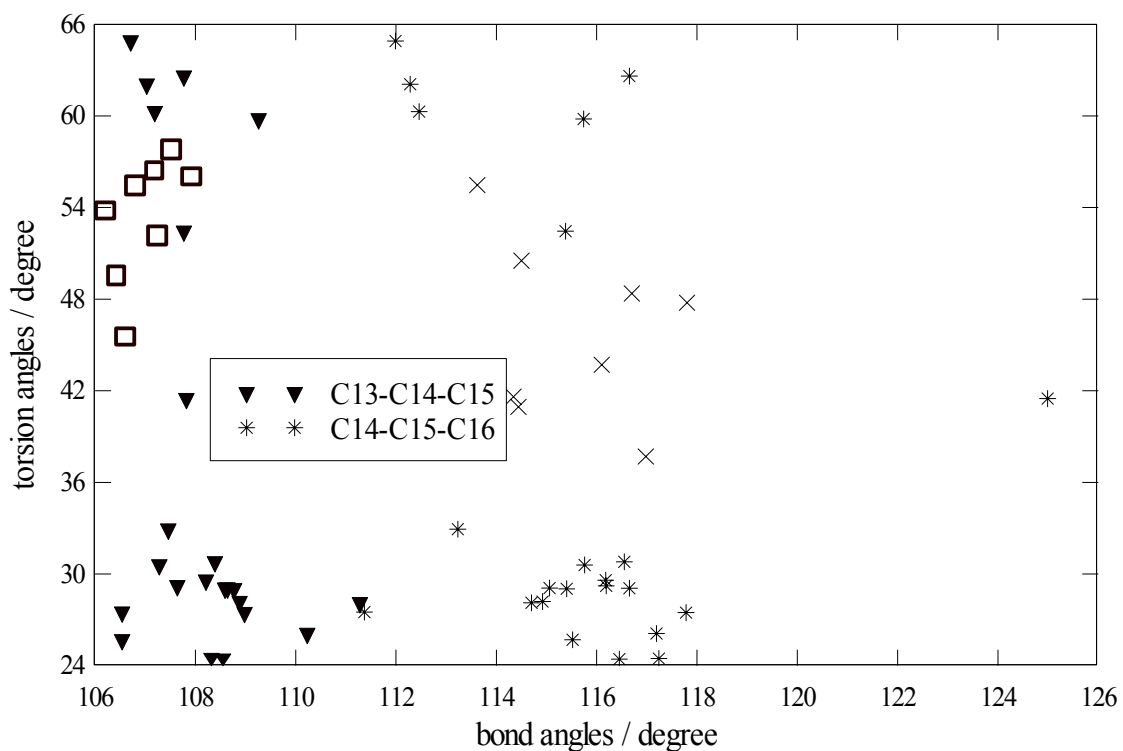
scatterplot of torsion angles(C13-C14-C8-C9) versus bond angles on ring C
compare between friedelane and olenane skeletons



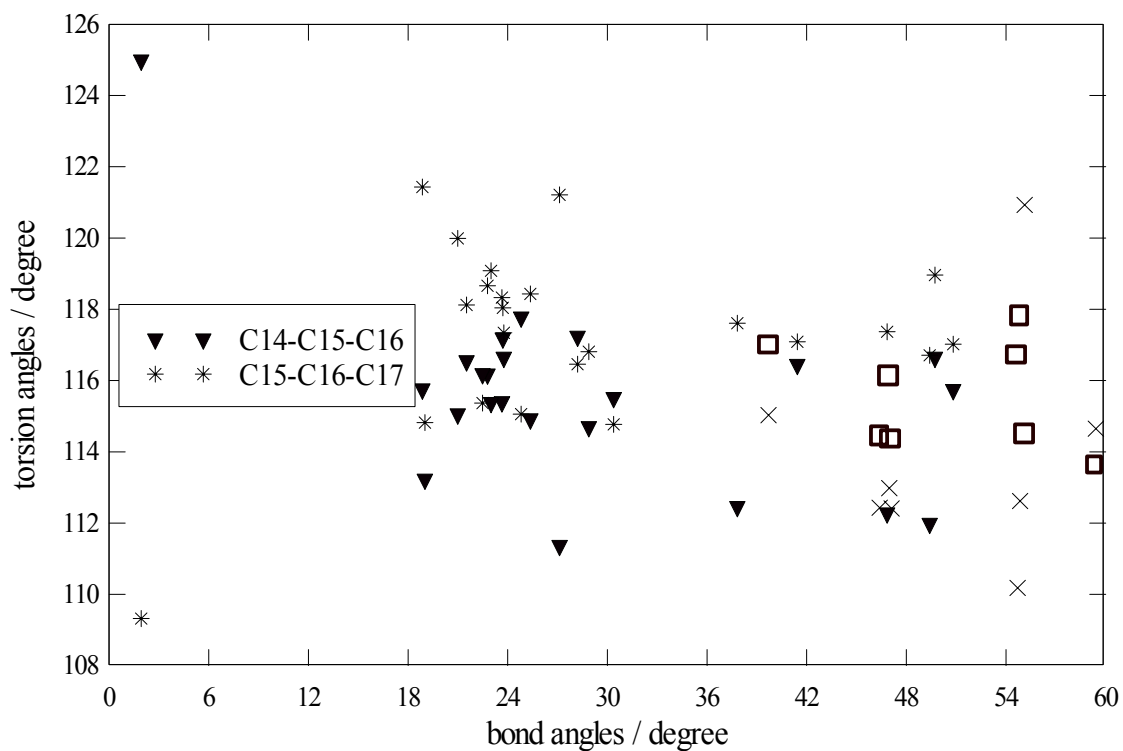
scatterplot of torsion angles(C18-C13-C14-C15) versus bond angles on ring D
at C13 and C14 compare between friedelane and olenane skeletons



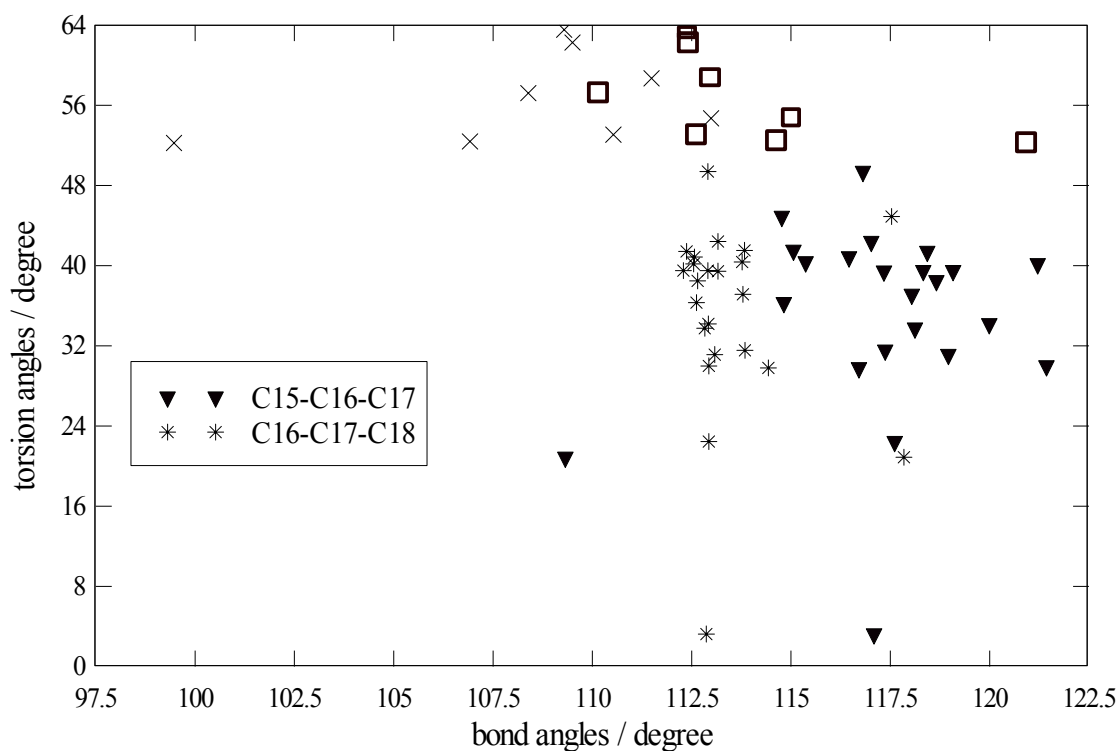
scatterplot of torsion angles(C13-C14-C15-C16) versus bond angles on ring D
compare between friedelane and olenane skeletons



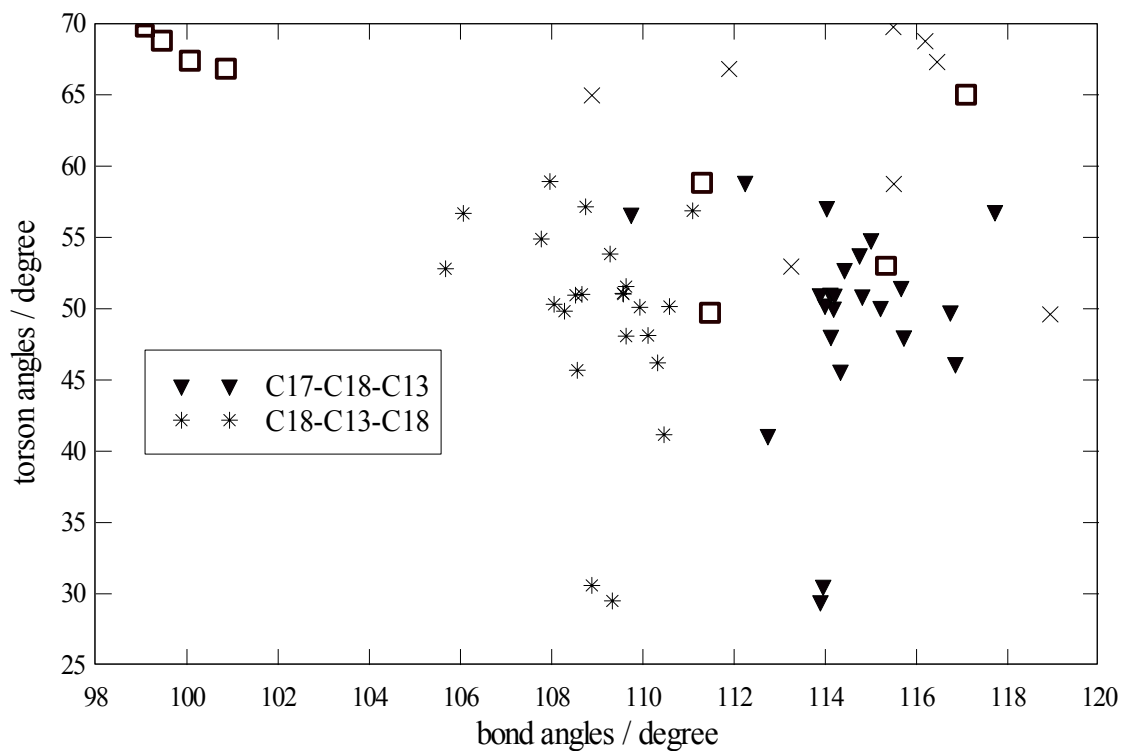
scatterplot of torsion angles(C14-C15-C16-C17) versus bond angles on ring D
compare between friedelane and oleanane skeletons



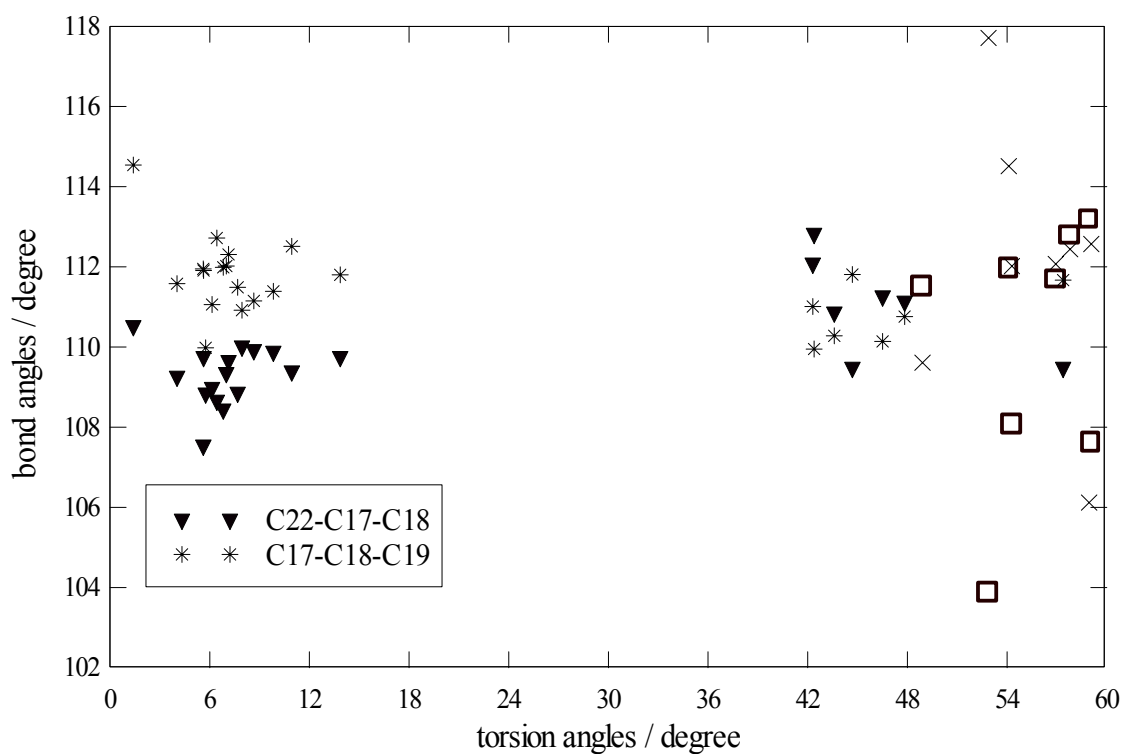
scatterplot of torsion angles(C15-C16-C17-C18) versus bond angles on ring D
compare between friedelane and oleanane skeletons



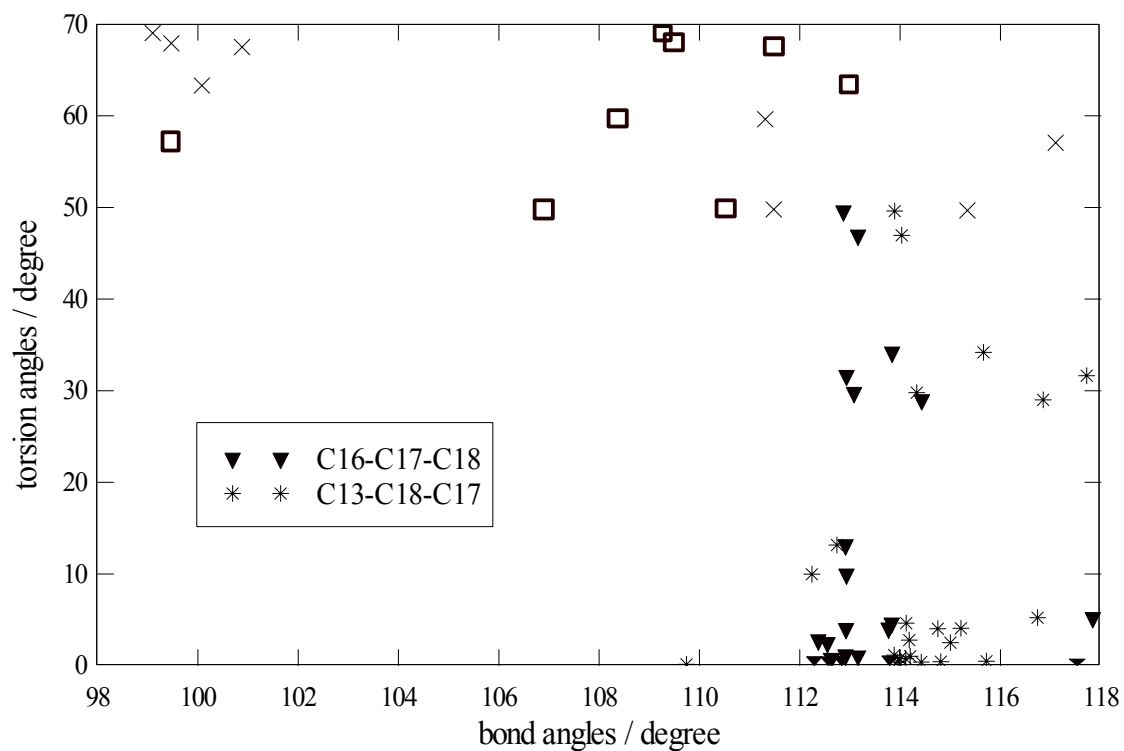
scatterplot of torsion angles(C17-C18-C13-C14) versus bond angles on ring D
compare between friedelane and olenane skeletons



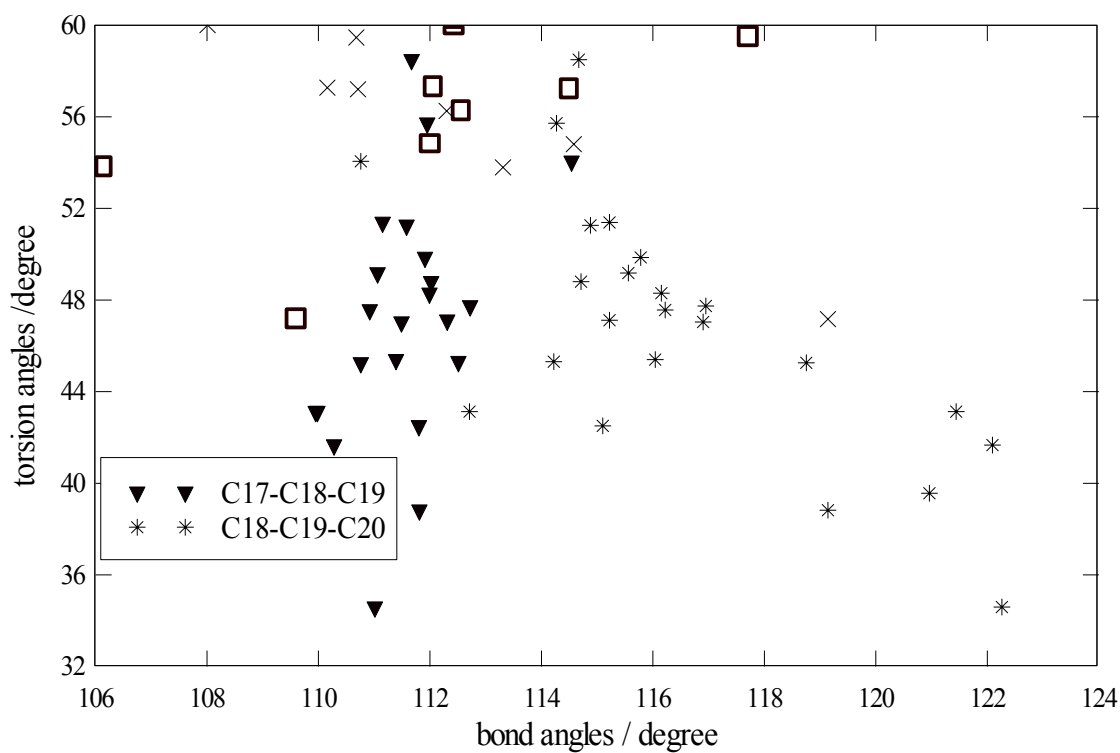
scatterplot of torsion angles(C22-C17-C18-C19) versus bond angles on ring E
at C18 compare between friedelane and olenane skeletons



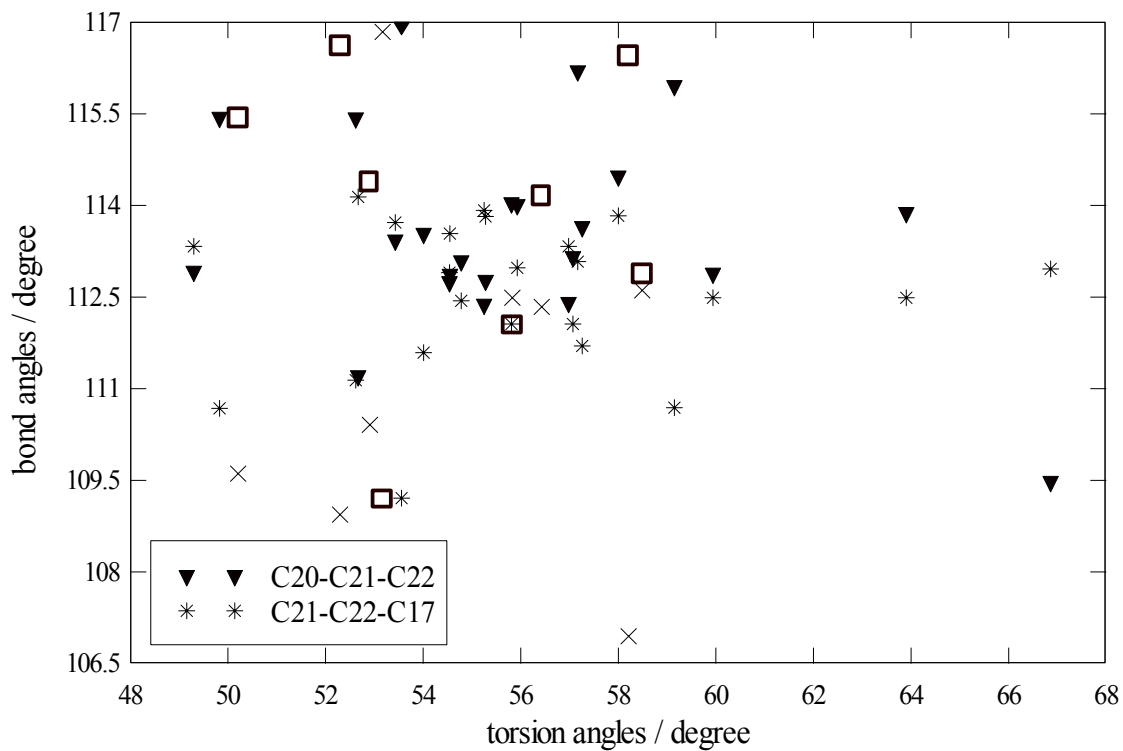
scatterplot of torsion angles(C16-C17-C18-C13) versus bond angles on ring D
compare between friedelane and olenane skeletons



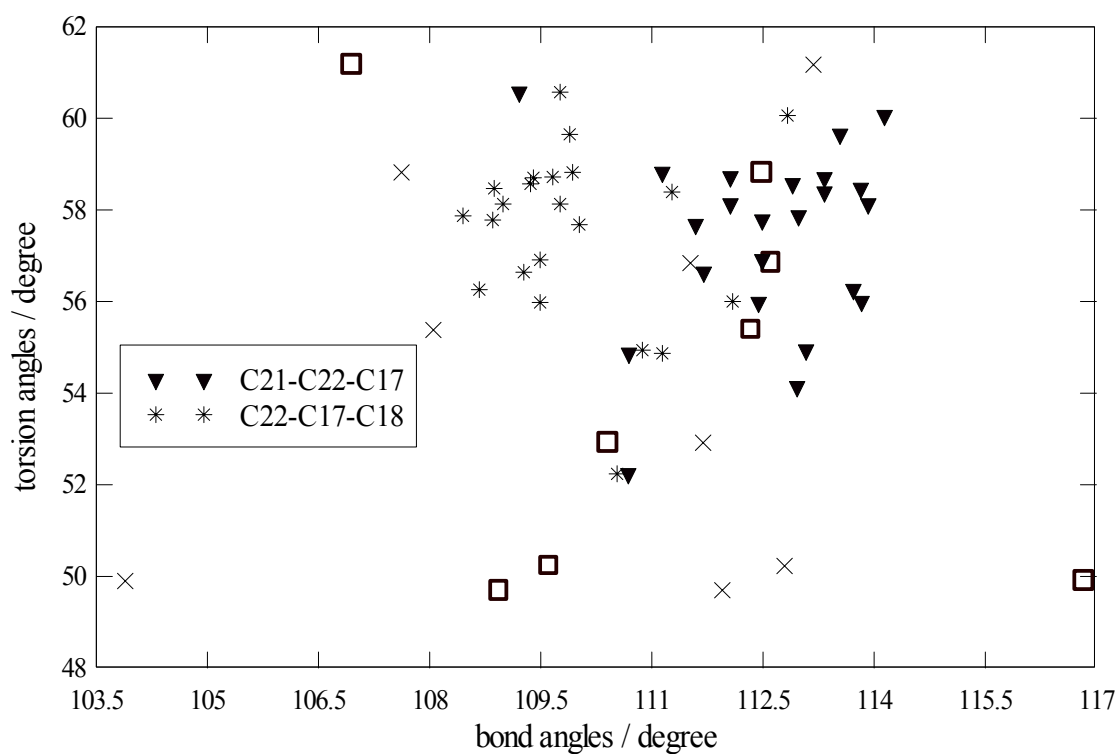
scatterplot of torsion angles(C17-C18-C19-C20) versus bond angles on ring E
compare between friedelane and olenane skeletons



scatterplot for torsion angles(C20-C21-C22-C17) versus bond angles at C21 and C22 on ring E compare between friedelane and olenane skeletons



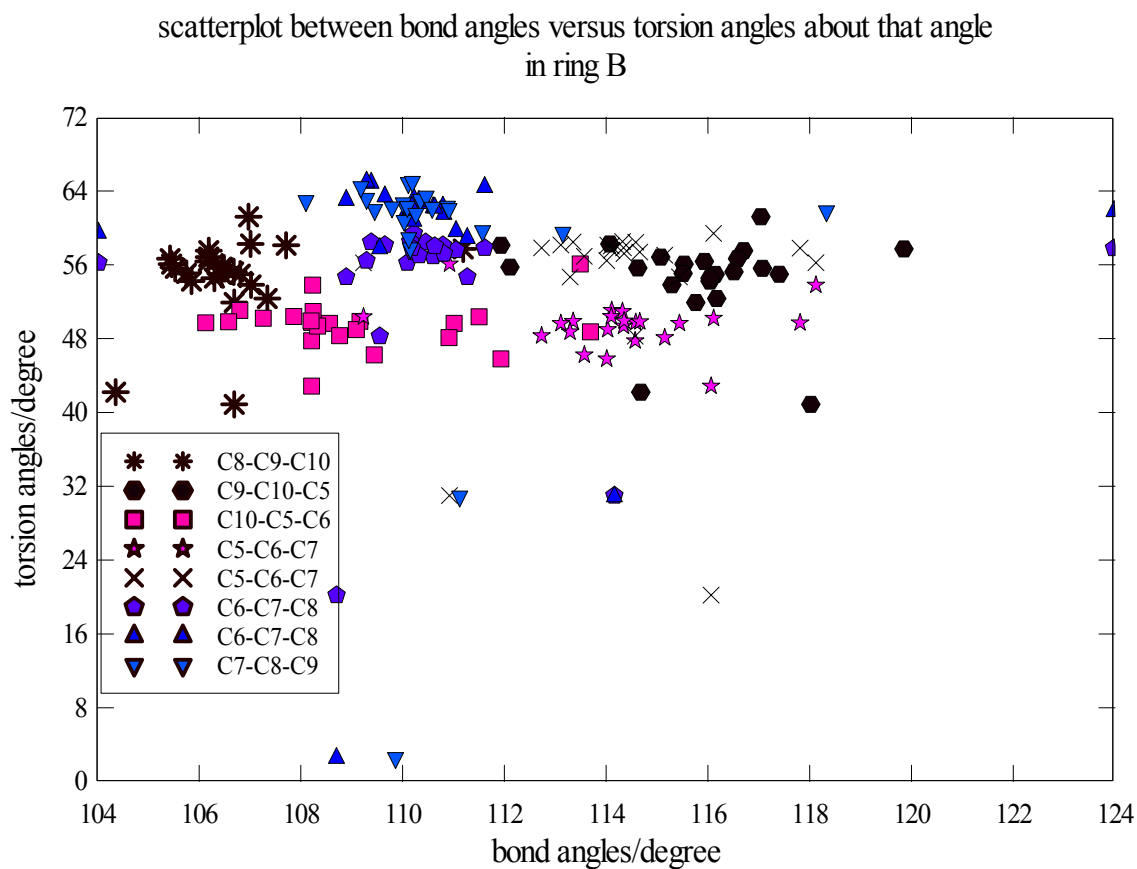
scatterplot of torsion angles(C21-C22-C17-C18) versus bond angles on ring E compare between friedelane and olenane skeletons



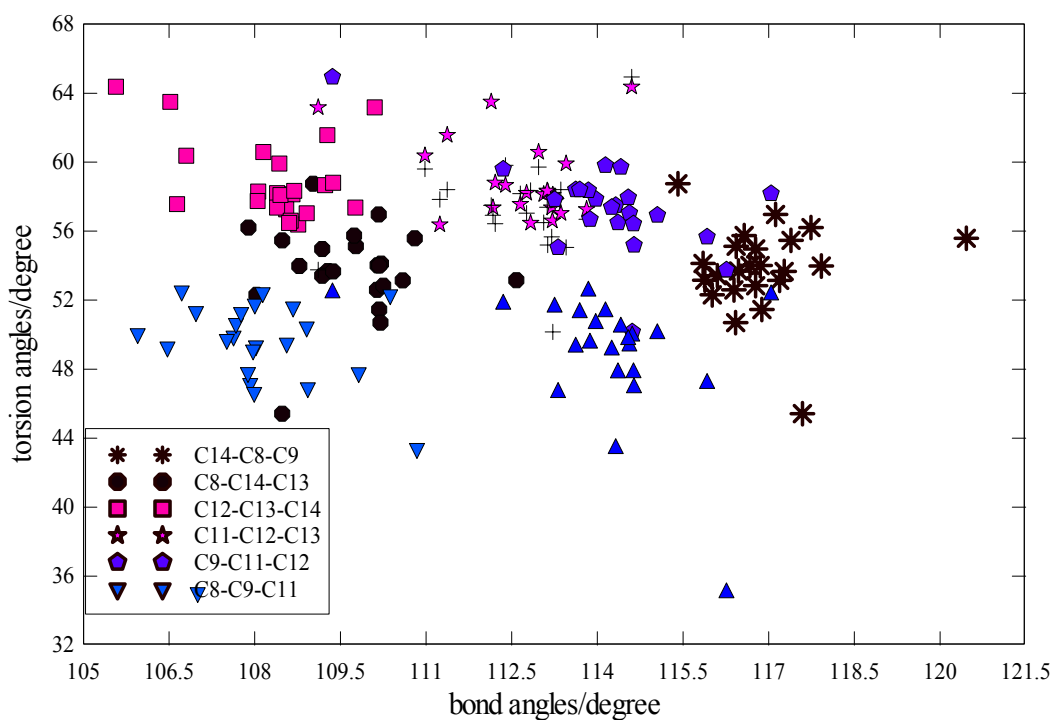
Appendix B2

Scatterplot Type 2

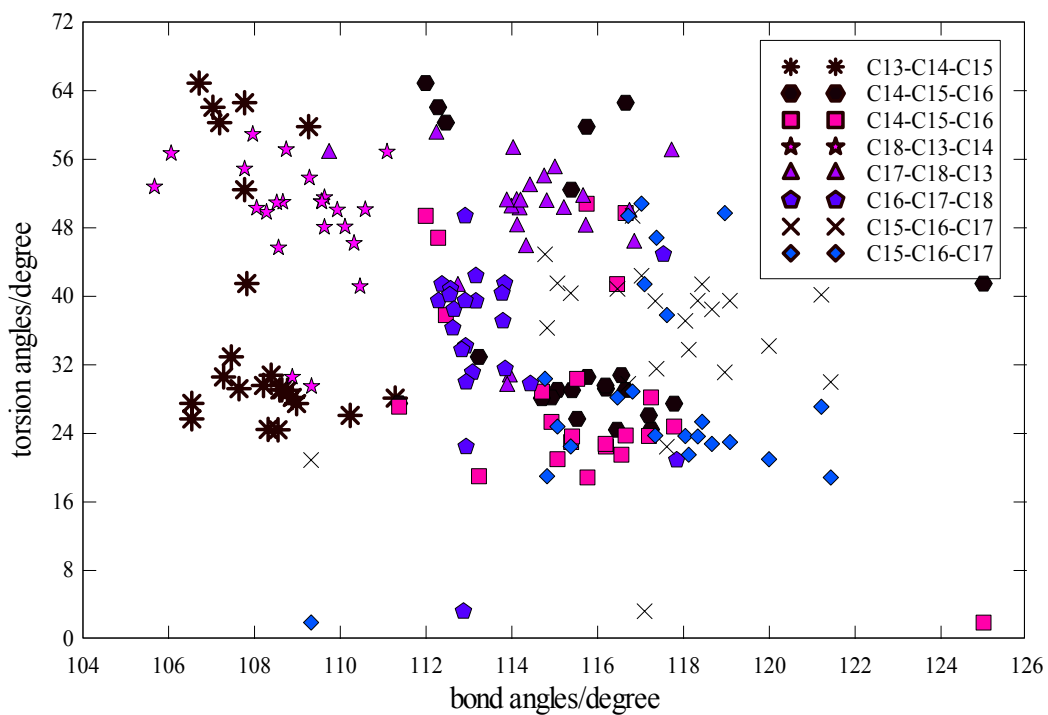
The scatterplot between bond angles with torsion angles related bonds in ring B-E of 23 friedelin and its derivatives compounds is indicative of the different carbon atom types, including secondary, tertiary, and quaternary carbon atoms, which belong to sp^3 hybridization but differ in endo-cyclic bond angles.



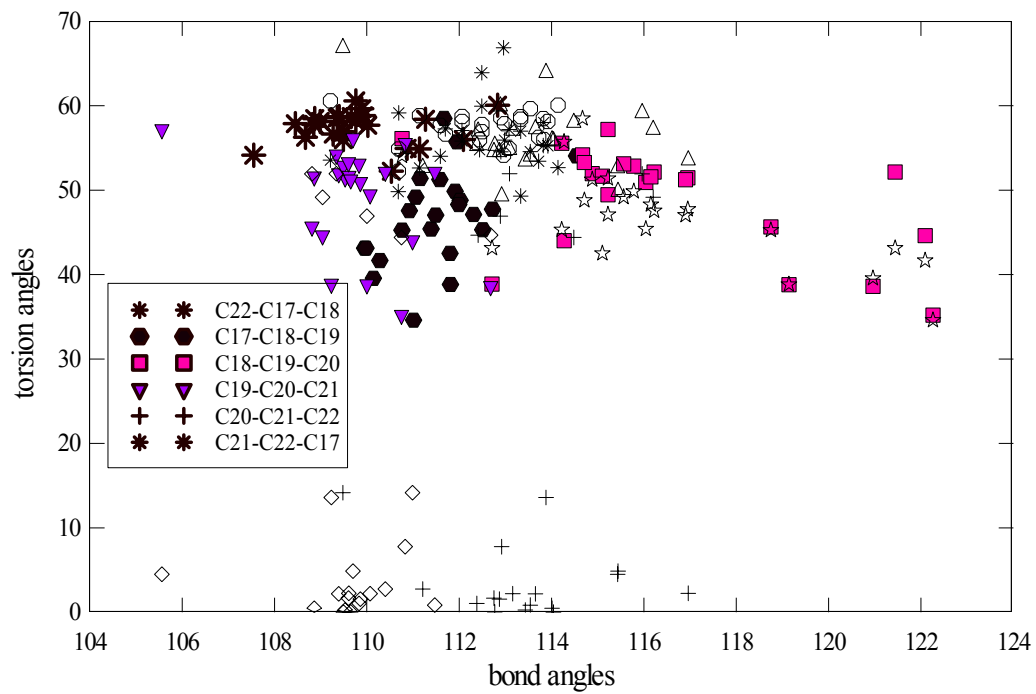
scatterplot between bond angles versus torsion angles about that angles
on ring C



scatterplot between bond angles versus torsion angles about that bond
on ring D



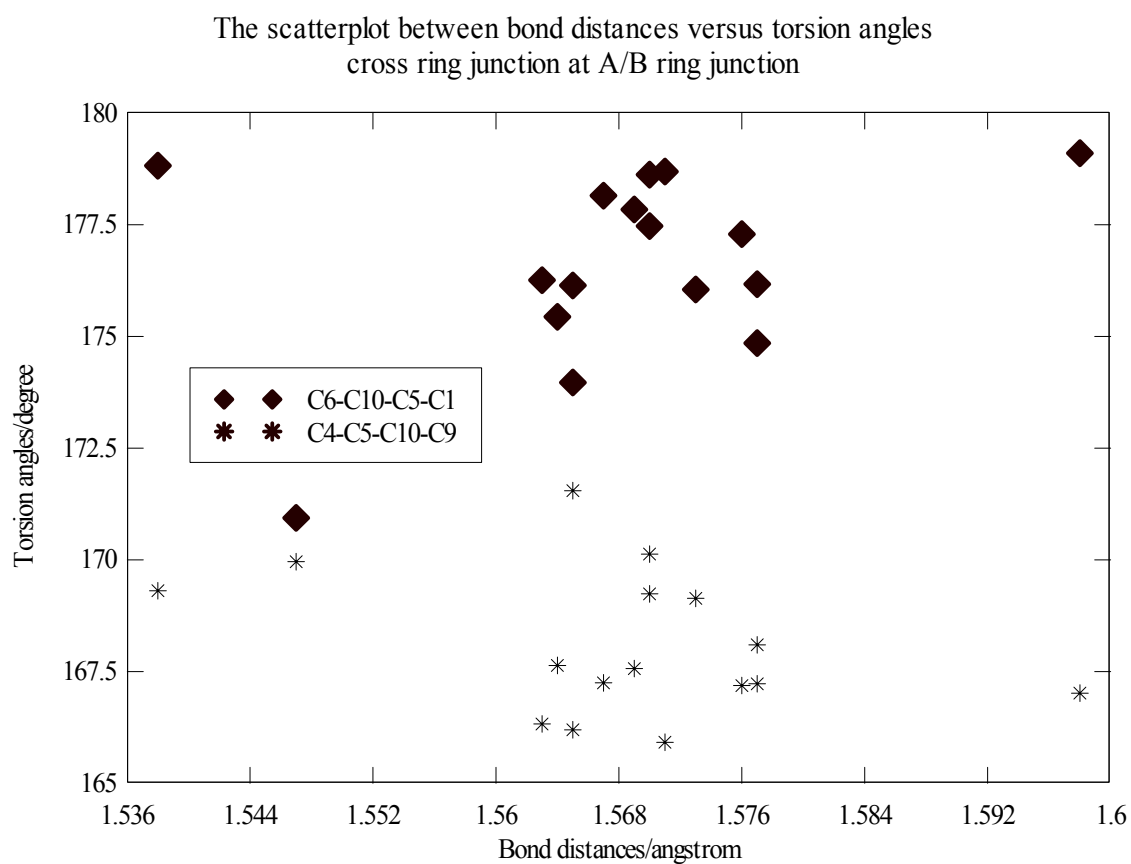
scatterplot between bond angles versus torsion angles about that bond
on ring E



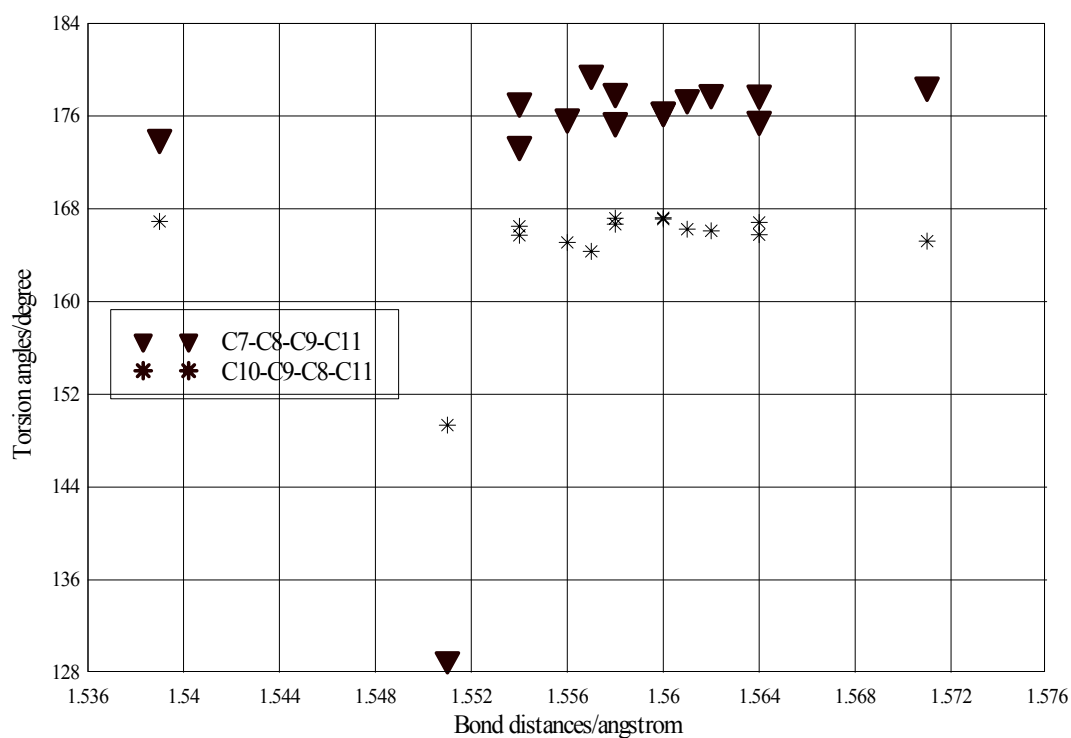
Appendix B3

Scatterplot Type 3

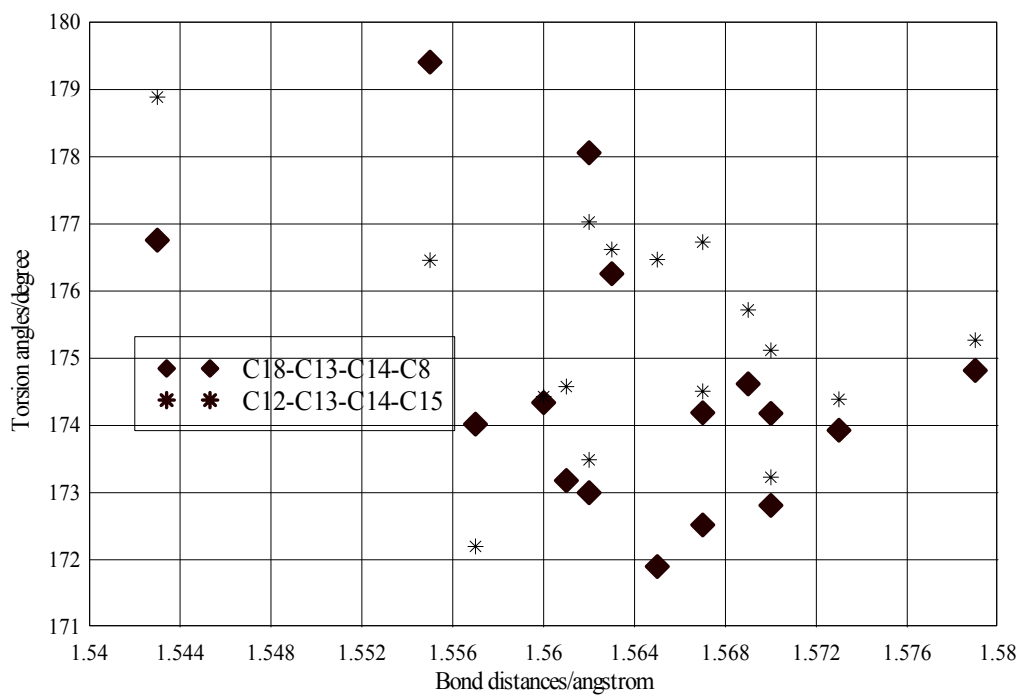
The scatterplot between bond distances versus torsion angles cross four carbon atoms at ring junction that indicate character of ring junction A/B, B/C, C/D and D/E of 18 compounds in friedelane skeletons.



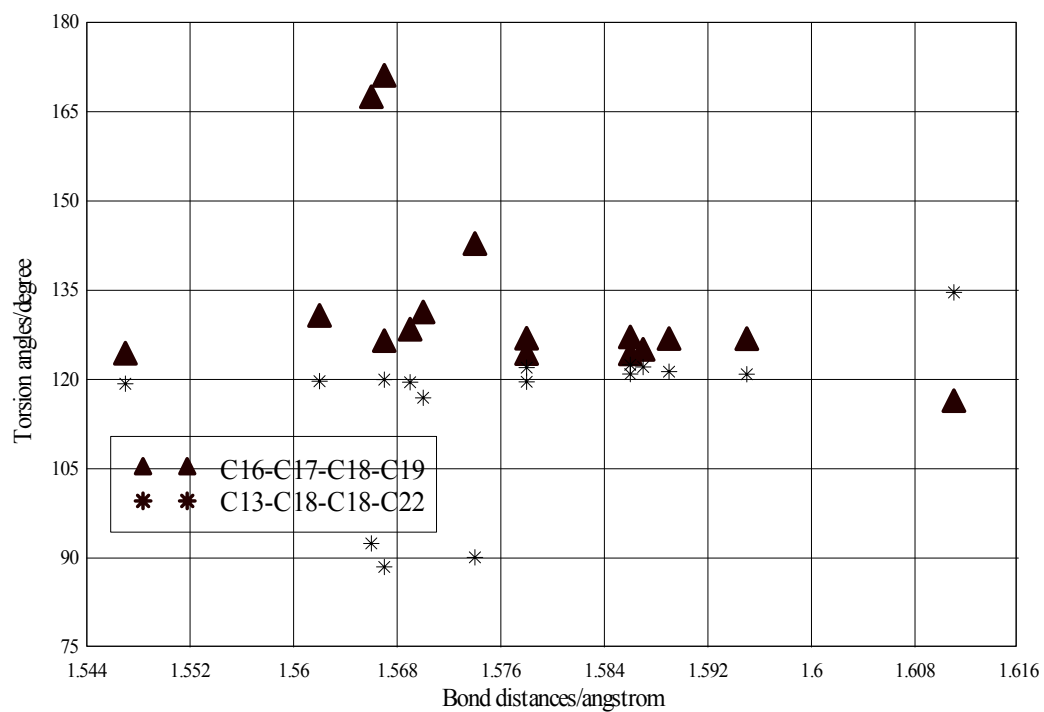
The scatterplot between bond distances versus torsion angles
at B/C ring junction



The scatterplot between bond distances versus torsion angles
at C/D ring junction



The scatterplot between bond distances versus torsion angles
at D/E ring junction



Appendix C

Least-Squares Mean Planes

Least-squares planes (x,y,z in crystal coordinates) and deviations from them of freidelane skeletons That use for indicated ring conformation, which separated considered each ring.

Bitsom

0.204 C1 -0.175 C2 0.205 C3 -0.254 C4 0.277 C5 -0.257 C10
Angle to previous plane = 12.80
0.154 C5 -0.196 C6 0.275 C7 -0.302 C8 0.261 C9 -0.191 C10
Angle to previous plane = 15.90
-0.192 C8 0.180 C9 -0.223 C11 0.273 C12 -0.274 C13 0.237 C14
Angle to previous plane = 14.21
-0.431 C13 0.361 C14 0.006 C15 -0.277 C16 0.215 C17 0.125 C18
Angle to previous plane = 11.30
0.197 C17 0.179 C18 -0.340 C19 0.148 C20 0.253 C21 -0.436 C22

Cerceh

0.188 C1 -0.167 C2 0.219 C3 -0.277 C4 0.295 C5 -0.257 C10
 $5.332 x + 3.703 y + 9.687 z = 2.989$
Angle to previous plane = 10.82
0.182 C5 -0.206 C6 0.269 C7 -0.292 C8 0.261 C9 -0.214 C10
 $1.376 x + 3.591 y + 10.998 z = 2.981$
Angle to previous plane = 17.26
-0.223 C8 0.175 C9 -0.191 C11 0.250 C12 -0.282 C13 0.270 C14
 $1.445 x + 3.776 y + 10.789 z = 2.923$
Angle to previous plane = 1.77
-0.293 C13 0.303 C14 -0.237 C15 0.155 C16 -0.146 C17 0.217 C18
 $4.069 x + 3.656 y + 10.274 z = 2.173$
Angle to previous plane = 11.06
-0.248 C17 0.262 C18 -0.243 C19 0.209 C20 -0.209 C21 0.228 C22

Cmpanl01

$6.265 x - 0.066 y - 3.114 z = 0.116$
-0.245 C1 -0.318 C2 0.543 C3 -0.207 C4 -0.355 C5 0.582 C10
 $5.808 x - 2.352 y + 10.111 z = 5.236$
Angle to previous plane = 28.43
-0.317 C5 0.385 C6 -0.034 C7 -0.388 C8 0.443 C9 -0.088 C10
 $5.047 x - 7.311 y + 8.371 z = 2.435$
Angle to previous plane = 21.93
-0.169 C8 0.133 C9 -0.190 C11 0.285 C12 0.307 C13 0.248 C14
 $4.997 x - 7.057 y + 9.814 z = 2.918$
Angle to previous plane = 3.08
-0.265 C13 0.352 C14 -0.276 C15 0.120 C16 -0.048 C17 0.118 C18
 $-3.508 x + 10.739 y + 9.005 z = 3.532$
Angle to previous plane = 43.48

-0.223 C17 0.140 C18 -0.105 C19 0.137 C20 -0.226 C21 0.276 C22

Epfred

- 0.339 x + 5.227 y - 16.803 z = 12.904

0.274 C1 -0.193 C2 0.154 C3 -0.178 C4 0.242 C5 -0.298 C10

- 0.244 x + 6.084 y - 8.467 z = 5.504

Angle to previous plane = 17.98

0.021 C5 0.021 C5 0.115 C7 -0.280 C8 0.322 C9 -0.198 C10

- 1.232 x + 6.292 y - 3.033 z = 0.882

Angle to previous plane = 11.69

-0.200 C8 .202 C9 -0.235 C11 0.260 C12 -0.246 C13 0.220 C14

- 4.739 x + 5.882 y - 4.376 z = 1.088

Angle to previous plane = 15.58

-0.438 C13 0.350 C14 0.032 C15 -0.301 C16 0.248 C17 .110 C18

3.798 x + 6.090 y - 0.047 z = 1.580

Angle to previous plane = 9.35

-0.275 C17 -0.159 C18 0.438 C19 -0.266 C20 -0.176 C21 0.438 C22

Epfred01

- 0.207 x + 5.352 y + 16.352 z = 5.248

0.239 C1 0.187 C2 -0.188 C3 0.229 C4 -0.268 C5 0.281 C10

- 1.197 x + 6.005 y + 10.232 z = 4.141

Angle to previous plane = 14.03

-0.193 C5 0.216 C6 -0.263 C7 0.278 C8 -0.253 C9 0.215 C10

- 1.142 x + 6.369 y + 2.936 z = 2.881

Angle to previous plane = 14.54

0.207 C8 -0.198 C9 0.225 C11 -0.252 C12 0.244 C13 -0.226 C14

- 4.424 x + 6.002 y + 4.271 z = 0.571

Angle to previous plane = 14.58

0.432 C13 -0.346 C14 -0.027 C15 0.291 C16 -0.219 C17 -0.131 C18

3.578 x + 6.189 y + 0.298 z = 0.051

Angle to previous plane = 8.57

0.241 C17 0.174 C18 -0.404 C19 0.230 C20 0.190 C21 -0.431 C22

Fadgew

5.179 x + 2.554 y - 7.466 z = 5.771

0.285 C1 -0.008 C2 -0.211 C3 0.158 C4 0.106 C5 -0.330 C10

5.636 x + 3.355 y - 5.358 z = 2.392

Angle to previous plane = 10.23

0.174 C5 -0.187 C6 0.255 C7 -0.306 C8 0.278 C9 -0.214 C10

- 6.112 x + 3.890 y - 1.504 z = 2.082

Angle to previous plane = 15.90

0.207 C8 -0.175 C9 0.197 C11 -0.245 C12 0.260 C13 -0.245 C14

- 5.720 x + 5.227 y - 1.402 z = 3.323

Angle to previous plane = 13.54

0.429 C13 -0.343 C14 -0.042 C15 0.314 C16 -0.242 C17 -0.116 C18

- 5.984 x + 4.835 y + 0.669 z = 4.507

Angle to previous plane = 9.87

-0.244 C17 -0.157 C18 0.386 C19 -0.219 C20 -0.184 C21 0.417 C22

Frdlon

$$7.377 x - 6.595 y + 5.328 z = 4.894$$

$$-0.183 C1 \quad 0.143 C2 \quad -0.190 C3 \quad 0.267 C4 \quad -0.294 C5 \quad 0.256 C10$$

$$6.596 x - 4.759 y + 5.994 z = 3.593$$

$$\text{Angle to previous plane} = 10.63$$

$$-0.180 C5 \quad 0.217 C6 \quad -0.274 C7 \quad 0.287 C8 \quad -0.251 C9 \quad 0.201 C10$$

$$5.376 x - 1.139 y + 6.605 z = 0.864$$

$$\text{Angle to previous plane} = 17.55$$

$$0.222 C8 \quad -0.194 C9 \quad 0.211 C11 \quad -0.247 C12 \quad 0.253 C13 \quad -0.246 C14$$

$$-2.239 x - 2.724 y + 6.595 z = 0.773$$

$$\text{Angle to previous plane} = 14.29$$

$$-0.447 C13 \quad 0.329 C14 \quad 0.064 C15 \quad -0.320 C16 \quad 0.220 C17 \quad 0.154 C18$$

$$-1.876 x - 1.065 y + 6.707 z = 2.317$$

$$\text{Angle to previous plane} = 7.41$$

$$0.253 C17 \quad 0.160 C18 \quad -0.400 C19 \quad 0.230 C20 \quad 0.188 C21 \quad -0.431 C22$$

Hfrdac

$$3.188 x + 5.944 y + 3.496 z = 13.188$$

$$0.204 C1 \quad -0.175 C2 \quad 0.221 C3 \quad -0.268 C4 \quad 0.281 C5 \quad -0.263 C10$$

$$3.335 x + 6.267 y - 0.110 z = 9.041$$

$$\text{Angle to previous plane} = 13.60$$

$$0.188 C5 \quad -0.204 C6 \quad 0.253 C7 \quad -0.284 C8 \quad 0.274 C9 \quad -0.227 C10$$

$$2.467 x + 6.336 y - 3.026 z = 4.614$$

$$\text{Angle to previous plane} = 13.03$$

$$-0.217 C8 \quad 0.200 C9 \quad -0.224 C11 \quad 0.259 C12 \quad -0.249 C13 \quad 0.231 C14$$

$$6.276 x + 5.632 y - 6.232 z = 5.760$$

$$\text{Angle to previous plane} = 17.65$$

$$-0.472 C13 \quad 0.354 C14 \quad 0.054 C15 \quad -0.327 C16 \quad 0.221 C17 \quad 0.170 C18$$

$$5.658 x + 5.503 y - 7.927 z = 3.510$$

$$\text{Angle to previous plane} = 7.97$$

$$0.275 C17 \quad 0.133 C18 \quad -0.386 C19 \quad 0.241 C20 \quad 0.173 C21 \quad -0.435 C22$$

Jampoc

$$2.866 x - 12.245 y + 5.662 z = 2.060$$

$$-0.190 C1 \quad 0.161 C2 \quad -0.214 C3 \quad 0.279 C4 \quad -0.302 C5 \quad 0.266 C10$$

$$3.080 x - 7.025 y + 6.070 z = 1.524$$

$$\text{Angle to previous plane} = 11.10$$

$$-0.186 C5 \quad 0.210 C6 \quad -0.274 C7 \quad 0.303 C8 \quad -0.268 C9 \quad 0.216 C10$$

$$3.111 x + 0.592 y + 6.266 z = 0.107$$

$$\text{Angle to previous plane} = 15.37$$

$$0.215 C8 \quad -0.194 C9 \quad 0.212 C11 \quad -0.246 C12 \quad 0.251 C13 \quad -0.239 C14$$

$$6.544 x + 1.199 y + 5.678 z = 2.053$$

$$\text{Angle to previous plane} = 15.07$$

$$0.435 C13 \quad -0.334 C14 \quad -0.030 C15 \quad 0.273 C16 \quad -0.193 C17 \quad -0.152 C18$$

$$5.943 x + 5.754 y + 5.677 z = 0.199$$

$$\text{Angle to previous plane} = 9.44$$

$$-0.251 C17 \quad -0.154 C18 \quad 0.387 C19 \quad -0.232 C20 \quad -0.178 C21 \quad 0.428 C22$$

Likud

$$-2.242 x + 9.203 y + 8.721 z = 1.238$$

$$-0.232 C1 \quad 0.216 C2 \quad -0.224 C3 \quad 0.244 C4 \quad -0.254 C5 \quad 0.251 C10$$

$$-3.682 x + 8.826 y + 8.087 z = 1.140$$

$$\text{Angle to previous plane} = 11.92$$

$$-0.291 C5 \quad 0.139 C6 \quad 0.026 C7 \quad -0.058 C8 \quad -0.088 C9 \quad 0.271 C10$$

$$-2.400 x + 11.113 y - 0.464 z = 1.698$$

$$\text{Angle to previous plane} = 36.35$$

$$0.120 C8 \quad -0.075 C9 \quad 0.155 C11 \quad -0.284 C12 \quad 0.318 C13 \quad -0.235 C14$$

$$-2.335 x + 11.181 y - 0.027 z = 1.895$$

$$\text{Angle to previous plane} = 1.99$$

$$0.251 C13 \quad -0.329 C14 \quad 0.267 C15 \quad -0.127 C16 \quad 0.057 C17 \quad -0.119 C18$$

$$2.922 x - 6.635 y + 9.059 z = 2.590$$

$$\text{Angle to previous plane} = 45.28$$

$$0.231 C17 \quad -0.159 C18 \quad 0.124 C19 \quad -0.149 C20 \quad 0.230 C21 \quad -0.277 C22$$

Paggao

$$3.227 x - 5.411 y + 10.107 z = 4.274$$

$$-0.180 C1 \quad 0.151 C2 \quad -0.185 C3 \quad 0.237 C4 \quad -0.260 C5 \quad 0.237 C10$$

$$2.909 x - 0.207 y + 10.671 z = 6.662$$

$$\text{Angle to previous plane} = 10.93$$

$$-0.195 C5 \quad 0.194 C6 \quad -0.234 C7 \quad 0.272 C8 \quad -0.276 C9 \quad 0.239 C10$$

$$2.921 x + 6.414 y + 10.321 z = 9.001$$

$$\text{Angle to previous plane} = 13.33$$

$$0.210 C8 \quad -0.175 C9 \quad 0.197 C11 \quad -0.249 C12 \quad 0.269 C13 \quad -0.253 C14$$

$$2.610 x + 4.687 y + 10.766 z = 8.516$$

$$\text{Angle to previous plane} = 4.58$$

$$0.290 C13 \quad -0.341 C14 \quad 0.248 C15 \quad -0.114 C16 \quad 0.071 C17 \quad -0.155 C18$$

$$1.560 x + 24.103 y + 5.837 z = 9.553$$

$$\text{Angle to previous plane} = 47.63$$

$$-0.226 C17 \quad 0.187 C18 \quad -0.164 C19 \quad 0.181 C20 \quad -0.237 C21 \quad 0.259 C22$$

Prisem

$$5.640 x + 12.530 y - 1.532 z = 18.842$$

$$0.211 C1 \quad -0.198 C2 \quad 0.236 C3 \quad -0.266 C4 \quad 0.271 C5 \quad -0.254 C10$$

$$6.020 x + 7.533 y - 2.291 z = 13.211$$

$$\text{Angle to previous plane} = 11.14$$

$$0.200 C5 \quad -0.222 C6 \quad 0.256 C7 \quad -0.287 C8 \quad 0.272 C9 \quad -0.219 C10$$

$$6.236 x + 0.984 y - 2.435 z = 6.399$$

$$\text{Angle to previous plane} = 13.44$$

$$-0.202 C8 \quad 0.199 C9 \quad -0.247 C11 \quad 0.294 C12 \quad -0.265 C13 \quad 0.222 C14$$

$$5.764 x + 0.777 y - 5.796 z = 4.528$$

$$\text{Angle to previous plane} = 14.46$$

$$0.431 C13 \quad 0.343 C14 \quad 0.036 C15 \quad -0.307 C16 \quad 0.232 C17 \quad 0.127 C18$$

$$5.979 x - 2.307 y - 4.492 z = 2.377$$

$$\text{Angle to previous plane} = 8.45$$

$$0.232 C17 \quad 0.190 C18 \quad -0.414 C19 \quad 0.216 C20 \quad 0.216 C21 \quad -0.441 C22$$

Vagcub

$$19.526 x + 3.174 y + 9.307 z = 9.228$$

$$0.270 C1 \quad -0.220 C2 \quad 0.192 C3 \quad -0.197 C4 \quad 0.233 C5 \quad -0.278 C10$$

$$12.241 x + 4.719 y + 10.844 z = 0.599$$

$$\text{Angle to previous plane} = 17.38$$

$$0.168 C5 \quad -0.191 C6 \quad 0.265 C7 \quad -0.311 C8 \quad 0.280 C9 \quad -0.210 C10$$

$$-4.135 x + 4.594 y + 11.755 z = 6.330$$

$$\text{Angle to previous plane} = 16.72$$

$$0.213 C8 \quad -0.191 C9 \quad 0.220 C11 \quad -0.267 C12 \quad 0.274 C13 \quad -0.249 C14$$

$$-3.559 x + 7.267 y + 10.835 z = 8.524$$

$$\text{Angle to previous plane} = 11.01$$

$$0.397 C13 \quad -0.348 C14 \quad -0.030 C15 \quad 0.336 C16 \quad -0.270 C17 \quad -0.086 C18$$

$$-3.763 x + 4.509 y + 11.791 z = 6.589$$

$$\text{Angle to previous plane} = 11.34$$

$$-0.163 C17 \quad -0.267 C18 \quad 0.400 C19 \quad -0.134 C20 \quad -0.292 C21 \quad 0.456 C22$$

Vefnid

$$6.333 x + 3.524 y + 7.352 z = 3.006$$

$$-0.192 C1 \quad 0.161 C2 \quad -0.212 C3 \quad 0.272 C4 \quad -0.298 C5 \quad 0.268 C10$$

$$6.684 x + 1.007 y + 4.564 z = 1.815$$

$$\text{Angle to previous plane} = 11.44$$

$$-0.184 C5 \quad 0.209 C6 \quad -0.265 C7 \quad 0.285 C8 \quad -0.258 C9 \quad 0.213 C10$$

$$-6.756 x - 2.105 y + 0.219 z = 0.287$$

$$\text{Angle to previous plane} = 15.02$$

$$-0.214 C8 \quad 0.190 C9 \quad -0.211 C11 \quad 0.253 C12 \quad -0.264 C13 \quad 0.247 C14$$

$$-6.524 x - 3.492 y + 4.730 z = 0.724$$

$$\text{Angle to previous plane} = 11.75$$

$$-0.414 C13 \quad 0.364 C14 \quad -0.033 C15 \quad -0.201 C16 \quad 0.174 C17 \quad 0.110 C18$$

$$-4.767 x - 10.368 y - 7.705 z = 8.861$$

$$\text{Angle to previous plane} = 41.49$$

$$0.248 C17 \quad -0.169 C18 \quad 0.125 C19 \quad -0.143 C20 \quad 0.219 C21 \quad -0.281 C22$$

Yegyoy

$$-2.144 x + 6.139 y + 9.547 z = 11.032$$

$$0.264 C1 \quad -0.202 C2 \quad 0.185 C3 \quad -0.211 C4 \quad 0.255 C5 \quad -0.291 C10$$

$$-1.888 x + 11.290 y + 8.249 z = 11.192$$

$$\text{Angle to previous plane} = 16.69$$

$$0.184 C5 \quad -0.209 C6 \quad 0.265 C7 \quad -0.285 C8 \quad 0.257 C9 \quad -0.211 C10$$

$$-2.162 x + 15.253 y + 6.297 z = 10.926$$

$$\text{Angle to previous plane} = 16.92$$

$$-0.204 C8 \quad 0.179 C9 \quad -0.206 C11 \quad 0.255 C12 \quad -0.264 C13 \quad 0.240 C14$$

$$-0.700 x + 15.999 y + 5.879 z = 11.081$$

$$\text{Angle to previous plane} = 11.36$$

$$-0.407 C13 \quad 0.317 C14 \quad 0.040 C15 \quad -0.288 C16 \quad 0.203 C17 \quad 0.136 C18$$

$$-0.851 x + 17.535 y + 4.670 z = 11.214$$

$$\text{Angle to previous plane} = 8.80$$

$$0.273 C17 \quad 0.134 C18 \quad -0.400 C19 \quad 0.265 C20 \quad 0.149 C21 \quad -0.421 C22$$

Zzzqai02

$$5.670 x - 1.652 y + 12.436 z = 5.547$$

$$0.216 C1 \quad -0.205 C2 \quad 0.237 C3 \quad -0.265 C4 \quad 0.269 C5 \quad -0.252 C10$$

$$6.042 x - 2.471 y + 7.333 z = 3.526$$

Angle to previous plane = 11.35

$$0.191 C5 \quad -0.207 C6 \quad 0.257 C7 \quad -0.280 C8 \quad 0.264 C9 \quad -0.224 C10$$

$$6.275 x - 2.278 y + 0.500 z = 1.458$$

Angle to previous plane = 13.99

$$-0.210 C8 \quad 0.201 C9 \quad -0.227 C11 \quad 0.253 C12 \quad -0.241 C13 \quad 0.225 C14$$

$$5.799 x - 5.706 y + 0.981 z = 1.109$$

Angle to previous plane = 14.82

$$-0.436 C13 \quad 0.346 C14 \quad 0.033 C15 \quad -0.299 C16 \quad 0.224 C17 \quad 0.133 C18$$

$$5.950 x - 4.753 y - 2.671 z = 0.644$$

Angle to previous plane = 8.46

$$0.245 C17 \quad 0.165 C18 \quad -0.397 C19 \quad 0.226 C20 \quad 0.193 C21 \quad -0.432 C22$$

Zzzqai1

$$5.667 x - 1.631 y + 12.566 z = 5.614$$

$$0.216 C1 \quad -0.187 C2 \quad 0.216 C3 \quad -0.258 C4 \quad 0.278 C5 \quad -0.265 C10$$

$$6.065 x - 2.455 y + 7.131 z = 3.460$$

Angle to previous plane = 12.02

$$0.202 C5 \quad -0.221 C6 \quad 0.255 C7 \quad -0.256 C8 \quad 0.242 C9 \quad -0.221 C10$$

$$6.280 x - 2.335 y + 0.491 z = 1.445$$

Angle to previous plane = 13.55

$$-0.191 C8 \quad 0.172 C9 \quad -0.207 C11 \quad 0.255 C12 \quad -0.261 C13 \quad 0.232 C14$$

$$5.809 x - 5.698 y + 1.176 z = 1.148$$

Angle to previous plane = 14.56

$$-0.445 C13 \quad 0.358 C14 \quad 0.029 C15 \quad -0.296 C16 \quad 0.221 C17 \quad 0.134 C18$$

$$5.977 x - 4.697 y - 2.295 z = 0.710$$

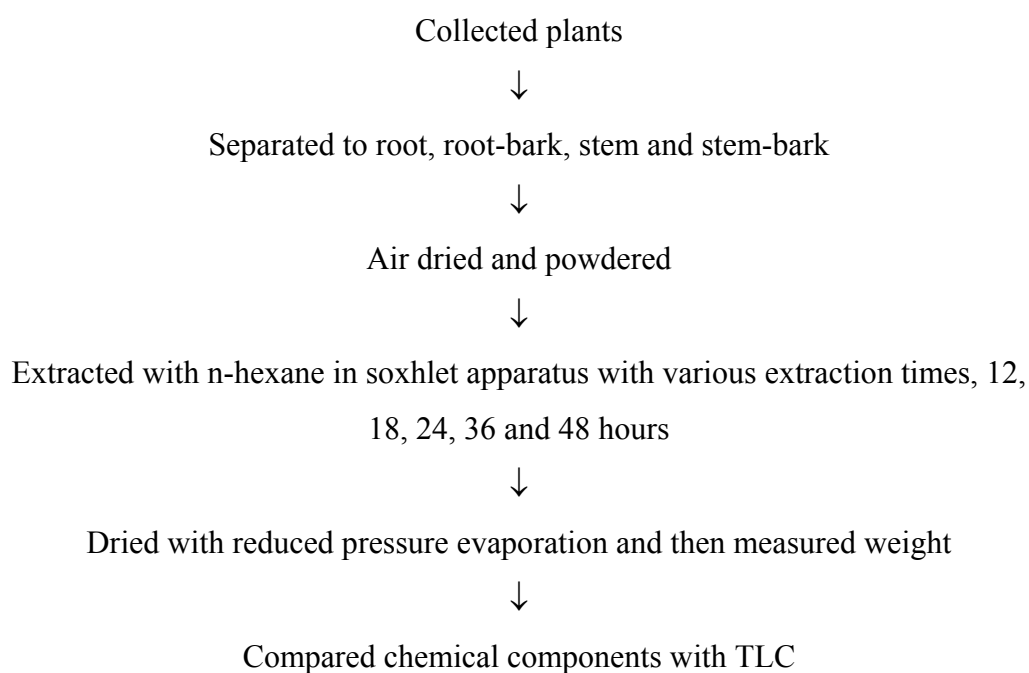
Angle to previous plane = 8.26

$$0.248 C17 \quad 0.181 C18 \quad -0.397 C19 \quad 0.213 C20 \quad 0.201 C21 \quad -0.445 C22$$

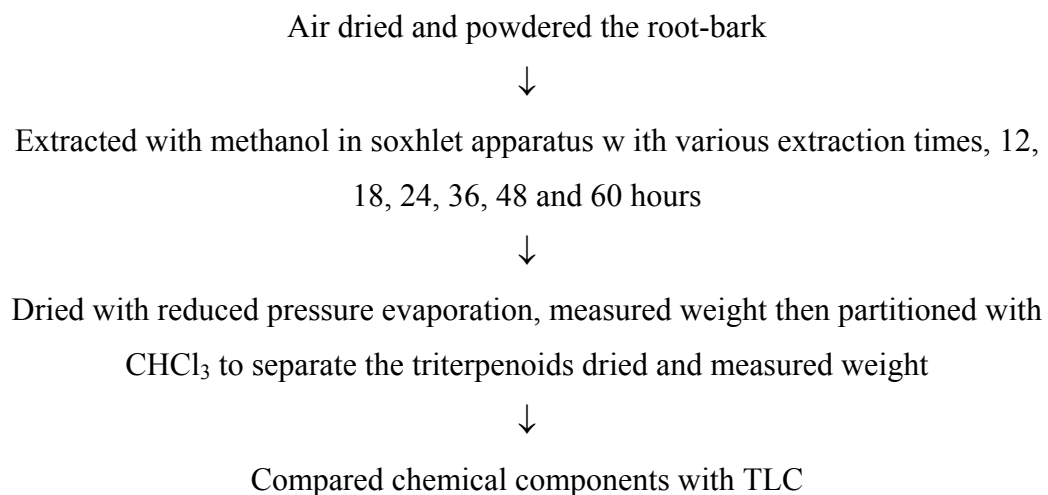
Appendix D

Isolation Study

n-hexane extraction



Methanol extraction



Purification

Crude extract was purified by column chromatography over silica gel (#7734) 200 gram with column diameter 5.00 cm and 50 cm length. Eluted starting with n-hexane and then gradually increasing polarity by increasing amount of CHCl_3 , EtOAc and EtOH respectively

Flow rate was 2.0 ml/min



Collected 500 ml fractions and tested purity by TLC



Chromatographed again over silica gel (#7729) on column diameter 2.50 cm and 50 cm length if a fraction was impure. Appropriate solvent determined from TLC or carried out on preparative tlc with silica gel # 7730

Curriculum Vitae

AUPHATHAM PHOTHIKANITH

Born: June 13, 1965, Khonkaen

Citizenship: Thai

Marital Status: Married

Education

- 1982-1986 B.Sc., Chemistry
Nakhon Ratchasima Teacher College, Nakhon Ratchasima, Thailand
- 1991-1993 M.Sc., Teaching Chemistry
Chiang Mai University, Chaing Mai, Thailand

Experience

- 1986-1994 Teaching Chemistry at Secondary School
Thali Vitaya Secondary School
Loei Province
- 1995-1997 Teaching Chemistry at four year college
Rajabhat Institute of Nakhon Ratchasima
Nakhon Ratchasima

Presentations

"Identification of a Disordered Friedelin Structure by Structure Correlation", (with K. J. Haller), 25th Congress on Science and Technology of Thailand, Pitsanuloke, Thailand: Abstract A-100, 1999.

"Preliminary Investigation of Natural Product Extraction from *Celatrus Paniculatus* Willd.", (with K. J. Haller), 26th Congress on Science and Technology of Thailand, Bangkok, Thailand: Abstract 18-I3P-16, 2000.

"X-Ray Structure Characterization of Disordered Friedelin-3-one and Epifriedelin-3-ol", (with K. J. Haller), AsCA'01, 4th Asian Crystallographic Association Meeting, Bangalore, India: Abstract A4-9, 2001.

Scholarships and Honors:

Graduate, Thai Government Scholarship, Secondary Education Quality Improvement Project, Ministry of Education.